

Elucidating the role of the Cpx envelope stress response in the colonization and virulence of
Citrobacter rodentium

by

Ashley Rebecca Gilliland

A thesis submitted in partial fulfillment of the requirements for the degree of

Master of Science

in

Microbiology and Biotechnology

Department of Biological Sciences
University of Alberta

© Ashley Rebecca Gilliland, 2022

Abstract

The murine attaching and effacing (A/E) pathogen, *Citrobacter rodentium*, is used as an infection model *in vivo* for the A/E pathogens enterohemorrhagic and enteropathogenic *Escherichia coli* (EHEC and EPEC). All three A/E pathogens harbor the Locus of Enterocyte Effacement (LEE) which encodes a Type III Secretion System (T3SS) and other virulence factors that are required for the adherence to intestinal epithelial cells, formation of pedestals and injection of effector proteins. During colonization, these pathogens face a myriad of challenges associated with the gastrointestinal tract including acidic pH, bile, oxygen gradients, mucus, and microbiome-mediated colonization resistance. To ameliorate the environmental stressors encountered, pathogens like *C. rodentium*, utilize two-component systems (TCS) to sense and appropriately respond to changes in the surrounding environment by moderating gene expression. The Cpx envelope stress response (ESR), consisting of the sensor histidine kinase CpxA and the response regulator CpxR, has previously been shown to be required for *C. rodentium* colonization and virulence *in vivo*. The purpose of this thesis was to investigate the observed attenuation by analyzing genes up and downregulated in the presence of the Cpx ESR to determine which, if any, were required for pathogenesis. Using transcriptomic and proteomic datasets from previous research as well as luminescent reporter assays to confirm Cpx-dependent upregulation, the genes *yebE*, *ygiB*, *bssR*, and *htpX* were chosen for further study. Here we showed that the virulence-inducing condition high-glucose Dulbecco's modified Eagle medium (HG-DMEM) strongly activated the Cpx ESR and further induced the expression of our four genes of interest. After gene deletion by allelic exchange, it was determined that only the $\Delta cpxRA$ mutant had reduced colonization and was attenuated *in vivo* in C57Bl/6J and C3H/HeJ mice, while the $\Delta yebE$, $\Delta ygiB$, $\Delta bssR$, and $\Delta htpX$ mutants remained virulent. To further

investigate the colonization defect seen in the $\Delta cpxRA$ mutant, we conducted growth experiments in buffered simulated colonic fluid (SCF). Interestingly, we were able to replicate the observed colonization abilities of our mutants seen *in vivo* as only the $\Delta cpxRA$ mutant experienced a growth defect in SCF. In addition, SCF highlighted an extreme sensitivity to sub-inhibitory levels of oxidative stress as well as various growth defects in our mutants. Niche differentiation and pathogen expansion via aerobic respiration is important for *C. rodentium* infection and our data suggests that the Cpx ESR is necessary in the colonic environment to mediate relevant stressors. Following these findings, we turned focus to investigate genes downregulated by the Cpx ESR. The downregulated genes *espV*, *mpc*, *kfcC*, *pspA* and *pspF*, identified from the transcriptomic and proteomic datasets, were confirmed to have reduced expression in the presence of the Cpx ESR in HG-DMEM. *espV* and *mpc* encode a non-LEE encoded T3SS and LEE regulator respectively, and the *kfc* operon encodes a putative fimbria. This data supports the notion that the Cpx ESR downregulates virulence factors and could implicate that controlled virulence gene expression contributes to cell viability *in vivo*. Finally, after bioinformatic analyses indicated an interaction between *yebE* and *pspACE*, all genes which undergo regulation impacted by the Cpx ESR, we generated various mutant strains and luminescent reporters to experimentally determine possible interactions. Here we found the presence of YebE influences the Phage Shock Protein (Psp) response, measured by *pspA-lux* expression, and the absence of an intact Psp response induces *yebE* expression. Overall, these data contribute to the overall knowledge surrounding *C. rodentium* colonization and virulence as well as proposes novel interactions between the inner membrane stress responses, CpxRA and Psp, as well as the inner membrane protein YebE.

Preface

Some of the content presented in this thesis has been submitted for publication to *Infection and Immunity* as: Gilliland AR, Gavino C, Gruenheid S, and Raivio TL (2021) “Simulated colonic fluid replicates the *in vivo* growth capabilities of *Citrobacter rodentium* mutants and highlights a critical role for the Cpx envelope stress response in mediating stressors encountered in the gastrointestinal tract” and is available as a preprint on bioRxiv, doi: <https://doi.org/10.1101/2021.12.13.472529>. I was responsible for collection and analysis of data in Figures 1, 2, 3, 5C-D, 6, 7, and 8 as well as manuscript composition. Gavino C collected and analyzed the mouse trial data presented in Figures 4 and 5A-B. Gruenheid S supervised mouse trials and provided funding for mouse trials. Raivio TL was the supervisory author and contributed with the formation of concepts, manuscript composition, and funding. All authors provided manuscript edits prior to submission.

The mouse trials conducted in Section 3.1.3 were completed in Dr. Samantha Gruenheid’s Lab by Christina Gavino under conditions specified by the Canadian Council on Animal Care and were approved by the McGill University Animal Care Committee.

The luminescence assays presented in Section 3.3 (Figures 3.3.2 to 3.3.5) were completed with assistance by Devanshi Pandit as a part of a BIOL 298 Undergraduate Research Project.

Acknowledgments

First and foremost, I would like to thank my supervisor and mentor Dr. Tracy Raivio for her unwavering support, uplifting demeanor, and thoughtful guidance throughout my degree. I am thankful for her mentorship and enthusiasm even through the challenging times faced in 2020 and 2021.

I would also like to thank my committee member Dr. Samantha Gruenheid who provided thoughtful feedback during my committee meeting, and manuscript preparation as well as Dr. Casey Fowler for serving as an arm's length examiner for my thesis defense.

A special thanks to the past and present Raivio lab members including graduate students, undergraduates, and post-doctoral fellows. Kat, Val, Tim, and Justin: Not only did we support each other throughout our graduate studies and the wild times of a global pandemic but the friendships I gained from each one of you is something I will treasure forever. Kat and Val, I am so thankful for our seemingly endless conversations at wine nights and mutual love for candles and hand cream, love you girls!

Finally, I would like to thank my loving family who, despite not really understanding what I was studying, was always there when I needed a chat and has provided constant encouragement and support throughout my life. A special thank you to my grandma, a University of Alberta alumni, whose experienced life as a graduate student and is a source of inspiration for my own academic endeavors.

I could not have completed this milestone without the support from all those mentioned previously, and I am excited to see where the future takes me.

"I am among those who think science has great beauty."

– Marie Curie

Table of Contents

Chapter 1. General Introduction.....	1
1.1 <i>Citrobacter rodentium</i>	2
1.1.1 Attaching and effacing pathogens.....	2
1.1.2 Locus of Enterocyte Effacement.....	4
1.1.3 LEE regulation	5
1.2 Colonization of the gastrointestinal tract by <i>C. rodentium</i>	7
1.2.1 Environmental challenges.....	8
1.2.2 Colonization resistance and the microbiome	12
1.3 The gram-negative bacterial cell envelope	15
1.3.1 Envelope structure	15
1.3.2 Stress responses	17
1.3.3 Two-component systems in <i>C. rodentium</i>	19
1.4 The Cpx envelope stress response	21
1.4.1 Inducing cues	22
1.4.2 Regulon members	22
1.4.3 Interactions with other stress responses.....	24
1.4.4 The Cpx response and <i>C. rodentium</i> pathogenesis	25
1.5 Thesis objectives and hypotheses	26

1.6 Figures.....	28
Chapter 2. Methods	31
2.1 Bacterial strains and growth conditions.....	32
2.2 Luminescence assays	32
2.2.1 Construction of <i>lux</i> -reporter plasmids	32
2.2.2 Luminescent assays in liquid media	33
2.2.3 Solid agar assays	34
2.3 Strain Construction	34
2.4 C57BL/6J and C3H/HeJ Mouse Infections.....	35
2.5 Growth curves.....	35
2.6 Tables.....	37
Chapter 3. Results.....	41
3.1 Individual Cpx-regulon members tested do not contribute to <i>C. rodentium</i> virulence however do impact bacterial fitness in simulated colonic fluid.....	42
3.1.1 Identification and confirmation of Cpx regulon members.....	42
3.1.2 The activity of the Cpx ESR is influenced by the absence of <i>htpX</i> and growth conditions.....	45
3.1.3 Cpx regulon members <i>yebE</i> , <i>ygiB</i> , <i>bssR</i> , and <i>htpX</i> are not individually required for colonization or virulence <i>in vivo</i>	46
3.1.4 Cpx-regulated genes impact <i>C. rodentium</i> fitness in simulated colonic fluid (SCF) ..	47

3.2 The Cpx response downregulates genes associated with virulence, large protein complexes, and the phage shock protein response.....	49
3.2.1 Simulated physiological conditions and the Cpx ESR impact the expression of the LEE master regulator <i>ler</i>	50
3.2.2 The Cpx ESR downregulates the genes <i>mpc</i> , <i>espV</i> , the <i>kfc</i> operon, and the Psp response genes, <i>pspA</i> and <i>pspF</i>	51
3.3 Evidence for an uncharacterized interaction between the Cpx and Psp envelope stress responses.....	53
3.3.1 The Cpx ESR and the Psp response can be differentially induced using alkaline or ethanol stress.....	54
3.3.2 The absence of YebE reduces the activity of the Psp response.....	55
3.3.3 PspF enhances the activity of the Psp response in <i>C. rodentium</i>	56
3.3.4 The Cpx ESR is not affected by the absence of PspF or PspA.....	57
3.3.5 The expression of <i>yebE</i> is increased in the absence of major Psp response components.....	57
3.4 Tables and Figures.....	59
Chapter 4. Discussion.....	79
4.1 Induction of the Cpx ESR over time is condition-specific.....	80
4.2 Elucidating the regulation of uncharacterized genes by the Cpx ESR.....	81
4.3 SCF is beneficial for determining colonization efficacy and susceptibilities of mutants to stressors.....	84

4.4 The presence of the Cpx ESR negatively impacts the expression of master LEE regulator, <i>ler</i>	87
4.5 Virulence factors are more stringently expressed in the presence of CpxRA	88
4.6 The Cpx ESR influences the activity of the Psp response	91
4.7 Interactions identified between Cpx-regulated YebE and the Psp response.....	95
4.8 Concluding remarks	97
References	99
Appendices.....	132
Appendix Table and Figures	133

List of Tables

Table 2.1. Strains and plasmids used in this study.

Table 2.2. Oligonucleotide primers used in this study.

Table 3.1.1. Mined RNA-Seq and SILAC data from Vogt *et al.* (210) and microarray data collected in Giannakopoulou *et al.* (232) for potential CpxRA upregulated genes.

Table 3.2.1. Mined RNA-Seq and SILAC data from Vogt *et al.* (210) and microarray data collected in Giannakopoulou *et al.* (232) for potential CpxRA downregulated genes.

Table S1. Average CPS/OD₆₀₀ of three biological replicates 1-hour post-resuspension in LB and high-glucose DMEM with MOPS for *cpxP*-, *yebE*-, *ygiB*-, *bssR*-, and *htpX-lux* reporter plasmids.

List of Figures

Figure 1.1. *Citrobacter rodentium* faces numerous challenges associated with transit through, and colonization of, the mouse gastrointestinal tract.

Figure 1.2. Model of the Cpx envelope stress response and the Psp response.

Figure 3.1.1. Confirmation of upregulated genes in the presence of CpxRA using lux-reporter assays in both LB and HG-DMEM.

Figure 3.1.2. Expression of *ygiB*- and *tolC-lux* over time indicates CpxRA-dependent regulation.

Figure 3.1.3. *yebE*, *ygiB*, and *bssR* exhibit expression profiles like that of *cpxP* over time in wild-type cells.

Figure 3.1.4. CpxRA is induced in the absence of *htpX*.

Figure 3.1.5. CpxRA activity is dependent on culturing conditions.

Figure 3.1.6. Genes of interest do not significantly contribute to *C. rodentium* colonization or virulence in C57Bl/6J mice.

Figure 3.1.7. Genes upregulated by the Cpx ESR do not impact *C. rodentium* colonization or virulence in C3H/HeJ mice.

Figure 3.1.8. Simulated colonic fluid (SCF) promotes *C. rodentium* growth whilst indicating fitness defects in $\Delta cpxRA$, $\Delta ygiB$, and $\Delta htpX$.

Figure 3.1.9. Simulated colonic fluid (SCF) highlights severe fitness defects in $\Delta cpxRA$ cells in response to sub-inhibitory levels of pH, oxidative, and copper stress.

Figure 3.1.10. $\Delta yebE$, $\Delta ygiB$ and $\Delta htpX$ cells experience fitness defects in simulated colonic fluid (SCF) with oxidative stress.

Figure 3.2.1. *C. rodentium* $\Delta cpxRA$ mutants show altered expression of LEE regulator, *ler*, in virulence-inducing conditions.

Figure 3.2.2. Expression of the LEE master regulator, *ler*, over time indicates reduced expression in the presence of CpxRA.

Figure 3.2.3. Virulence genes and the Psp response components, *pspA* and *pspF*, have reduced expression in the presence of CpxRA.

Figure 3.3.1. The activity of the Cpx response is strongly induced by alkaline pH while the Psp response is strongly induced by ethanol stress over time.

Figure 3.3.2. $\Delta yebE$ mutants exhibit lower levels of Psp activity relative to wild-type cells.

Figure 3.3.3. The Psp response regulator PspF is required for full and proper expression of *pspA* over time.

Figure 3.3.4. The activity of the Cpx response does not depend on the presence of an intact Psp response.

Figure 3.3.5. The absence of the Psp response members, *pspA* and *pspF*, moderately increases the expression of *yebE*.

Figure S1. Luminescence on solid LB agar for reporters of confirmed Cpx regulon members and *cpxP-lux* in Cpx-regulated gene mutants.

Figure S2. Growth curve of luminescent reporter strains grown and measured over 12 hours.

List of Symbols, Nomenclature, and Abbreviations

Symbols

Δ : gene deletion

Abbreviations

A/E: attaching and effacing

ABC: ATP-binding cassette

AMR: antimicrobial resistance

ATP: adenosine triphosphate

BFP: bundle-forming pilus

Cam: chloramphenicol

CFUs: colony forming units

CPS: counts per second

DAP: diaminopimelic acid

DNA: deoxyribonucleic acid

EAF: enteropathogenic *Escherichia coli* adherence factor

EHEC: enterohemorrhagic *Escherichia coli*

EPEC: enteropathogenic *Escherichia coli*

ESR: envelope stress response

HG-DMEM: high-glucose Dulbecco's modified Eagle medium

H-NS: histone-like nucleoid structuring protein

IHF: integration host factor

Kan: kanamycin

LB: lysogeny broth

LEE: locus of enterocyte effacement

LG-DMEM: low-glucose Dulbecco's modified Eagle medium

LPS: lipopolysaccharide

MCS: multiple cloning site

MOPS: 3-morpholinopropane-1-sulfonic acid

OD: optical density

OD₆₀₀: optical density at 600nm

PBS: phosphate buffered saline

PCR: polymerase chain reaction

PMF: proton motive force

RNA: ribonucleic acid

ROS: reactive oxygen species

RT-qPCR: quantitative reverse transcriptase PCR

SCF: simulated colonic fluid

SILAC: stable isotope labeling by amino acids in cell culture

sRNA: small ribonucleic acid

T3SS: type III secretion system

T6SS: type VI secretion system

TCS: two-component system

Chapter 1. General Introduction

1.1 *Citrobacter rodentium*

Citrobacter rodentium is a Gram-negative attaching and effacing (A/E) pathogen of mice with the two most studied strains being ICC168 and DBS100 (1–4). It is a non-motile, facultative anaerobe and colonizes the cecum and colon of mice (2, 5–7). *C. rodentium* causes colonic crypt hyperplasia in mice which results in severe inflammation in the colon (2, 3, 6, 8–10). Colonic crypt hyperplasia is characterized by elongation of the intestinal crypts, disruption of the microvilli, and inflammation which results in dehydration and diarrhea (6, 11). Infections are lethal for some mouse strains like C3H/HeJ, while C57Bl/6 mice experience self-limiting infections (12, 13). C3H/HeJ mice have a mutation in *tlr4* making them unable to respond to bacterial lipopolysaccharide (LPS) (13, 14). However, the specific sensitivity to *C. rodentium* infection by C3H/HeJ was found to be independent of LPS responsiveness and instead was due to the locus identified as *Cri1* (*Citrobacter rodentium* infection 1) (13, 14). The susceptible *Cri1* allele is conserved in the mouse strains C3H/HeJ, C3H/HeOuJ, FVB, and AKR/J, which all succumb to *C. rodentium* infection, and it was determined mouse susceptibility from the *Cri1* locus was not due to altered *C. rodentium* colonization (14–16). Instead, the *Cri1* locus contains the gene *Rspo2*, encoding the secreted protein R-spondin 2, which is strongly upregulated in the subepithelial stromal cells of the colonic mucosa in susceptible mouse strains upon infection with *C. rodentium* and causes the activation of Wnt signalling resulting in inhibition of colonic epithelial differentiation and disrupted intestinal homeostasis (16).

1.1.1 Attaching and effacing pathogens

C. rodentium is used as a model for the human A/E pathogens, enterohemorrhagic and enteropathogenic *Escherichia coli* (EHEC and EPEC, respectively), which are essentially non-

pathogenic in mice (3, 11, 17). A/E pathogens utilize a type III secretion system (T3SS) to adhere to the intestinal epithelial cells allowing them to inject effector proteins which disrupt host cell function (3, 17, 18). *C. rodentium* is suspected to have undergone convergent evolution with human pathogenic *E. coli* with 67% of its genes also found in EPEC and EHEC (10, 19). Given this, there are a few differences between EHEC, EPEC, and *C. rodentium* which are important to note in the context of their epidemiology, pathology, and *in vivo* localization. EHEC O157:H7 is a Shiga toxin encoding gastrointestinal pathogen and is a large contributor of food-borne illness in industrialized nations with bovine reservoirs capable of shedding the pathogen which contributes to its high transmissibility and outbreaks (10, 20–23). On the other hand, EPEC, like *C. rodentium*, does not encode a Shiga toxin and is a common water-borne pathogen causing disease in children throughout the developing world (10, 22–24). EPEC also encodes a Type IV fimbria known as the bundle-forming pilus (BFP) on the EPEC adherence factor (EAF) plasmid which is integral in initial adherence to epithelial cells (25–29). While *C. rodentium* doesn't have an EAF encoded BFP, its genome contains 19 putative fimbrial operons including *kfc*, *gcf*, and a putative Type IV pili in the *cfc* operon (19, 30, 31). The *cfc* operon has significant homology to some of the genes that encode the BFP of EPEC and the components CfcC and CfcI are required for colonization *in vivo* (29, 30). Other differences are exemplified by *C. rodentium* having 29 T3SS effector proteins, including the 22 found in EPEC E2348/69 as well as *C. rodentium* harbors two Type VI secretion systems (T6SS), whereas EHEC only contains one T6SS which is genetically distinct (19). The *C. rodentium* T6SS genes are clustered into CTS1 and CTS2 where CTS1 conferred a growth advantage *in vivo* during an interspecies competition assay while CTS2 is predicted to be non-functional (19, 32).

In humans, both EPEC and EHEC colonize the gastrointestinal mucosa with EPEC favoring the small intestine and EHEC localized initially to Peyer's patches in the small intestine followed by colonization in the large bowel (23, 33–36). Similarly to EHEC, *C. rodentium* has been shown to initially colonize a lymphoid structure in the cecum known as the cecal patch followed by colonization of the colon and rectum (9, 10, 37, 38). While differences in epidemiology and pathology exist between EHEC, EPEC, and *C. rodentium*, due to limitations of studying EPEC/EHEC in animal models, studying the model organism *C. rodentium* in the context of mechanisms required for pathogenesis in a mouse model of infection is an important area for developing insights into A/E pathogen colonization and virulence.

1.1.2 Locus of Enterocyte Effacement

The A/E pathogens EPEC, EHEC, and *C. rodentium* all harbor the Locus of Enterocyte Effacement (LEE) pathogenicity island that contains five operons (LEE1-5) encoding key proteins which are responsible for the hallmark lesions formed upon intimate attachment to intestinal epithelial cells (39, 40). The LEE in *C. rodentium* is organized with LEE1, LEE3, LEE5 and LEE4 on the positive strand and LEE2 and R1/R2 on the negative strand (39). LEE1 encodes the master regulator *ler* along with structural proteins for the T3SS. LEE3 is a polycistronic operon which encodes the regulator *mpc* and important structural proteins like the translocase, EscV, and ATPase, EscN (41–45). LEE5/Tir contains the genes *tir* and *eae* which encode the proteins Tir and intimin, respectively, and are required for the intimate attachment to epithelial cells (4, 39). LEE4 largely contains *esp* genes which encode for effector proteins secreted by the T3SS while LEE2 contains genes for structural proteins, chaperones, and secreted proteins (39).

In terms of homology, the LEE of *C. rodentium* contains significant differences from the LEE found in EHEC and EPEC. In particular, the *C. rodentium* LEE is approximately 36kb whereas the EHEC/EPEC LEE is closer to 34 kb (39). The *C. rodentium* LEE contains two intergenic regions which differ from that of EHEC/EPEC and its R1/R2 operon is located on the opposite side of the LEE: downstream and in the opposite direction of LEE4, as opposed to EHEC/EPEC R1/R2 which is upstream and in the opposite direction of LEE1 (39). In addition, within the LEE of *C. rodentium* the homology of highly conserved proteins relative to EHEC/EPEC, which have 100% identity and similarity, is typically less than 95% (*orf2*, *orf3*, *escS*, *cesD*, *escJ*, *orf12/mpc*, *orf15*, *escF*) (39). Lastly, the *C. rodentium* LEE is located in between the insertion sequence element, IS679, also found in the EAF plasmid, with the region upstream of IS679 homologous to plasmids in *Salmonella* and EHEC, and an ABC transporter operon (39). In EPEC and EHEC, the LEE is located within the *selC* tRNA gene (39). Despite these apparent differences in the LEE organization, gene homology, and location in the chromosome between A/E pathogens, the virulence mechanism of these organisms are highly similar indicating conservation for this mode of pathogenesis (39).

1.1.3 LEE regulation

There are numerous LEE-encoded regulators that influence LEE expression. The master regulator, Ler, is a transcriptional activator encoded in the LEE1 operon and activates the expression of LEE1-5 (46). Ler is a histone-like nucleoid structuring protein (H-NS) paralog which is thought to disrupt H-NS binding to the LEE thus enabling the transcription of LEE1-5 (46–49). Ler also activates expression of the transcriptional activator, GrlA, and repressor, GrlR, encoded in the Ler-regulated *grlRA* operon (R1/R2) that act upon LEE1 thus forming a

regulatory loop (10, 39, 50, 51). GrlA contains a helix-turn-helix DNA binding motif and is required for the activation of *ler* likely by direct interaction with a *cis*-acting element upstream of LEE1 while GrlR represses GrlA activity through the formation of GrlR-GrlA heterodimers utilizing a surface-exposed Glu-Asp-Glu-Asp motif on the GrlR β -barrel (51, 52). There is also another, less characterized LEE-encoded regulator known as Mpc/CesL/*10036/orf12* which is the first gene in the polycistronic LEE3 operon (41, 44, 53). The presence of Mpc is essential for the expression of translocator proteins located in LEE3 and prevents premature secretion of effector proteins in conjunction with gatekeepers SepL/SepD, while overexpression of Mpc suppresses the LEE through interactions with Ler, suggesting that Mpc is important for the correct timing of the LEE-encoded T3SS assembly and activity (18, 41, 44, 53, 54).

In addition to LEE-encoded regulators, there are numerous other direct and indirect regulators of the LEE studied in EHEC, EPEC, and *C. rodentium* which activate or inhibit its expression based on growth, cellular need, and sensed environmental stressors (50, 55, 56). In general, the LEE is largely regulated by nucleoid associated proteins (NAPs) which are highly conserved across Eukarya, Bacteria, and Archeae (56). *ler* is transcriptionally activated by the integration host factor (IHF) and the factor for inversion stimulation (FIS), as well as repressed by histone-like nucleoid structuring proteins H-NS and HhA (49, 56–61). It has been demonstrated in EHEC and EPEC that Ler alleviates repression by H-NS allowing for the transcription of the LEE operons and other virulence factors (49, 62, 63).

Environmental factors also play a large part in the correct regulation of the LEE. While limited studies have been conducted on *C. rodentium* LEE regulation in response to various environmental conditions, the literature is much more expansive for EHEC and EPEC (55, 56). In EHEC, numerous environmental signals have been implicated in the regulation of the LEE

such as quorum-sensing molecules, glycolytic and gluconeogenic carbon sources, ethanolamine, fucose, butyrate, and biotin (reviewed by 56). In EPEC, growth phase, growth conditions, nutrient deprivation, and envelope stress responses are all associated with the altered regulation of the LEE (55). In *C. rodentium*, H-NS represses the σ^{70} promoter of *grlA* while RegA, an AraC-like regulatory protein, activates it in the presence of bicarbonate ions (50, 61, 64, 65). In addition, the leucine-responsive regulatory protein, Lrp, also directly represses transcription of *ler* which subsequently impacts the expression of other LEE genes, while the stationary phase sigma factor RpoS has been implicated in the positive regulation of the LEE (66, 67). ExuR, a sugar acid metabolism transcription factor, was shown to be required for the expression of Ler in EHEC with a putative binding site located in the regulatory region upstream of the P1 promoter of *ler* in EHEC (68). Reduced expression of LEE-encoded genes was also demonstrated in a *C. rodentium* Δ *exuR* mutant relative to wild-type cells suggesting this regulatory mechanism is conserved (68). The complex and multi-faceted regulation of the LEE suggests that A/E pathogenesis relies on the ability of cells to adequately sense the environment and correctly regulate the expression of virulence mechanisms to cause disease.

1.2 Colonization of the gastrointestinal tract by *C. rodentium*

As thoroughly reviewed by Collins *et al.* (10), *C. rodentium* colonization begins upon entrance into the gastrointestinal tract, where the bacteria initially colonize the caecum, followed by the colon and rectum (9, 37, 38). Like other A/E pathogens, there are three general phases of infection: initial adherence, T3SS-dependent translocation of effectors, and intimate attachment (10). The current model for *C. rodentium* initial attachment is proposed to be through the use of fimbria, pili or adhesins, in a similar manner to that of EPEC which utilizes its BFP to adhere to

human cells, and while the exact mechanism has yet to be characterized, speculations have been attributed to the Type IV Cfc pilus, the Kfc fimbria, and the adhesin AdcA of *C. rodentium* (10, 28, 30, 64). Following attachment, A/E pathogens utilize the LEE-encoded T3SS to form a pore in the host cells membrane and inject the protein Tir followed by both LEE and non-LEE encoded effector proteins (10, 69). Tir inserts into the host cells membrane via a hairpin-loop structure and is required for the formation of pedestals via actin reorganization, colonization, and colonic hyperplasia (10, 70). Following translocation of Tir, the protein intimin, encoded by the *eae* gene, is localized to the bacterial membrane, and binds to Tir thus forming a stronger attachment to the intestinal cell (9, 10). This attachment promotes actin reorganization via translocated effector proteins which results in a pedestal being formed underneath the bacterial cell. The effector proteins cause cytoskeleton rearrangements that result in pedestal formation and microvilli effacement as well as impact numerous signaling pathways involved in cell health, integrity, and immune response (9, 10). Following intimate attachment, *C. rodentium* clonally expands to form microcolonies known as A/E lesions (71). The initial formation of these lesions via adherence of luminal planktonic bacteria is limited to the first 18 hours of infection and largely determines the severity of infection (71).

1.2.1 Environmental challenges

The gastrointestinal tract provides numerous physical challenges to colonization that *C. rodentium* must tolerate (see Figure 1.1). One of the most notable is the widely varying pH throughout the gut. The mouse stomach has a pH of approximately 3-3.5 which has been reported to increase to anywhere from 5-7 in the distal colon and feces (72–74). Strong acids and weak acids have differing effects on bacterial cells. In *E. coli*, the inner membrane is a barrier

which prevents the uptake of protons from strong acids with a pH of 5, which, when coupled with the buffering capacity of the cytoplasm, allows maintenance of a physiological cytoplasmic pH (75). In the stomach, weak organic acids are more easily able to pass through the inner membrane and overcome the buffering capacities of the cytoplasm which results in acid shock and can disrupt proton motive force (PMF) which is important for cellular energetics (75). The gastric acid present in the stomach has been shown previously to reduce the survivability of enteric pathogens and limit their ability to cause infection (76, 77).

Acid-tolerance by EPEC and EHEC have been well-characterized over the years. *E. coli* has four currently identified mechanisms which are used to tolerate acid stress at levels below pH 3: the oxidative or glucose-repressed system, as well as the fermentative systems including glutamate- (GadABC), arginine- (AdiAC), and lysine-dependent acid resistance (CadAB) (75, 78, 79). The oxidative acid response system was the first acid response system identified, does not require an external amino acid to mediate acidic stress and is thought to be modulated by the availability of key internal and external intermediates involved in cell metabolism (80). The amino acid-dependent mechanisms, which are more concisely defined, consist of a decarboxylase, which consumes a proton, and an antiporter, that exports a net positive charge out of the cell (75). The oxidative system is thought to utilize the decarboxylase from the glutamate-dependent acid resistance mechanism to mediate acid stress in stationary-phase cells in the absence of glucose (80). Utilizing simulated gastric fluid, both EPEC and EHEC have shown enhanced resistance and recovery to stress caused by acid (81, 82). The alternative sigma factor σ^s , encoded by *rpoS*, which responds to conditions like nutrient deprivation, unfavourable conditions (pH, osmolarity, temperature), and stationary phase, is required for the activation of the oxidative acid response system, regulates the glutamate-dependent acid response system, and

is associated with the survival of various EHEC and EPEC strains in response to acid stress *in vitro* and *in vivo* (75, 79, 83–86). Regulators which influence the most-studied glutamate-dependent acid resistance system (GadABC) include the EvgSA and PhoPQ two-component systems (TCS), the TrmE (MnmE) and ArcAB circuit, the GadXW AraC-like regulators, and sRNA GadY, which are largely condition-, pH-, and growth phase-dependent and contribute to the tightly controlled induction of *gadA*, *gadBC*, and *gadE* (75). A relatively new finding in the field of *E. coli* response to, and mediation of, acid stress involves the TCS CpxRA which upregulates the fatty acid biosynthesis genes *fabAB* resulting in altered membrane permeability and maintenance of pH homeostasis (87).

Like *E. coli*, *C. rodentium* employs the alternative sigma factor RpoS in response to stress which contains 92% sequence identity with EPEC and EHEC strains (66). While the role of RpoS in *C. rodentium* tolerance to acid has not been tested directly, its importance in resistance to oxidative stress and tolerance to heat has been demonstrated (66). Different from other enteric pathogens, *C. rodentium* has lost the genes for glutamate-dependent acid-resistance which are found in *E. coli* and it has been shown that the addition of exogenous glutamate, proline, and lysine does not improve *C. rodentium* survival in acid shock media (78, 88). Cheng *et al.* (78) postulate this is because *C. rodentium*, a murine pathogen, is only required to withstand a stomach pH of 3 as opposed to *E. coli* which must tolerate the pH of a human stomach that is closer to 2.

Bile is secreted by the liver where it disperses either to the small intestine for digestive purposes or to the gall bladder for storage (89, 90). Bile is considered an antimicrobial, primarily because it can disrupt the phospholipid bilayer and membrane proteins of bacteria (89, 91). Gram-negative enteric pathogens have resistance mechanisms in order to adapt to the toxic

effects of bile including the presence of LPS and use of efflux pumps (89, 92, 93). While mechanisms for bile resistance have yet to be characterized in *C. rodentium*, it has been demonstrated to grow efficiently in bile although becomes sensitive to elevated bile concentrations which reduce its colonization ability and increase its clearance rate *in vivo* (93, 94).

Oxygen gradients are prevalent both longitudinally and latitudinally in the gastrointestinal tract. In relative terms, the colon is more anoxic than the stomach, while the lumen is more anoxic than the mucosal surface (95, 96). Oxygenation of the gastrointestinal tract can also be impacted temporally as blood flow increases during active digestion which in turn raises oxygen levels while inflammation can reduce oxygen in the mucosa (96). An obvious stressor associated with the presence of oxygen is the development of reactive oxygen species (ROS) which are deleterious to cell function by numerous mechanisms including from direct killing by oxidative damage (97). On the other hand, the difference in oxygen levels within the gut contributes to the spatial organization of microbiome members where obligate anaerobes have higher prevalence in the colonic lumen whereas facultative anaerobes, like pathogens, are able to thrive closer to the epithelial cell surface (98–100). *C. rodentium* utilizes this spatial heterogeneity to its advantage during colonization. It has been demonstrated that *C. rodentium* can disrupt mitochondrial oxidative phosphorylation resulting in a switch to glycolysis which in turn increases the oxygen concentration in the colonic mucosa resulting in rapid luminal pathogen expansion via aerobic respiration (101–103). This interruption to hypoxia at the intestinal epithelial has been proposed as a mechanism for niche differentiation and overcoming competitors in the colonic mucosa (101, 102).

Lastly, a prominent barrier in the gastrointestinal tract is the intestinal mucus that is

produced by goblet cells in the intestinal epithelial layer (104). In the colon, goblet cells are found along the crypts of the colon and secrete enough mucus, mostly consisting of the glycoprotein mucin 2 (Muc2), to form two layers above the epithelial cells (104). The top layer, closest to the lumen, is less-defined relative to the lower layer and contains mucus, bacteria, and dietary material (104). The bottom layer is maintained at a relatively constant thickness and is virtually free of bacteria. Relative to the small intestine, the colon secretes less antimicrobial peptides because the presence of bacteria is important for the generation of metabolites like short chain fatty acids and vitamins, therefore the antimicrobial peptides it does secrete are more geared towards inhibiting bacteria from crossing the mucosal barrier via size-exclusion and inhibiting motility (104). *C. rodentium* utilizes mucinases to breakdown the mucus layer in order to reach the intestinal epithelial cells (105). In addition, research has shown that breakdown of the mucus barrier by dysbiosis of the microbiome or diseases like inflammatory bowel disease or hyperglycemia can increase the susceptibility of hosts to gastrointestinal pathogens (104). The success of *C. rodentium* colonization and the subsequent colitis that is induced has been strongly associated with the breakdown or disruption of the mucosal barrier either from antibiotic treatment, improper diet, or genetic defects in immune regulatory genes (104, 106–111).

1.2.2 Colonization resistance and the microbiome

C. rodentium colonization is not only impacted by the physical parameters of the gastrointestinal tract but also the microbiome members present (see Figure 1.1). Colonization resistance occurs when the native microbiome prevents incoming bacteria, like pathogens, from colonizing the gastrointestinal tract by limiting the availability of space and nutrients, and producing deterrents like bacteriocins (112–115). As previously mentioned, *C. rodentium*

oxygenates the lumen via aerobic respiration to promote pathogen expansion and perhaps overcome microbiome competitors that are more sensitive to oxygen (101, 102). However, prior to the development of colonic crypt hyperplasia and aerobic respiration, it has been demonstrated that *C. rodentium* utilizes host derived H₂O₂ in order to facilitate anaerobic respiration which generates a specific niche for it to occupy in the early stages of colonizing the epithelial surface (116). Obligate anaerobes are typically sensitive to H₂O₂ which suggests this is a mechanism *C. rodentium* uses to subvert colonization resistance (116).

As another strategy to overcome colonization resistance, *C. rodentium* is able to use numerous carbon sources demonstrated *in vivo* and *in vitro*, like galacturonic acid, monosaccharides like fructose, citric acid cycle intermediates including succinate, fumarate, and malate, as well as mono- and polyunsaturated fats (68, 111, 117–120). In addition, it has been demonstrated that *C. rodentium* upregulates the expression of amino acid biosynthesis enzymes which are required when there is a microbiota present *in vivo*, suggesting that it avoids competition for amino acids in the gut as a strategy to overcome colonization resistance (119, 121, 122).

The ability to stimulate, and duration of, *C. rodentium* colonization in the gastrointestinal tract has been shown to be highly dependent on the microbiome. Disruption to the microbiome from the exposure of the host to psychological stress or treatment with antibiotics improved *C. rodentium* colonization (106, 123). In addition, a western-style diet has been shown to influence the progression of *C. rodentium* colonization where it is initially lower but is able to persist in mice due to changes in microbiome composition (118). Interestingly, upon supplementation with a mouse commensal Proteobacteria, the western-diet fed mice were able to reduce the persistence of *C. rodentium* as were gnotobiotic mice that underwent fecal transplantation with feces derived

from normally fed mice (118). The concept of dysbiosis was further explored when mice were treated with either kanamycin, metronidazole, or vancomycin which differentially alter the microbiome (124). It was determined that only pre-treatment with kanamycin displaced *C. rodentium* colonization suggesting that specific commensal microbiome members are required for successful *C. rodentium* infection (124). This was supported by the finding that while *C. rodentium* could grow in germ-free mice to high titers, it was localized to the content of the cecum as opposed to cecal or colonic tissue (124). This data indicates that while dysbiosis aids in *C. rodentium* colonization, perhaps through the reduction of, or disruption to, colonization resistance, the presence of certain microbiome members is also required for proper *C. rodentium* infection. One member that has been shown to be beneficial for *C. rodentium* pathogenesis is *Bacteroides thetaiotaomicron* whose presence increases gut permeability through accelerated degradation of the mucus layer and possibly regulates virulence mechanisms through the production of signaling metabolites like succinate (125).

While some members of the microbiota are important for *C. rodentium* colonization, other members are deleterious. *C. rodentium* colonization, persistence or induced colitis was negatively impacted upon supplementation of the microbiome with phytonutrients causing increased levels of *Clostridia* species, probiotics, hyaluronan, Bifidobacteria produced surface exopolysaccharide, lactobacilli-enriched commensal culture, or dietary quercetin (108, 126–131). Upon investigation into why the composition of the microbiome impacts *C. rodentium* colonization, Osbelt *et al.* (117) found that the presence of butyrate-producing bacteria and higher levels of short chain fatty acids like butyrate, propionate, and acetate were associated with increased resistance to infection. It was also shown that exogenous supplementation of butyrate lowered the susceptibility of mice to *C. rodentium* infection once a certain concentration of

butyrate had been reached in the cecum (117). In addition, commensal microbiome members, including *E. coli*, have been shown to compete with *C. rodentium* for monosaccharides which results in reduced colonization and increased pathogen clearance (120). These studies highlight the reliance of *C. rodentium* colonization and persistence on the presence, composition, and symbiosis of the microbiome.

1.3 The gram-negative bacterial cell envelope

The gram-negative bacterial cell envelope, consisting of an outer membrane, periplasm, and inner membrane, is responsible for differentiating and protecting the cell from the surrounding environment. It plays an important role in the maintenance of cellular homeostasis, the import and export of nutrients and toxins, energizing the cell, and sensing external cues including physical stressors and chemical signals.

1.3.1 Envelope structure

The outer membrane is made up of an inner leaflet of phospholipids and an outer leaflet of glycolipids, mainly lipopolysaccharide (LPS) (132). LPS is an endotoxin and functions as a barrier to protect cells from hydrophobic molecules like detergents and antibiotics as well as stressors like harsh pH (132–134). LPS consists of lipid A (endotoxin), a conserved inner core oligosaccharide, a more variable outer core, and a highly variable region known as the O-antigen (134). Embedded in the outer membrane are mainly β -barrel proteins which are folded and inserted by the Bam (β -barrel assembly machine) complex and are largely associated with the transport of molecules across the outer membrane into or out of the periplasm or cytoplasm (132,

135). For example, TolC is an outer membrane β -barrel protein that, in conjunction with AcrAB, works as a transmembrane efflux pump to export toxic molecules, like antibiotics, from the cytoplasm out of the cell (132, 136, 137). The combination of LPS with the membrane-embedded β -barrel proteins allows for the selective permeability of the outer membrane (132). Lipoproteins are proteins connected to a lipid which can integrate into either the outer or inner membrane via the Sec or Tat translocon (see below) and the Lol (localization of lipoproteins) export pathway (132, 138). The most abundant protein in *E. coli* is the lipoprotein Lpp, which functions to connect the outer membrane to the peptidoglycan layer in the periplasm (132, 139).

The periplasm of Gram-negative bacteria contains a thin peptidoglycan layer made up of crosslinked repeating disaccharide units consisting of N-acetyl glucosamine and N-acetyl muramic acid which forms a “mesh” around the cell and helps with cell shape and rigidity (132). Within the periplasmic space that is not occupied by peptidoglycan, there are metabolites, solutes, and numerous proteins, both soluble and membrane associated. These proteins include degradative enzymes, periplasmic binding proteins, and chaperones and proteases, which aid in the folding and/or degradation of proteins as well as the facilitation of proteins moving from the inner to the outer membrane (132).

The last component of the gram-negative cell envelope is the inner membrane which consists of a phospholipid bilayer that is studded with numerous transmembrane and membrane-associated proteins. Proteins associated with the inner membrane have a wide range of functions like those involved in energetics through the generation of adenosine triphosphate (ATP) and proton motive force (PMF), quality control, envelope stress, motility, and secretion systems as well as numerous uncharacterized proteins. The proteins are either transported across the membrane via the Sec translocon or the twin-arginine translocation (Tat) pathway (132). The Sec

translocon consists of inner membrane proteins SecYEG, which form a channel in the inner membrane, cytoplasmic export factor SecA, chaperone SecB, and an auxiliary component, the insertase YidC (140). Proteins can either be transported co- or post-translationally as unfolded peptides in a chaperone-dependent or -independent manner (140). If proteins are destined for the inner membrane, they can either be inserted via SecYEG directly, or with the assistance of the auxiliary insertase YidC, or solely by YidC (140–142). On the other hand, if proteins are to be transported to the periplasm, they are typically met by a chaperone, such as SurA, DegP, Skp or DsbA, to assist with proper protein folding (132). The other form of translocation is via the Tat pathway which moves folded proteins across the membrane relying solely on PMF (143). The Tat pathway was recently demonstrated as important for *C. rodentium* resistance to bile and fitness *in vivo* (93).

1.3.2 Stress responses

Due to the integral role of the envelope in overall cell health, it contains numerous proteins which are involved in sensing perturbations to this compartment known as stress responses. A well-known and conserved mechanism for the altered regulation of genes is through the production of alternative sigma factors which can be generated in response to several different stressors. The *E. coli* general stress response consisting of the alternative sigma factor σ^S , encoded by *rpoS*, is required when cells experience stress in stationary phase (86, 144). It competes with σ^{70} , the housekeeping sigma factor, for RNA polymerase which results in the increased expression of genes that can enhance survival of the bacterial cell by making it generally more resistant to stress (144). The regulatory networks of σ^S are very complicated but it

is known to affect regulation at the transcription, translation, and protein and transcript degradation levels of σ^S -dependent genes as well as some already expressed by σ^{70} (86).

A specific stress response associated with the maintenance of the outer membrane and periplasm is the σ^E envelope stress response (ESR). Thoroughly reviewed by Hews *et al.* (145), σ^E is an extracytoplasmic sigma factor, encoded by *rpoE* and essential in *E. coli*, that senses misfolded or mistranslocated outer membrane proteins in the outer membrane and periplasmic space. Regulation of the σ^E response involves the inhibitors RseA and RseB, which are localized to the inner membrane and periplasm, respectively (146). RseA inhibits σ^E activity in the cytoplasm, which is amplified by RseB (147). Upon induction by misfolded proteins in the periplasm, the proteases DegS and then RseP, cleave RseA thus releasing RseA- σ^E into the cytoplasm upon which it is further cleaved by ClpXP after binding to SspB (145, 148–151). The σ^E ESR is induced by numerous stressors like heat or acid shock, oxidative stress, and carbon starvation, which can cause disruptions to LPS and outer membrane biogenesis by impacting protein folding and translocation within the periplasm (145, 152).

A much less understood ESR is the Phage Shock Protein (Psp) inner membrane stress response that consists of the *pspABCDE* operon, the response enhancer *pspF*, and auxiliary gene *pspG* (Figure 1.2) (153). In *E. coli*, the Psp response is required for bacterial survival in the presence of β -lactam antibiotics despite its small regulon suggesting it has a crucial role as an effector in reducing cell susceptibility under stress (154). The Psp response is thought to sense disruptions to the cell envelope and PMF as it is induced by numerous factors including mislocalization of outer membrane pore-forming proteins known as secretins, temperature extremes, ethanol, and compounds that disrupt PMF (153, 155, 156). Upon induction, the transmembrane proteins PspBC alter conformation which recruits the periplasmic protein PspA

to the inner membrane (155, 157, 158). Apart from this, PspB and PspC are also important in the prevention of cell death from mislocalized secretins (159, 160). Upon recruitment to the inner membrane, PspA releases its inhibition of the response enhancer, PspF, which binds upstream of the σ^{54} -driven promoter for the *pspABCDE* operon and *pspG* to promote their transcription (153, 155, 157, 161–164). *pspF* is an auto-regulated gene under the control of a σ^{70} promoter, therefore its transcription is maintained at a constant low level (163, 165, 166). PspA has also been shown to form large multimers which are thought to bind to the inner membrane to help stabilize it while under stress (167). When the stress to the inner membrane has been relieved, PspA resumes its inhibition of PspF by binding to it in the cytoplasm which reduces transcription of the *pspABCDE* operon and *pspG* gene to essentially turn off the Psp response (153, 155, 166). The Psp response has been mainly studied in non-pathogenic *E. coli* as well as *Yersinia enterocolitica*, a T3SS-utilizing pathogen like *C. rodentium*, which requires the Psp ESR for full virulence (168–170). The Psp response has not been studied in *C. rodentium* though its genome indicates the presence of *pspABCD* and *pspG*, therefore it is unclear how it contributes to *C. rodentium* fitness and virulence (19).

1.3.3 Two-component systems in *C. rodentium*

Beyond alternative sigma factors and the Psp response, bacterial cells have numerous two-component systems (TCS) which sense a variety of environmental stressors. TCS consist of a membrane-bound sensor histidine kinase that autophosphorylates and transfers a phosphoryl group to a cytoplasmic response regulator which goes on to bind to specific sites upstream of genes and function as a transcription factor (171, 172). The general steps for TCS activity are signal detection, kinase activation, phosphotransfer, and response generation (171, 172). Some

histidine kinases also act as a phosphatase to deactivate the response regulator in non-inducing conditions (171, 172). *C. rodentium* has 26 identified TCS with the RcsBC, ArcAB, and CpxRA ESRs strongly associated with pathogenesis *in vivo* where mutants lacking the respective response regulators were significantly attenuated relative to wild-type cells (173). The TCS RstAB, UhpAB, and ZraRS also had a significant impact on *C. rodentium* pathogenesis, though their effect on survival post-infection was less significant than the TCS previously mentioned (173).

The RcsBC ESR is a modified version of a TCS called a phosphorelay, as it uses the sensor histidine kinase RcsC and response regulator RcsB which are induced by a plethora of signals such as those from perturbations to peptidoglycan, cell surface sensing like LPS integrity, and disruptions to lipoprotein localization (174). However, the full Rcs phosphorelay requires the RcsF lipoprotein in the outer membrane to sense outer membrane perturbations and the inner membrane localized regulators IgaA and RcsD (174–176). IgaA interacts with and inhibits RcsD in the absence of induction, which is a phosphotransfer protein in the inner membrane that transfers the phosphoryl group from RcsC to RcsB, the response regulator (174, 177, 178). RcsA is an additional regulator that, in conjunction with RcsB, affects the transcription of a specific suite of genes like those involved in flagella or capsule synthesis (174, 179, 180). The absence of the Rcs phosphorelay was shown to reduce *C. rodentium* virulence *in vivo*, possibly due to altered capsule production, while colonization levels remained unaffected (173).

Another TCS that significantly alters *C. rodentium* virulence is the ArcAB ESR (173). In this TCS, ArcB, the histidine kinase, is induced in oxygen limiting conditions (anaerobic and microaerobic), where it phosphorylates the response regulator ArcA which then represses genes involved in the tricarboxylic acid (TCA) cycle and glyoxylate pathways to allow adaptation to

the redox environment (181, 182). Thomassin *et al.* (2017) showed that *C. rodentium* Δ *arcB* mutants could localize to the mucosal surface but had a significant adherence and colonization defect *in vitro* and *in vivo*, respectively, which was attributed to severely affected T3SS regulation and expression.

1.4 The Cpx envelope stress response

Originally identified in the 1990s, the Cpx (conjugative pilus expression) ESR is a TCS which consists of the sensor histidine kinase CpxA and the response regulator CpxR (Figure 1.2) (183–185). CpxA is in the inner membrane and consists of two transmembrane domains, a periplasmic loop, and a large cytosolic domain (186). Upon activation, CpxA autophosphorylates and transfers a phosphoryl group to CpxR, which then binds to a consensus sequence upstream of Cpx regulon members leading to altered gene expression (145, 184, 185, 187). The CpxR binding consensus sequence 5'-GTAAA(N)₄₋₈GTAAA-3' is conserved to varying degrees however nucleotide deviations from the consensus sequence do not predict the strength of the Cpx regulation of the downstream gene (188–190).

There are two auxiliary proteins associated with the regulation of the Cpx ESR in response to stress. CpxP is a periplasmic protein strongly regulated by the Cpx ESR which has structural homology to the periplasmic chaperone Spy (145, 190–193). When overexpressed or tethered to the inner membrane, it inhibits Cpx response activation, hypothetically through interactions with the periplasmic domain of CpxA (185, 194–197). It is currently hypothesized that under stressful conditions, CpxP is titrated away from CpxA thus relieving repression of the sensor kinase to allow for increased phosphorylation (198). The second auxiliary protein,

associated with Cpx response activation is the outer membrane lipoprotein NlpE (199).

Overexpression of NlpE induces the Cpx response and the lipoprotein has been shown to interact with CpxA when the cell is experiencing lipoprotein trafficking and oxidative folding defects (145, 199, 200).

1.4.1 Inducing cues

While the sensing mechanism used by CpxA is poorly defined, inducing cues of the Cpx ESR include alkaline pH, salt, defects in peptidoglycan synthesis, antimicrobial peptides, and misfolded or defective secretion of inner membrane and periplasmic proteins (145, 185, 189–191, 201–203). In addition, the level with which the Cpx ESR is activated is dependent on the type of signal and the growth phase of the cells as it has been shown to be more active during stationary phase (187, 204, 205). It is thought that these signals can induce the Cpx ESR in different ways as they can affect either the cytosol, like metabolism and growth cues, which activate CpxR independently of CpxA, be sensed by the transmembrane domains of CpxA, or are sensed by the outer membrane lipoprotein NlpE which then activates CpxA (202, 206). Some signals also rely entirely on CpxA to be sensed like alkaline pH, P pilus subunit overexpression, and envelope damage caused by EDTA (185, 206).

1.4.2 Regulon members

The Cpx ESR regulon was first characterized in *E. coli* strain MC4100 using both a Cpx null and overactivation mutants as well as luminescent reporters (190). Genes that were strongly induced by the Cpx ESR included members *cpxP*, *degP*, *dsbA*, *yebE*, *yccA*, *spy*, *ppiA* and *cpxRA*,

supporting previous findings (188, 190). The majority of these genes are involved in envelope biogenesis or maintenance specifically with regards to protein folding (190). Besides *cpxP*, *degP* and *dsbA* are two of the most studied regulon members of the Cpx ESR. DegP is a periplasmic protease inducible by the heat shock response, σ^E (207). It was first identified as a member of the Cpx regulon in 1995 by Danese *et al* (207). Later, it was shown that DegP could degrade CpxP in the periplasm and this proteolysis was increased in the presence of misfolded proteins (198, 208). In addition to interactions with CpxP, DegP has also been implicated in the regulation of the T3SS in EPEC and its presence is required for *C. rodentium* pathogenesis (209, 210).

Another prominent member of the Cpx regulon, DsbA, is a thiol disulfide oxidoreductase which along with DsbB aids in the formation of disulfide bonds in envelope proteins (188, 211). Like DegP, DsbA is required for T3SS elaboration in EPEC along with efficient expression as well as assembly of the bundle-forming pilus required by EPEC for colonization (209, 212, 213). The expression of two other Cpx regulon members, *yebE* and *yccA* are both copper-inducible in a CpxRA-dependent manner and encode predicted inner membrane proteins (189, 214, 215). The function of YebE is uncharacterized (216). YccA is a proposed substrate for the protease FtsH and it acts to inhibit or limit FtsH-mediated degradation of SecY when the cell's translocation machinery is jammed and could lead to cell death (215, 217). Finally, *spy* and *ppiA* both encode proteins, a chaperone and isomerase respectively, which are important for proper protein folding in the cell envelope (188). The identification and characterization of these Cpx regulon members supported the model that the Cpx response is induced by improper inner membrane and periplasmic protein folding and therefore upregulates the expression of genes which encode proteins that could alleviate those stressors (185, 187).

1.4.3 Interactions with other stress responses

As previously reviewed, the Cpx regulon also appears to include the regulators of other stress responses providing evidence for the Cpx ESR to act as a modulator of other stress responses (185, 187, 218). The Cpx ESR has been shown to downregulate the operon encoding the alternative sigma factor, σ^E , which senses disruptions to outer membrane biogenesis (185, 187). It also induces the expression of the inner membrane-localized protein MzrA, which activates the EnvZ/OmpR stress response through direct interaction between MzrA and EnvZ (185, 187, 219, 220). The EnvZ/OmpR stress response is induced via changes in osmolarity and regulates the porins OmpF and OmpC, whose expression is also influenced by the presence of CpxRA (187, 221, 222). The BaeSR TCS has a regulon which largely overlaps with the Cpx ESR and is most well characterized as a regulator for the *mdt-bae* operon, which encodes a multidrug transporter, and *tolC*, an outer membrane channel that works in conjunction with efflux pumps to remove toxic metabolites from the cell (187, 218, 223). In addition, BaeSR, the Rcs phosphorelay, induced by perturbations to the outer membrane and peptidoglycan, and the Cpx ESR have been shown to activate the expression of the chaperone *spy* (195, 218, 224). The Rcs phosphorelay and the Cpx ESR are also induced by some of the same extracytoplasmic stressors such as defects in lipoprotein trafficking and outer membrane biogenesis, the presence of certain antibiotics like polymyxin B, adhesion to surfaces and disruptions to peptidoglycan (201, 218, 225–227). A CpxRA-RcsBC interaction associated with virulence has also been suggested whereby the Cpx ESR may repress the Rcs phosphorelay which in turn affects the expression of the Ysc-Yop T3SS in *Yersinia pseudotuberculosis* (228). Lastly, as another inner membrane stress response, the Psp response has been associated with the Cpx ESR by induction under similar conditions and overlap in some regulon members (218, 229). Thus, it has been

proposed that the Cpx ESR may act as a modulator of other envelope stress responses thus incorporating numerous signals that generates a highly regulated response to encountered stressors (187, 218, 225).

1.4.4 The Cpx response and *C. rodentium* pathogenesis

Previous studies investigating the role of the Cpx ESR in other pathogens have suggested mechanisms by which the Cpx ESR may impact, both negatively and positively, colonization and virulence. Some of these mechanisms in EPEC include the negative regulation of *perC* resulting in reduced *ler* expression, efficient expression of the bundle-forming pilus involved in initial host cell attachment, and induction of genes required for maintaining envelope protein integrity and the regulation of virulence factors (55, 145, 209, 212, 230). Overall, it has been concluded that the Cpx ESR facilitates adaptation to envelope stressors because it downregulates virulence genes and large protein complexes while upregulating envelope and protein modifying factors, although the specific reasons for its impact on pathogenesis *in vivo* have not been definitively demonstrated in most cases (145).

In *C. rodentium*, it has been concluded that the Cpx ESR is activated *in vivo* based on the observation of increased expression levels of *cpxP* (231). Given that *C. rodentium* is an A/E pathogen relying on the LEE and the encoded T3SS for virulence, it is important to note that the absence of CpxRA does not impact the secretion of T3SS effector proteins *in vitro*, indicating its presence has a limited impact on the overall activity of the LEE (210, 231). Differing results have been observed in terms of cell health and the presence of CpxRA when grown in virulence-inducing conditions. Thomassin *et al.* (231) measured an extended lag phase for cells lacking

CpxRA while Vogt *et al.* (210) found no growth defect in similar conditions. The Cpx regulon in *C. rodentium* has been previously defined by microarray, RNA-seq, and SILAC proteomic analysis (210, 232). The data produced from these two studies was extensive and the impacts of numerous genes of interest on virulence have not been investigated. Giannakopoulou *et al.* (232) determined that the auxiliary proteins, CpxP and NlpE, were not required for colonization or virulence in *C. rodentium*. On the other hand, Vogt *et al.* (210) showed that the Cpx regulon members *degP* and *dsbA* were required for *C. rodentium* virulence in C3H/HeJ mice, however the Cpx regulation of these genes was not responsible for the virulence defect seen when *cpxRA* was absent. The Cpx regulon is extensive with the presence of CpxRA contributing to the differential expression of over 330 transcripts in *C. rodentium* (210, 232). The roles of some of the more strongly upregulated genes in both studies, such as *yebE*, *ygiB*, *bssR* and *htpX* which are investigated in this thesis, are not defined in *C. rodentium*.

1.5 Thesis objectives and hypotheses

1. **Investigate genes in the Cpx regulon to determine whether their Cpx-dependent expression could contribute to the attenuation of the $\Delta cpxRA$ mutant.** We hypothesized that the $\Delta cpxRA$ mutant was avirulent because members of the Cpx regulon were not being appropriately expressed thus negatively impacting cell health and colonization ability.
2. **Identify interactions between the Cpx ESR, the Psp response, and the uncharacterized inner membrane protein YebE utilizing knockout mutants and luminescent reporters.**

Overall, the research conducted for this thesis was carried out to further elucidate the ever-expanding role for the Cpx ESR in *C. rodentium* colonization and virulence as well as to characterize novel interactions between the Cpx response and its regulon members.

1.6 Figures

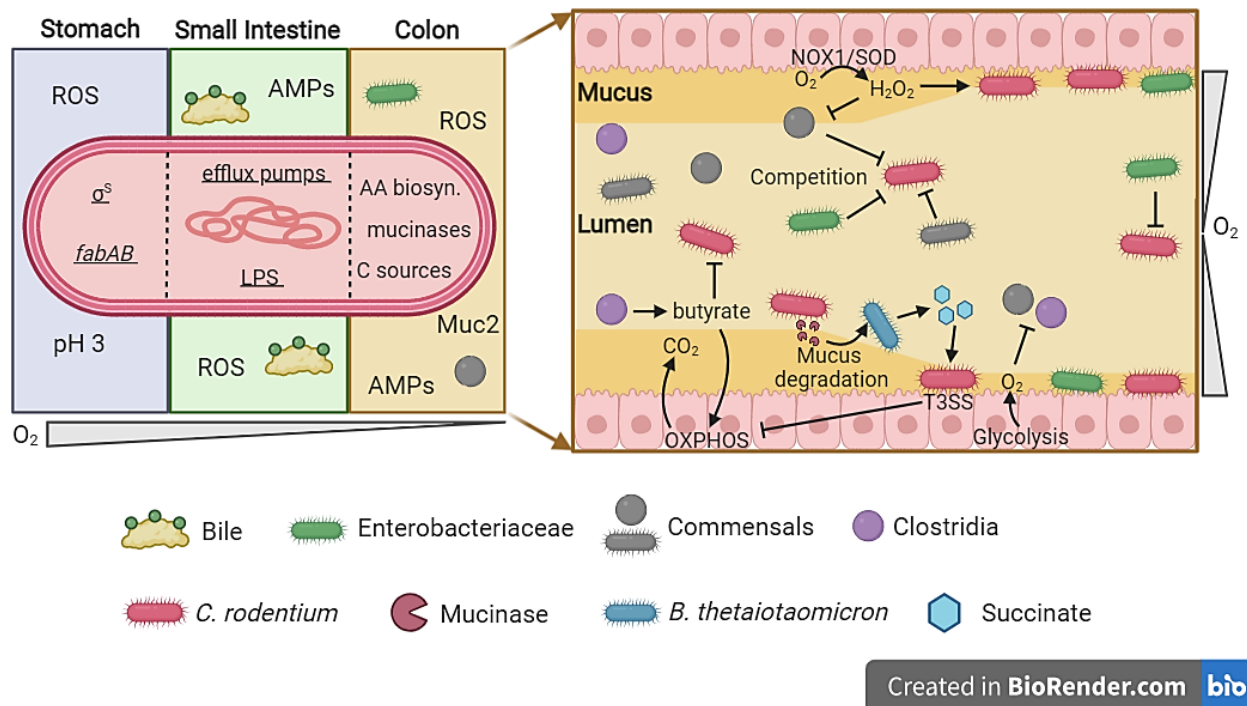


Figure 1.1. *Citrobacter rodentium* faces numerous challenges associated with transit through, and colonization of, the mouse gastrointestinal tract. During gastrointestinal transit, *C. rodentium* viability is challenged by the presence of reactive oxygen species (ROS) and antimicrobial peptides (AMPs) as well as various stressors unique to the stomach, small intestine, and colonic environments. In the stomach, the highly acidic environment from the presence of gastric juice activates the general stress alternative sigma factor σ^s , as well as the transcription of genes associated with fatty acid biosynthesis to maintain the cells pH homeostasis (evidence for underlined terms demonstrated in *Escherichia coli*). As *C. rodentium* passes through the small intestine, its lipopolysaccharide (LPS) layer as well as the expression of efflux pumps protects it from bile which disrupts bacterial membranes and membrane proteins. Once *C. rodentium* has reached the colon, it competes with host microbiome members for nutrients by activating genes involved in amino acid (AA) biosynthesis and using alternative carbon (C) sources. Its ability to infect is also negatively impacted by the butyrate produced by Clostridia species that contributes to the oxidative phosphorylation (OXPHOS) carried out by intestinal epithelial cells (IECs) mitochondria which promotes the presence of mucosal-associated obligate anaerobes through the maintenance of an anerobic environment. To successfully reach and adhere to the IECs, *C. rodentium* breaks down the mucus layer, largely consisting of the glycoprotein mucin 2 (Muc2) utilizing mucinases. The degradation of mucus causes the commensal member *Bacteroides thetaiotaomicron* to secrete succinate, which is a signal expression of the type III secretion system (T3SS) used by *C. rodentium*. Upon attachment

via the T3SS, *C. rodentium* utilizes H₂O₂, derived from IEC's NADPH oxidase 1 (NOX1) as well as superoxide dismutase (SOD), to anaerobically respire prior to the development of colonic crypt hyperplasia. Following secretion of effector proteins by the T3SS, the IEC's mitochondria switch from OXPHOS to glycolysis which oxygenates the colonic mucosal surface resulting in a change in microbiome composition and reduction of butyrate-producing obligate anaerobes which further reduces OXPHOS. Oxygenation allows *C. rodentium* and other facultative anaerobes like those in Enterobacteriaceae to rapidly expand in the colon. In a mild model of infection, Enterobacteriaceae also contributes to the clearance of avirulent luminal *C. rodentium*. Figure created with BioRender.com and adapted from (6, 233).

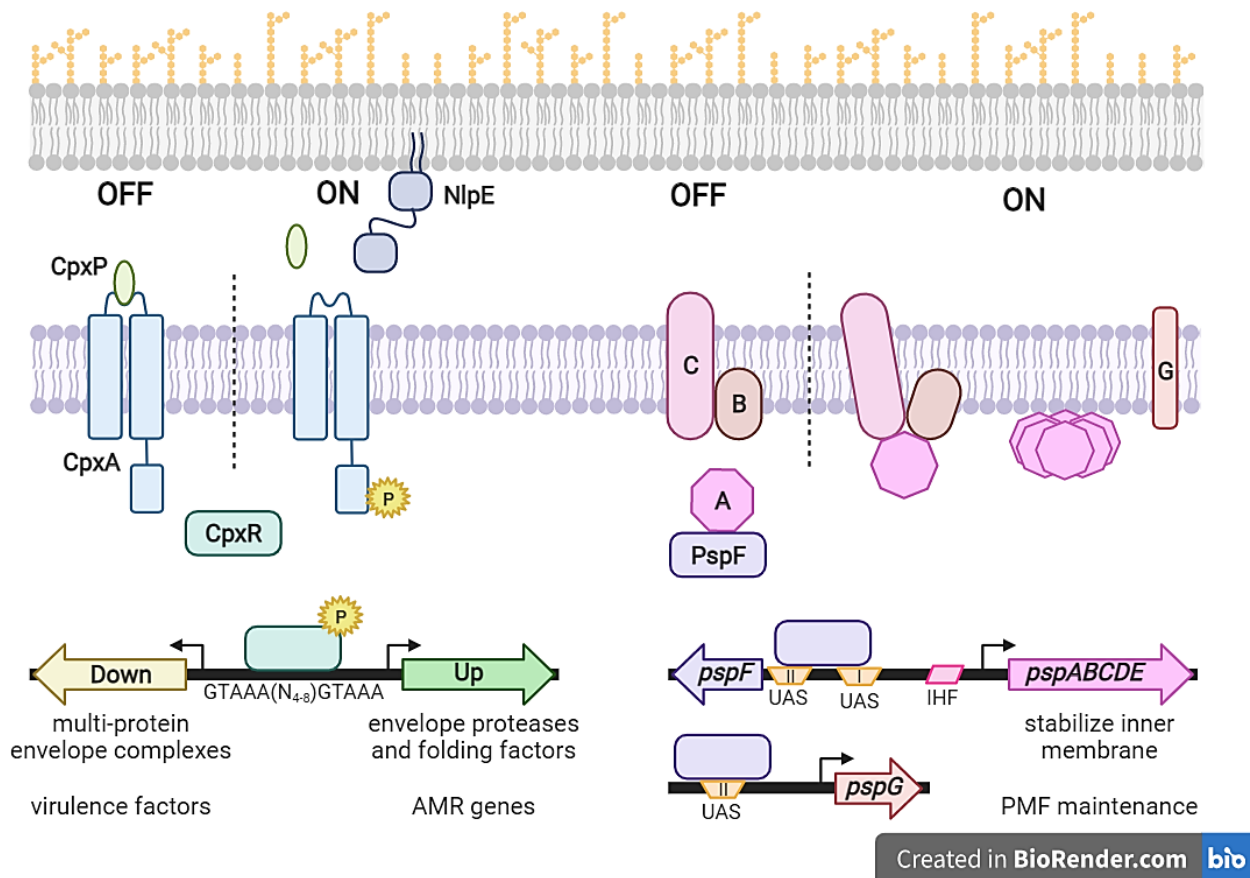


Figure 1.2. Model of the Cpx envelope stress response and the Psp response. The Cpx ESR is a two-component system consisting of the sensor histidine kinase CpxA and the response regulator CpxR, along with the auxiliary proteins CpxP (inhibitor) and NlpE (activator) which are localized to the periplasm and outer membrane, respectively. Upon induction by envelope stress, CpxA autophosphorylates and transfers a phosphoryl group to CpxR in the cytoplasm where it binds to the consensus sequence 5'-GTAAA(N₄₋₈)GTAAA-3' and influences the expression of downstream genes. Genes upregulated by the Cpx ESR include envelope proteases and folding factors as well as genes associated with antimicrobial resistance (AMR). Induction of the Cpx ESR also results in reduced expression of multi-protein envelope complexes and virulence factors. In *E. coli*, the Psp response is made up of proteins encoded in the *pspABCDE* operon, the upstream gene *pspF* as well as *pspG* which is located elsewhere on the chromosome. PspA is a negative regulator of the Psp response and effector capable of forming multimeric complexes that localize to the inner membrane. PspB and PspC are inner membrane proteins which alter conformation upon induction and bind PspA to relieve repression of PspF. PspF is an enhancer binding protein under negative autogenous regulation which binds upstream from the σ^{54} promoters of *pspABCDE* and *pspG*. PspF is required to fully activate the Psp response which aids in membrane stabilization and the maintenance of proton motive force. Figure created with BioRender.com and adapted from (145, 155, 234).

Chapter 2. Methods

2.1 Bacterial strains and growth conditions

Bacterial strains and plasmids used are listed in Table 2.1. Unless otherwise indicated, cells were grown in either lysogeny broth (LB; 10 g/L tryptone, 5 g/L yeast extract, and 5 g/L NaCl), high-glucose Dulbecco's Modified Eagle Medium with no phenol (Gibco™, cat. no. 31053028) (HG-DMEM), low-glucose Dulbecco's Modified Eagle Medium (Gibco™, cat. no. 11885084) (LG-DMEM), or simulated colonic fluid first developed by Beumer *et al.* (235), using ox bile in lieu of porcine bile (SCF; 6.25 g/L proteose-peptone, 2.6 g/L glucose, 0.88 g/L NaCl, 0.43 g/L KH₂PO₄, 1.7 g/L NaHCO₃, 2.7 g/L KHCO₃, and 4.0 g/L ox bile). Cultures were grown at 37°C with aeration at 225 rpm and LB agar plates were incubated at 37°C for 16-18 hours. For luminescence assays and growth curves, HG-DMEM, LG-DMEM and SCF were buffered with 0.1M MOPS to maintain physiological pH of 7.4 and 7.0, respectively, unless otherwise indicated. SCF was prepared fresh for each experiment and filter sterilized. When required, media was supplemented with; 30 ug/ml kanamycin, 100 ug/ml ampicillin, 25 ug/ml chloramphenicol, 0.3mM diaminopimelic acid, 5% sucrose (filter-sterilized).

2.2 Luminescence assays

2.2.1 Construction of *lux*-reporter plasmids

Luminescent reporters were constructed using the pNLP10 *lux*-reporter plasmid (190). Primers listed in Table 2.2 were designed to amplify ~500bp upstream and 50 bp downstream of the translation start site apart from *ygiB*, where the amplified promoter was a ~300 bp region. The restriction enzymes EcoRI and BamHI were incorporated into the forward and reverse primers, respectively (unless otherwise indicated). Promoter regions were amplified by PCR

using *Taq* polymerase (Invitrogen, USA), cloned into pNPL10 and transformed into OneShot TOP10 chemically competent cells (Invitrogen, USA). TOP10 colonies harboring the pNLP10 plasmid were confirmed for insert presence using colony PCR with primers flanking the pNLP10 multiple cloning site as well as with Sanger sequencing. Plasmids with the correct insert were mini-prepped and transformed into electrocompetent *C. rodentium* DBS100 wild-type or mutant cells.

2.2.2 Luminescent assays in liquid media

For spin down induction assays, cells were grown overnight in LB containing kanamycin in biological triplicate, then subcultured 1:100 and grown to an OD of 0.4-0.6. After approximately 2 hours growth, 1 ml of culture was centrifuged, the supernatant was removed, and the cells were resuspended in 1 ml pre-warmed induction media containing kanamycin (T = 0). 200 ul of induced cells were transferred into a black walled clear bottom 96-well plate and incubated at 37°C shaking, unless otherwise stated. For growth curve luminescence assays, cells were grown overnight in LB containing kanamycin in biological triplicate, then subcultured 1:100 directly into a black walled clear bottom 96-well plate containing LB with kanamycin and incubated at 37°C shaking. For all assays, empty wells were left between strains to prevent contaminating luminescence from adjacent wells. OD₆₀₀ and luminescence measurements were taken over time using the Victor X3 2030 multilabel plate reader (Perkin Elmer). *lux* activity was measured in counts per second (CPS) and normalized using the measured OD₆₀₀ of the same well to accommodate for differences in cell number between cultures. Luminescence assays were repeated at least twice in biological triplicate.

2.2.3 Solid agar assays

Overnight cultures of strains harboring luminescent reporters in LB with kanamycin were standardized to an OD₆₀₀ of 1.0 and serially diluted to 10⁻⁶ in 1X Phosphate Buffered Saline (PBS). 10 ul of each dilution was spotted onto LB supplemented with kanamycin and grown for 18 hours at 37°C. Luminescence was measured using a ChemiDoc MP imaging system (Bio-Rad). Assays were repeated twice with one representative plate shown.

2.3 Strain Construction

All deletion mutants were generated using allelic exchange in the methods described by Vogt *et al.* (210). In summary, in-frame deletion constructs were generated using overlap extension PCR with Phusion *Taq* polymerase (Invitrogen, USA) and the primers listed in Table 2.2. Amplicons were then digested using the restriction enzymes XbaI and SphI/PaeI, ligated into pUC18, and transformed into OneShot TOP10 chemically competent cells (Invitrogen, USA). Plasmids were mini-prepped and sent for Sanger sequencing for amplicon confirmation. Once confirmed, the deletion construct was digested from pUC18 and ligated into the suicide vector, pRE112, where it was transformed by electroporation into MFDpir cells (236, 237). MFDpir cells containing the deletion construct underwent conjugation with *C. rodentium* DBS100 and single-crossover colonies were selected with chloramphenicol and confirmed by PCR using primers designed to flank the deletion site by ~50 bp on each side (Table 2.2). Loss of pRE112 was determined by plating on LB -NaCl with 5% sucrose (filter-sterilized) and grown on

benchtop for 2 days. Colonies that were sucrose-resistant and chloramphenicol-sensitive were screened by PCR using *Taq* polymerase (Invitrogen, USA) to confirm intended deletion.

2.4 C57BL/6J and C3H/HeJ Mouse Infections

All animal experiments were performed under conditions specified by the Canadian Council on Animal Care and were approved by the McGill University Animal Care Committee. C57BL/6J and C3H/HeJ mice were purchased from the Jackson Laboratory (Bar Harbor, ME, USA). Five-week-old female mice (n = 5 per group) were infected by oral gavage with 0.1 ml of LB medium containing $2-3 \times 10^8$ colony-forming units (CFU) of bacteria. The infectious dose was verified by plating serial dilutions of the inoculum onto MacConkey agar (Difco). For survival analysis of C3H/HeJ mice, the mice were monitored daily and were killed if they met any of the following clinical endpoints: 20% body weight loss, hunching and shaking, inactivity, or body condition score of <2 (238). To monitor bacterial colonization, fecal pellets or the terminal centimeter of the colon were homogenized in PBS, serially diluted, and plated on MacConkey agar. Plates containing between 30 and 300 colonies were counted. Spleens were removed and weighed, and splenic indexes were calculated [$\sqrt{(\text{weight of spleen} \times 100/\text{weight of mouse})}$]. The mouse data represents a single trial for each mouse strain.

2.5 Growth curves

C. rodentium wild-type and mutant strains were grown in biological triplicate overnight. Cells were washed and standardized to an OD₆₀₀ of 1.0 in 1X PBS and diluted 1:100 into growth media pre-aliquoted in a clear 96-well plate. Plates were read in an Epoch2 microplate reader

(Biotek, USA) set to 37°C with continuous orbital shaking at a frequency of 237 cpm (4mm) at slow speed. Blank wells were subtracted from corresponding culture wells prior to calculations. Biological triplicates were averaged with the standard deviation indicated by error bars. Growth curves were completed at least twice with the data from one experiment shown. Susceptibility assays were prepared in the same manner with the addition of hydrogen peroxide or copper chloride to a final concentration of 1mM.

2.6 Tables

Table 2.1. Strains and plasmids used in this study.

Strain or Plasmid	Description	Source or Reference
<i>Citrobacter rodentium</i> strains		
DBS100	<i>Citrobacter rodentium</i> ATCC 51459	(2)
DBS100 $\Delta cpxRA$		(231)
DBS100 $\Delta yebE$		This study
DBS100 $\Delta ygiB$		This study
DBS100 $\Delta bssR$		This study
DBS100 $\Delta htpX$		This study
DBS100 $\Delta pspF$		This study
DBS100 $\Delta pspA$		This study
<i>Escherichia coli</i> strains		
MFDpir	Conjugal donor for biparental matings; DAP auxotroph	(237)
Plasmids		
pNLP10	Very low copy luminescence reporter plasmid containing promoterless <i>luxCDABE</i> operon; Kan ^R	(190)
pNLP10P _{<i>cpxP</i>}	<i>C. rodentium cpxP</i> promoter cloned into pNLP10; Kan ^R	This study
pNLP10P _{<i>yebE</i>}	<i>C. rodentium yebE</i> promoter cloned into pNLP10; Kan ^R	This study
pNLP10P _{<i>ygiB</i>}	<i>C. rodentium ygiB</i> promoter cloned into pNLP10; Kan ^R	This study
pNLP10P _{<i>bssR</i>}	<i>C. rodentium bssR</i> promoter cloned into pNLP10; Kan ^R	This study
pNLP10P _{<i>htpX</i>}	<i>C. rodentium htpX</i> promoter cloned into pNLP10; Kan ^R	This study
pNLP10P _{<i>tolC</i>}	<i>C. rodentium tolC</i> promoter cloned into pNLP10; Kan ^R	This study
pNLP10P _{<i>ler</i>}	<i>C. rodentium ler</i> promoter cloned into pNLP10; Kan ^R	This study
pNLP10P _{<i>mpc</i>}	<i>C. rodentium mpc</i> promoter cloned into pNLP10; Kan ^R	This study
pNLP10P _{<i>espV</i>}	<i>C. rodentium espV</i> promoter cloned into pNLP10; Kan ^R	This study
pNLP10P _{<i>kfcC</i>}	<i>C. rodentium kfcC</i> promoter cloned into pNLP10; Kan ^R	This study
pNLP10P _{<i>pspA</i>}	<i>C. rodentium pspA</i> promoter cloned into pNLP10; Kan ^R	This study
pNLP10P _{<i>pspF</i>}	<i>C. rodentium pspF</i> promoter cloned into pNLP10; Kan ^R	This study
pUC18	General cloning vector; Amp ^R	Thermo Fisher Scientific
pRE112	Suicide vector for allelic exchange; Cam ^R	(236)

Table 2.2. Oligonucleotide primers used in this study.

Primer Name	Sequence*	Use
pNLP10 F	GCTTCCCAACCTTACCAGAG	Amplify MCS of pNLP10 (190)
pNLP10 R	CACCAAATAATGATTGCAC	Amplify MCS of pNLP10 (190)
crepXP_F3_EcoRI	TTTGAATTCGGGATGTCAACTCTCGG TCAT	<i>cpxP</i> promoter for <i>lux</i> plasmid pNLP10
crepXP_R3_BamHI	AAAGGATCCCTGAATGCCAGCGTTG AGG	<i>cpxP</i> promoter for <i>lux</i> plasmid pNLP10
yebE_F_EcoRI	TTATAGAATTCCTGAGTCATTGTGCG	<i>yebE</i> promoter for <i>lux</i> plasmid pNLP10
yebE_R_BamHI	AAATAGGATCCCGAGCAACGATTGT A	<i>yebE</i> promoter for <i>lux</i> plasmid pNLP10
ygiB_F_EcoRI	TTATAGAATTCACTAAGCGTTACCCG ATGG	<i>ygiB</i> promoter for <i>lux</i> plasmid pNLP10
ygiB_R_BamHI	ATATAGGATCCGTGCGCTCCAGTTTT TAC	<i>ygiB</i> promoter for <i>lux</i> plasmid pNLP10
bssR2_F_EcoRI	ATATAGAATTCTCTGCATCGTCATAG CTCGGG	<i>bssR</i> promoter for <i>lux</i> plasmid pNLP10
bssR2_R_BamHI	TATGGATCCCTGTTTCAGCAGGTCGGT TC	<i>bssR</i> promoter for <i>lux</i> plasmid pNLP10
htpX_2_F_XhoI	ATTACTCGAGTTGCCCGCTTCAATGC G	<i>htpX</i> promoter for <i>lux</i> plasmid pNLP10
htpX_2_R_KpnI	TATCGACTGGTACCCGGTCAGACTCA G	<i>htpX</i> promoter for <i>lux</i> plasmid pNLP10
tolC_F_EcoRI	ATATAGAATTCTGGTGTATAAGCCG CG	<i>tolC</i> promoter for <i>lux</i> plasmid pNLP10
tolC_R_BamHI	TACTAGGATCCACTTGCATCAGGTTC TCTG	<i>tolC</i> promoter for <i>lux</i> plasmid pNLP10
ler_F_EcoRI	TTTGAATTCACGCGATCTGTTGCC TG	<i>ler</i> promoter for <i>lux</i> plasmid pNLP10
ler_R_BamHI	TTTGGATCCTCAGCTGAATGTATGG CTTG	<i>ler</i> promoter for <i>lux</i> plasmid pNLP10
mpc_F_EcoRI	TGTGAATTCGTCAAACCACCTAAAA CACC	<i>mpc</i> promoter for <i>lux</i> plasmid pNLP10
mpc_R_BamHI	TTGGATCCTTCAACACGATTATCAAG C	<i>mpc</i> promoter for <i>lux</i> plasmid pNLP10
espV_F_EcoRI	TTGAATTCGATGACAGCCATTC	<i>espV</i> promoter for <i>lux</i> plasmid pNLP10
espV_R_BamHI	TTGGATCCTCATCATTTGCCCC	<i>espV</i> promoter for <i>lux</i> plasmid pNLP10
kfcC_F_EcoRI	TTTGAATTCGACGAATAGAAAAGCC CCATC	<i>kfcC</i> promoter for <i>lux</i> plasmid pNLP10
kfcC_R_BamHI	TTGGATCCATTAACAGTACCGCTGTT C	<i>kfcC</i> promoter for <i>lux</i> plasmid pNLP10
pspA_F_EcoRI	TTTGAATTCATCAAGAAACAGCG	<i>pspA</i> promoter for <i>lux</i> plasmid pNLP10
pspA_R_BamHI	TTTGGATCCTTCTGCGGATCTTCC	<i>pspA</i> promoter for <i>lux</i> plasmid pNLP10
pspF_F_EcoRI	TTTGAATTCGCGTATCTTCCACCAGC GTCA	<i>pspF</i> promoter for <i>lux</i> plasmid pNLP10
pspF_R_BamHI	TTTTGGATCCTCCAGAAAGCTATTGG CTTCGC	<i>pspF</i> promoter for <i>lux</i> plasmid pNLP10

yebEupF	TCCGGAGTATTACATTTTTGCCCTC AAGTACTGACAA	Overlap extension PCR for $\Delta yebE$
yebEupR_XbaI	TTTCTAGAAGTTCTCCGGAACCCAAT AACATC	Overlap extension PCR for $\Delta yebE$
yebEdnF_SphI 2	TTTGCATGCATCAGCGTTTCCCACTG	Overlap extension PCR for $\Delta yebE$
yebEdnR	CAAAAATGTAATACTCCGGATGCAG CATGTTTCGC	Overlap extension PCR for $\Delta yebE$
ygiBupF_XbaI	TTTTCTAGAGACAAGCCGCAGCCGG TG	Overlap extension PCR for $\Delta ygiB$
ygiBupR	TCCATGCGGATCACATATTCGTCTTC CAGGAC	Overlap extension PCR for $\Delta ygiB$
ygiBdnF	AGACGAATATGTGATCCGCATGGAA AGAGTCAGTATC	Overlap extension PCR for $\Delta ygiB$
ygiBdnR_SphI	AAAGCATGCGTCGCCAAACTTCGGC AG	Overlap extension PCR for $\Delta ygiB$
bssRupF_XbaI	TTTTCTAGACGTGCGGATACGGATAG ACG	Overlap extension PCR for $\Delta bssR$
bssRupR	CCTTGTGTCAGGCGAACATACTTCGT TCCTCC	Overlap extension PCR for $\Delta bssR$
bssRdnF	CGAAGTATGTTTCGCTGACACAAGG G	Overlap extension PCR for $\Delta bssR$
bssRdnR_SphI	TTTGCATGCTGATAAAAAGCCATTCC GCTGAC	Overlap extension PCR for $\Delta bssR$
htpXupF_XbaI	TTTTCTAGAGCGCTGACCGAGGCG	Overlap extension PCR for $\Delta htpX$
htpXupR	GCCAGTGATAACCGTCGCTTACTTCA TCATAATTTCTTTTAACC	Overlap extension PCR for $\Delta htpX$
htpXdnF	GAAAATTATGATGAAGTAAGCGACG GTTATCACTG	Overlap extension PCR for $\Delta htpX$
htpXdnR_SphI	TTTGCATGCGGACCAACGATTGCC	Overlap extension PCR for $\Delta htpX$
pspAupF_XbaI	TTTTCTAGAGACGTGCGCCTGTGCC	Overlap extension PCR for $\Delta pspA$
pspAupR	CCGCCAGATCTTATTAACCCATAATT CAATCCTCAC	Overlap extension PCR for $\Delta pspA$
pspAdnF	GGATTGAATTATGGGTAAATAAGAT CTGGCGGCGTCTG	Overlap extension PCR for $\Delta pspA$
pspAdnR_SphI	TTTGCATGCGGTAAAATTAGCTGTCA ATGC	Overlap extension PCR for $\Delta pspA$
pspFupF_XbaI	TTTTCTAGAACTCCTTACAGGTGATG AACGGC	Overlap extension PCR for $\Delta pspF$
pspFupR	GCAGTAATCGCTAAATCATGATGAA TTTCGCC	Overlap extension PCR for $\Delta pspF$
pspFdnF	TTCATCATGATTTAGCGATTACTGCC ACCTGATCG	Overlap extension PCR for $\Delta pspF$
pspFdnR_SphI	TTTGCATGCCTTATCGGTATTGAACG CCAGATAG	Overlap extension PCR for $\Delta pspF$
yebEgene_F2	ATAATTTGCGCATCTTTTGCCG	Flanking <i>yebE</i> to confirm knockouts
yebEgene_R2	TCGGCAGCATGTCCTGTTTC	Flanking <i>yebE</i> to confirm knockouts
ygiBgene_F2	CCGCCTTCTCGCTTCATTTTCAAC	Flanking <i>ygiB</i> to confirm knockouts
ygiBgene_R2	GAAACCGTATTCAGTAGCTTTATCGC G	Flanking <i>ygiB</i> to confirm knockouts

bssRgene_F2	TTCCCGGTGAATTATTGATCTTTGGC A	Flanking <i>bssR</i> to confirm knockouts
bssRgene_R2	AGCGAGGGGGCGCAAC	Flanking <i>bssR</i> to confirm knockouts
htpXgene_F	TAGCCACACTACCCATACGATGTG	Flanking <i>htpX</i> to confirm knockouts
htpXgene_R	TTTCAGAGTTACCGTTTTGCCGGATG	Flanking <i>htpX</i> to confirm knockouts
pspAgene_F	AAGGCTTAAAAAGTTGGCACG	Flanking <i>pspA</i> to confirm knockouts
pspAgene_R	TACTCCTTACAGGTGATGAACGG	Flanking <i>pspA</i> to confirm knockouts
pspFgene_F	ATGTACAGATTTACCTCAGCCTG	Flanking <i>pspF</i> to confirm knockouts
pspFgene_R	CAGGTAAAAATCACGACGG	Flanking <i>pspF</i> to confirm knockouts

*Restriction sites are underlined, enzymes indicated in primer name.

Chapter 3. Results

Note: The data presented in Figure 3.1.6 and Figure 3.1.7A-B was collected and analyzed by Christina Gavino from the Gruenheid lab at McGill University.

Note: Devanshi Pandit assisted with the collection of data presented in Figure 3.3.2, Figure 3.3.3, Figure 3.3.4, and Figure 3.3.5 as well as did the transformation to generate the Δ pspF strain harboring the pspA-lux reporter plasmid

3.1 Individual Cpx-regulon members tested do not contribute to *C. rodentium* virulence however do impact bacterial fitness in simulated colonic fluid

3.1.1 Identification and confirmation of Cpx regulon members

Previous research done by two independent groups collected proteomic, RNA-seq and microarray data to identify genes that were differentially expressed in the absence of CpxRA (210, 232). Using the data collected, the 11 genes listed in Table 3.1.1 were selected for further study based on their predicted function, expression levels, and/or lack of previous investigation. *htpX* and *yebE* were selected as they had some of the highest transcript abundance changes besides *cpxP* and *yccA*, which have both been previously investigated in *C. rodentium* (210). SILAC data for *htpX* was insignificant due to the detection of only 1 peptide while *yebE* had a *P*-value of 0.08. *ygiB*, *malE*, and *dps* had significantly higher transcript abundances in one or both transcriptomic studies as well as peptide counts in the presence of CpxRA as indicated by bolded values (*dps* microarray; *P*-value = 0.081) (Table 3.1.1). *tolC* was also included as it is located 198 bp upstream of *ygiB* and has previously been presumed to be expressed in an operon with *ygiBC* (239). The additional maltose transporter complex genes including *malG*, *malK*, and *lamB* were included due to the significant increase in sequence abundance uncovered by microarray in the presence of CpxRA (232). *bssR* and *bdm* are involved in biofilm regulation and had significantly higher transcript abundance in wild-type cells in both transcriptomic studies despite an absence of detection in the SILAC data (Table 3.1.1).

Using the *lux*-reporter plasmid pNLP10, reporters for the 11 genes of interest as well as the Cpx-regulated gene *cpxP*, used as a positive control and indicator of Cpx activity, were constructed and initially screened in LB and LB with alkaline pH for Cpx-dependent expression (data not shown). While some of these genes, namely *yebE* and *htpX*, have had Cpx-dependent

expression confirmed experimentally in previous studies using other bacterial strains, their expression has never been studied in *C. rodentium* DBS100 (189, 190, 240, 241). Following this, reporter strains were tested in LB broth as well as the virulence-inducing media, high-glucose Dulbecco's Modified Eagles Medium, which lacked phenol red and was buffered with 0.1M MOPS (HG-DMEM) (70, 190, 242). Of the 11 reporters initially selected, *yebE*, *ygiB*, *bssR*, and *htpX* along with the positive control, *cpxP*, had significantly higher luminescence in wild-type cells relative to the $\Delta cpxRA$ mutants in both LB broth and HG-DMEM (Table S1, Figure 3.1.1A). Interestingly, the re-suspension of log-phase cells in HG-DMEM significantly activated the Cpx ESR as seen by the near 10-fold increase in *cpxP-lux* activity relative to re-suspension in LB, indicating that HG-DMEM is a stress-inducing condition for *C. rodentium* (Figure 3.1.1A). Of the four remaining genes of interest, *yebE-lux* relied the most on the Cpx ESR for its expression as seen by minimal luminescence detected in both LB and HG-DMEM in the absence of CpxRA (Figure 3.1.1A, Table S1). Furthermore, like the *cpxP-lux* reporter, *yebE-lux* expression was not induced in HG-DMEM in the $\Delta cpxRA$ mutant relative to LB expression (Figure 3.1.1A). On the other hand, the expression of *ygiB*-, *bssR*-, and *htpX-lux* reporters exhibited higher levels of expression in HG-DMEM relative to LB regardless of the Cpx ESR. When comparing *ygiB*-, *bssR*-, and *htpX-lux* reporters between wild-type and $\Delta cpxRA$ cells, there is a clear indication that the presence of the Cpx ESR results in higher expression in both medias tested (Figure 3.1.1A, Table S1). Finally, each gene of interest, except for *yebE*, had increased luminescence in wild-type cells when grown on solid LB agar relative to $\Delta cpxRA$ cells (Figure 3.1.1B, Figure S1A). Luminescence produced by the *yebE-lux* reporter on LB agar was below the threshold of detection therefore we could not determine the impact of the Cpx ESR on *yebE* expression using this assay.

tolC was originally included in this study due to its proximity to the predicted translation initiation site of downstream *ygiB* and the presumption that it resides in an operon with *ygiBC* (239). To confirm whether these genes were in an operon together, their expression in both LB and HG-DMEM (without MOPS) was measured over 6 hours. From this, we determined there was no measurable difference in the expression of *tolC* between the wild-type and $\Delta cpxRA$ mutant in LB (Figure 3.2.1A). In HG-DMEM, the transcription of *tolC* reduced over time in wild-type cells and increased in $\Delta cpxRA$ cells (Figure 3.1.2B). This contrasts with the higher levels of luminescence detected from the *ygiB-lux* reporter in wild-type cells when grown in either medium (Figure 3.1.2A-B). Finally, as indicated by Figure 3.1.2C, a putative CpxR binding site is located in between *tolC* and *ygiB*, 91 base pairs upstream from the predicted translation initiation site of *ygiB* (188). From this, we can conclude that *tolC* and *ygiBC* are perhaps transcribed together as suggested by Dhamdhare *et al.* (2010), however when required, the Cpx ESR has the ability to differentially express these two genes in both conditions tested.

To determine how the four selected genes of interest, *yebE*, *ygiB*, *bssR*, and *htpX*, are being expressed over time relative to the phases of cellular growth, *lux*-reporter activity was monitored for 12 hours from initial inoculation to stationary phase growth in LB. Interestingly, *yebE-lux* activity followed a near identical trend to the expression of the positive control *cpxP-lux* reporter in both wild-type and $\Delta cpxRA$ cells (Figure 3.1.3A). This suggests that the expression of *yebE-lux* is almost entirely dependent on the Cpx ESR or at least utilizes the same mechanisms that are responsible for the expression of *cpxP*, furthering curiosity as to its proposed function in terms of stress response and overall cell health. In addition, *ygiB-lux* and *bssR-lux* reporters showed a similar trend of expression to that of *cpxP-lux* in wild-type cells with a lower level of activity in $\Delta cpxRA$ cells (Figure 3.1.3B-C). It is evident for both *ygiB* and

bssR that, unlike *yebE*, there are other regulators for these genes outside of CpxRA as they both had measurable basal expression, well above the low background levels seen for the *cpxP*- and *yebE-lux* reporters in Δ *cpxRA* cells. In addition, the peak of luminescence for *cpxP*-, *yebE*-, *ygiB*- and *bssR-lux* in wild-type cells was reached after approximately 7-8 hours growth which coincides with late exponential phase (Figure 3.1.2A-C, Figure S2). This supports previous studies which have shown that the Cpx ESR is most active during late exponential and early stationary phase (204, 205). On the other hand, *htpX-lux* had higher luminescence in wild-type cells and was consistently expressed over the measured 12 hours of growth suggesting that its expression is less dependent on growth phase (Figure 3.1.3D). It should however be noted that the presence of CpxRA allowed for the maintenance of *htpX-lux* activity throughout late exponential and stationary phase as opposed to the steady decline in luminescence seen in the Δ *cpxRA* cells (Figure 3.1.3D, Figure S2). This further highlights the importance of the Cpx ESR for gene regulation in stationary phase growth.

3.1.2 The activity of the Cpx ESR is influenced by the absence of *htpX* and growth conditions

Provided our evidence indicates *yebE*, *ygiB*, *bssR*, and *htpX* rely on the presence of CpxRA for proper expression, we questioned whether the absence of these genes would impact the envelope stress experienced by cells thus altering the activity of the Cpx ESR. Using allelic exchange, *C. rodentium* knockout mutants were generated for *yebE*, *ygiB*, *bssR*, and *htpX*. These strains were transformed with the reporter *cpxP-lux* and grown in LB or HG-DMEM where the luminescence was measured. Our results indicate that only Δ *htpX* cells had significantly increased expression of *cpxP*, supporting previously reported findings observed in *E. coli* K-12

strain MC4100 (Figure 3.1.4A-B, Figure S1B) (240). This could be seen on LB agar plates as well as in both LB broth and HG-DMEM at an increase of 2.1- and 1.9-fold, respectively (Figure 3.1.4A-B, Figure S1B).

Unexpectedly, it was determined the expression pattern over time of *cpxP-lux* and by extension, the activity of the Cpx ESR, differs vastly depending on the media used for growth. When the same subculture was split and re-suspended in either LB or HG-DMEM, despite having similar growth trends over 6 hours, *cpxP-lux* activity increased over time when grown in LB but decreased over time in HG-DMEM (Figure 3.1.5A-B). In addition, while having a less substantial impact on the activity of the Cpx ESR, cultures that were grown shaking in LB induced *cpxP-lux* more so than static cultures, whereas the opposite was true for HG-DMEM cultures where static cultures had higher *cpxP-lux* activity (Figure 3.1.5C-D). These results suggest that while the Cpx ESR may be influenced by growth and is most active in late exponential or early stationary phase in LB broth, the same may not remain true for cells experiencing perhaps more stressors or other Cpx ESR inducing signals when grown in HG-DMEM.

3.1.3 Cpx regulon members *yebE*, *ygiB*, *bssR*, and *htpX* are not individually required for colonization or virulence *in vivo*

With *yebE*, *ygiB*, *bssR*, and *htpX* expression confirmed to be upregulated by the presence of CpxRA, we then tested whether these genes were required for the colonization or virulence of *C. rodentium* which could provide a possible explanation for why the removal of *cpxRA* is detrimental to pathogenesis (210, 231, 232). In our first set of experiments, we used C57Bl/6J

mice which experience a self-limiting form of disease to determine whether colonization was negatively impacted by any of the mutants (12). As seen in Figure 3.1.6A-C, only $\Delta cpxRA$ cells could not consistently colonize to the same level as wild-type and the other mutants (Day 4; $*P<0.05$, Day 9 and 12; $**P<0.01$, Mann-Whitney U Test). While the $\Delta yebE$ mutant exhibited a slight lag in colonization levels on day 9 ($*P<0.05$) and the $\Delta bssR$ mutant showed an increase in colonization of the colon on day 12 ($*P<0.05$), these minor statistical significances are not reflected in the degree of disease-state measured using a splenic index (Figure 3.1.6D). All strains caused a similar level of disease relative to wild-type except for $\Delta cpxRA$, which had a significantly lower splenic index indicating attenuated virulence, thus confirming the results of previous studies (Figure 3.1.6D) (231, 232).

Similarly, in a C3H/HeJ mouse trial, testing disease progression and survival, only the $\Delta cpxRA$ mutant exhibited a colonization defect as seen by an approximate 2-fold reduction in colony forming units (CFUs) for three mice and undetectable levels in two on day 4 post-infection (Figure 3.1.7A). In addition, the $\Delta cpxRA$ mutant had significant attenuation of virulence as seen by the fact that all five infected mice survived until day 30 (Figure 3.1.7B).

3.1.4 Cpx-regulated genes impact *C. rodentium* fitness in simulated colonic fluid (SCF)

Previous research has shown differing results regarding the effect of removing the Cpx ESR on *C. rodentium* growth. Vogt *et al.* (210) showed no growth defects associated with a $\Delta cpxRA$ mutant in shaking LB broth or static HG-DMEM with 5% CO₂. On the other hand, although the exact nature of the culture conditions used are unclear, Thomassin *et al.* (231) found that *C. rodentium* $\Delta cpxRA$ cultures had a longer lag phase in DMEM but eventually would grow

to a comparable OD to the wild-type and complemented strains. In this study, all the mutants tested grew comparably in LB, however in buffered HG-DMEM, all the mutants grew to a reduced level relative to wild-type cells, with the most significant reduction experienced by $\Delta cpxRA$ cells (Figure 3.1.8A-B). One predominant issue to note with *C. rodentium* in HG-DMEM is an overall poor growth phenotype as seen by the OD maximum of 0.2 (Figure 3.1.8B). To circumvent this as well as to mimic the *in vivo* conditions experienced by *C. rodentium* cells during colonization, the strains were grown in simulated colonic fluid (SCF), first developed by Beumer *et al.* (235). Interestingly, when comparing unbuffered and buffered growth in SCF, it becomes evident that while unstable pH is toxic to $\Delta cpxRA$ cells, resulting in zero growth, there is also a growth defect evidenced by a longer lag phase in MOPS buffered SCF at pH 7 (Figure 3.1.8C-D). Importantly, when pH is controlled in buffered SCF, only the $\Delta cpxRA$ cells grow significantly different from wild-type cells, mimicking the colonization defect seen in both C57Bl/6J and C3H/HeJ mice (Figure 3.1.6A-C, Figure 3.1.7A, Figure 3.1.8D). The $\Delta cpxRA$ cells also exhibited severe growth defects when grown in buffered SCF and challenged with the presence of either oxidative or copper stress, suggesting an extreme sensitivity to sub-inhibitory levels of stressors in the colonic environment (Figure 3.1.9). An additional observation to be noted in unbuffered SCF is that both the $\Delta ygiB$ and $\Delta htpX$ mutants experienced an extended lag phase as well as had increased variability between biological replicates (Figure 3.1.8C). This could indicate a susceptibility to unstable pH as well as suggests a contributing factor to the pH sensitivity experienced by $\Delta cpxRA$ cells (Figure 3.1.8C).

Due to the susceptibility to stressors exhibited by the $\Delta cpxRA$ mutant in SCF, we investigated whether our Cpx-regulated gene mutants also experienced increased sensitivity when in the presence of oxidative stress. While growth was observed in the presence of oxidative

stress in buffered LB, the knockout mutants $\Delta yebE$, $\Delta ygiB$, and $\Delta htpX$ all exhibited varying degrees of susceptibility to sub-inhibitory levels of hydrogen peroxide when grown in buffered SCF, with $\Delta ygiB$ and $\Delta htpX$ mutants showing the greatest defects (Figure 3.1.10). Finally, a reduction in OD indicating cell lysis was also observed in SCF buffered with MOPS as cells transitioned from exponential to stationary phase (Figure 3.1.8D, Figure 3.1.10B-D). The cause of this reduction requires further study. These results indicate that SCF mimics the colonization defect of the $\Delta cpxRA$ mutant measured *in vivo* which suggests that it may be a better media to use when evaluating potential *in vivo* growth phenotypes. In addition, SCF appears to be a media that can highlight subtle growth defects that might not be as easily detected in an animal model as seen with the $\Delta yebE$, $\Delta ygiB$, and $\Delta htpX$ mutants.

3.2 The Cpx response downregulates genes associated with virulence, large protein complexes, and the phage shock protein response

To develop a well-rounded understanding of the role of the Cpx ESR in colonization and virulence, we next looked at identifying genes with reduced expression in the presence of CpxRA as their proper regulation may also be important for colonization and infection. The Cpx ESR has been associated with the downregulation of virulence genes and large protein complexes (reviewed by 145). Like EPEC and EHEC, *C. rodentium* contains the LEE pathogenicity island which encodes virulence factors and a T3SS required to attach and efface intestinal epithelial cells (39, 40). Since the Cpx ESR is required for *C. rodentium* virulence and has been shown to impact LEE gene expression in EPEC and EHEC, we hypothesized that the Cpx ESR may alter the expression of the LEE master regulator *ler*, in *C. rodentium*, which may

contribute to the attenuation of virulence *in vivo* (231, 243, 244). In addition, we also wanted to investigate genes previously identified in transcriptomic and proteomic datasets, that had reduced expression in the presence of the Cpx ESR and could play a role in colonization and virulence such as those encoding fimbria or pili components (210, 232). In EPEC, the Cpx ESR plays an important role in the timing of expression and elaboration of the bundle-forming pilus (212). Under Cpx-inducing conditions, the Cpx ESR inhibits the *bfp* gene cluster, however under normal conditions, the Cpx ESR is required for proper pilus expression and formation likely through the upregulation of protein folding factors like DegP and CpxP (212). Therefore, using luminescent reporter genes, we proceeded to further explore the Cpx ESRs effect on the LEE master regulator *ler*, as well as confirm and evaluate the role of the Cpx ESR in the reduced expression of genes identified by transcriptomic and proteomic studies (210, 232).

3.2.1 Simulated physiological conditions and the Cpx ESR impact the expression of the LEE master regulator *ler*.

Previous studies have demonstrated the *C. rodentium* Δ *cpxRA* mutant does not have a significantly altered T3SS secreted protein profile *in vitro*, while there is reduced transcription of LEE operons upon activation of CpxRA and reduced expression and secretion of translocator proteins in EPEC and EHEC (210, 231, 243, 244). Utilizing *lux* reporter genes, we asked whether the attenuation of the *C. rodentium* Δ *cpxRA* mutant could be in part due to altered transcription of the LEE operon by measuring the luminescence of a *ler-lux* reporter. When cells were grown statically in simulated colonic fluid (SCF), a media that simulates the lumen of the colon, the expression of *ler* was independent from the presence of the Cpx ESR (Figure 3.2.1A) (235). On the other hand, when cells were grown statically in the virulence-inducing condition,

HG-DMEM, *ler* expression was higher in $\Delta cpxRA$ mutant cells indicating that the presence of the Cpx ESR reduces the expression of *C. rodentium*'s primary LEE regulator (Figure 3.2.1B). These results could be reproduced in both high- and low-glucose DMEM as well as in static and shaking conditions (Figure 3.2.2). Therefore, in media simulating the colonic lumen, the Cpx ESR has no impact on the expression of *ler* while in the virulence-inducing condition DMEM, the presence of the Cpx ESR was associated with reduced *ler* expression.

3.2.2 The Cpx ESR downregulates the genes *mpc*, *espV*, the *kfc* operon, and the Psp response genes, *pspA* and *pspF*

From microarray, RNA-seq, and SILAC data previously collected, ten genes of interest were selected based on their reduced expression in the presence of CpxRA and predicted function for confirmation utilizing luminescent reporters (Table 3.2.1) (210, 232). One gene of interest was *pspA*, which encodes a negative regulator and effector of the Psp response, as it had significantly reduced expression in the presence of CpxRA in all three datasets (155, 245, 246). Since PspF is the transcriptional activator for the Psp response, it was also included even though the RNA-seq dataset showed higher levels of *pspF* expression in wild-type cells relative to the $\Delta cpxRA$ mutant while the microarray showed reduced expression (Table 3.2.1) (163). Despite only appearing in the microarray data, *cfcC* was of specific interest due to its predicted protein function as a Type IV pilus biogenesis protein while *cfcA*, which encodes the Cfc fimbrial subunit, was included as it has been previously identified to have a ribosome binding site upstream and therefore is likely an operon leader of the *cfc* gene cluster (30). Vogt *et al.* (210) previously confirmed the Cpx-mediated downregulation of the *kfc* operon, which encodes a K99 fimbrial homolog, utilizing RT-qPCR of *kfcC* (64). Therefore, we used a *kfcC-lux* reporter as a

positive control as well as data evaluating its expression over time could contribute to the overall understanding of its Cpx-mediated regulation. We also included *kfcF* as it was significantly downregulated in both transcriptomic studies while *kfcC* was only downregulated in the RNA-seq data (Table 3.2.1). *ctsIG*, *espV*, and *mpc* also had predicted functions involving the structure or regulation of virulence secretion systems and had significantly higher expression in the absence of CpxRA in the microarray data (232). *ctsIG* is in the CTS1 T6SS gene cluster and is predicted to encode a protein in the valine-glycine repeat (VgrG) family that forms the tip of the T6SS apparatus (19, 32, 232). *espV* encodes a non-LEE T3SS effector protein while *mpc* is the first gene in LEE3 associated with LEE regulation in EHEC and EPEC (19, 41, 53, 247). *yehD*, a fimbrial protein, was included due to its significantly reduced expression in the presence of CpxRA in the RNA-seq dataset and the previously demonstrated role of the Cpx ESR in regulating the expression of adhesive structures, although the microarray data indicates contradictory findings (Table 3.2.1).

Of the ten reporters constructed in the pNLP10 luminescent reporter gene plasmid and tested in the virulence-inducing condition HG-DMEM buffered with 0.1M MOPS, *mpc*-, *espV*-, *kfcC*-, *pspA*-, and *pspF-lux* constructs had reduced expression in the presence of CpxRA (Figure 3.2.3) (70, 190, 242). In the Δ *cpxRA* mutant, *mpc-lux* expression increased sharply, relative to the wild-type control, between 0.5 and 1 hour followed by a slow decrease in expression over the next 5 hours (Figure 3.2.3A). In addition, the standard deviation for *mpc-lux* activity was larger relative to wild-type cells despite growth between Δ *cpxRA* replicate cultures having little variability suggesting uncontrolled expression (Figure 3.2.3A; growth data not shown). The *espV-lux* plasmid also had a small increase in expression between 0.5 and 1 hour in the Δ *cpxRA* mutant relative to wild-type cells which then proceeded to decline over time (Figure 3.2.3B).

kfcC-lux expression had an approximate 4-fold increase in the absence of CpxRA at 2 hours post-induction relative to wild-type cells indicating that the presence of the Cpx ESR moderates its expression which supports previous RT-qPCR results (Figure 3.2.3C) (210). The data presented here highlights the importance for the presence of the Cpx ESR to reduce the expression of virulence factors in a virulence-inducing condition.

Furthermore, the presence of the Cpx ESR was confirmed to negatively impact the expression of the Psp response genes *pspA* and *pspF* (Figure 3.2.3D-E). The activity of the *pspA-lux* reporter overtime remained low in wild-type cells but increased between 4 to 6 hours post-induction in the Δ *cpxRA* mutant (Figure 3.2.3D). More intriguingly, the reporter for *pspF*, which is thought to maintain a low level of expression regardless of stressors encountered due to its autoregulation and weak promoter, had an increased level of expression in the absence of CpxRA as well as high variability between replicates (Figure 3.2.3E) (155, 165). This suggests that perhaps either the Cpx ESR negatively regulates the expression of *pspA* by reducing or controlling the transcription of the *psp* operon activator, *pspF*, or in the absence of CpxRA, there is a disruption to PMF which induces the Psp response.

3.3 Evidence for an uncharacterized interaction between the Cpx and Psp envelope stress responses

After investigation into the function of YebE, the bioinformatics database BioGRID v.4.4.203, which is a repository for protein and genetic interaction data, showed interactions between *yebE* and *pspACE* based on data collected from a high-throughput quantitative genome-wide genetic interaction screen in *E. coli* W3110 (BioGRID alias: Y75_p1822) (248–250). This

screen demonstrated aggravating growth defects in the double mutants $\Delta yebE\Delta pspA$ and $\Delta yebE\Delta pspE$ while $\Delta yebE\Delta pspC$ alleviated growth defects (250). PspA is a cytoplasmic negative regulator which acts by inhibition of PspF, as well as is a membrane-associated oligomeric protein that has been proposed to aid in the maintenance of membrane potential (155, 245, 246). PspC is an inner membrane transmembrane protein, which along with PspB, is thought to undergo a conformational change under inducing conditions that results in recruitment of PspA and subsequent release of the repression of PspF which binds to regions upstream of *pspA* to enhance the transcription of the *pspABCDE* operon (see model in Figure 1.2) (163, 234, 245). In light of our previous evidence indicating a role for the Cpx ESR in the regulation of *yebE* and *pspA* gene expression and the negative interaction identified by high-throughput genetic screening, we assayed luminescent reporter gene expression in a variety of genetic backgrounds to investigate potential connections between YebE and the Cpx and Psp ESRs (Figure 3.1.1A, Figure 3.1.3A, Figure 3.2.3D) (250).

3.3.1 The Cpx ESR and the Psp response can be differentially induced using alkaline or ethanol stress

We wished to identify a way to induce the Cpx and Psp responses distinctly to further study potential Cpx ESR, YebE, and Psp response interactions. It is known that the Cpx ESR is induced by alkaline pH and the Psp response is transiently induced by ethanol stress, but it was important to determine if either stressor would also have an impact on the opposite response (191, 251). Utilizing the luminescent reporters *cpxP-lux* and *pspA-lux* for the Cpx and Psp responses respectively, wild-type cells were grown in either LB, LB pH 8, or LB with 5% ethanol to measure the influence of each stressor on both stress responses. As seen in Figure

3.3.1A, alkaline pH strongly induced the activity of the Cpx ESR while ethanol had a minimal effect at 0.5- and 6-hours post-induction though it did induce the response relative to LB between 1- and 4- hours. On the contrary, while the induction is delayed, the expression of *pspA-lux* is significantly higher during ethanol stress as opposed to alkaline stress where expression is minimally different from the activity measured in LB (Figure 3.3.1B). These results indicate that these two stress responses are both induced to varying levels by alkaline and ethanol stress, however the Cpx ESR responds more strongly to alkaline pH while stress induced by ethanol activates the Psp response more so than high pH.

3.3.2 The absence of YebE reduces the activity of the Psp response

To further investigate the genetic interaction predictions presented in BioGRID from Babu *et al.* (250), we wanted to determine whether the presence of YebE would affect the expression of *pspA* thus confirming an interaction between YebE and the Psp response (248, 249). Using luminescent reporter genes, we found that in LB, the presence of YebE had little to no influence on the activity of the Psp response as seen by the luminescence produced from *pspA-lux* (Figure 3.3.2A). Interestingly, when cells were grown in LB at a pH of 8, a condition known to induce the Cpx stress response, the activation of the Psp response was higher when YebE was present relative to the $\Delta yebE$ mutant (Figure 3.3.2B) (191). Moreover, in the Psp-inducing condition of 5% ethanol, the same trend could be seen where *pspA-lux* expression was increased in wild-type cells relative to the $\Delta yebE$ mutant (Figure 3.3.2C). These results indicate an influence of YebE on the expression of *pspA* in the presence of alkaline and ethanol stress which coincides with the genetic interactions between *yebE* and the genes *pspACE* presented by BioGRID (248–250).

3.3.3 PspF enhances the activity of the Psp response in *C. rodentium*

The Psp response has been studied most in *Yersinia enterocolitica* and *E. coli* whereas its function and regulation in *C. rodentium* has not been characterized (245). Originally identified in *E. coli*, PspF is encoded in the opposite direction from *pspABCDE* and is under the control of a σ^{70} promoter where it undergoes negative transcriptional auto-regulation to remain at low intracellular concentrations (163, 165). It has been identified as an enhancer of the Psp response under inducing-conditions through transcriptional activation of a σ^{54} promoter upstream of *pspABCDE* (163). To test the reliance of the Psp response on PspF in *C. rodentium*, we did luminescence assays in LB and LB with 5% ethanol in wild-type and Δ *pspF* mutant cells harboring a *pspA-lux* reporter. In LB, it was evident that wild-type cells had higher *pspA-lux* expression relative to the Δ *pspF* mutants however there was still luminescence, or Psp response activity, in the absence of PspF (Figure 3.3.3A). When cells were exposed to ethanol stress, *pspA-lux* activity in the Δ *pspF* mutant was highly variable over time and in between replicates relative to wild-type cells (Figure 3.3.3B). This could be attributed to the slight growth defect measured for the Δ *pspF* mutant in ethanol stress which is perhaps a result from the inability to properly regulate the Psp response (growth data not shown). These results highlight how PspF is required for the proper expression of the *pspABCD* operon however its removal does not abolish the activity of the Psp response completely.

3.3.4 The Cpx ESR is not affected by the absence of PspF or PspA

As previously demonstrated, both *pspA* and *pspF* expression are negatively influenced by the presence of the Cpx ESR (Figure 3.2.3D-E). To determine if the Cpx ESR is influenced by the presence of the Psp response, *cpxP-lux* activity was measured in both Cpx- and Psp-inducing conditions in Δ *pspA* and Δ *pspF* mutant strains. The Δ *pspF* mutant strain has reduced Psp response activity in LB while the Δ *pspA* mutant would be expected to lose the effector abilities of an oligomeric PspA complex which is associated with stabilizing the membrane and PMF (Figure 3.3.3A) (155, 245, 246). Regardless of condition, the level of *cpxP-lux* expression measured was consistent between wild-type and both mutant strains (Figure 3.3.4A-C). While this assay should be replicated, this preliminary data indicates that the Cpx ESR mediates envelope stress caused by alkaline pH and ethanol stress independently from the presence of Psp response components.

3.3.5 The expression of *yebE* is increased in the absence of major Psp response components

Whilst the presence of YebE had an impact on the Psp response, it was important to investigate the impact of Psp response components on the expression of *yebE*. In LB, there was no significant difference in *yebE-lux* between wild-type, Δ *pspA* and Δ *pspF* over time (Figure 3.3.5A). Upon Cpx-induction in LB pH 8, the overall expression of *yebE-lux* was increased relative to LB alone (Figure 3.3.5A-B). Interestingly, there was also a further increase in the activity of the *yebE-lux* construct in both the Δ *pspA* and Δ *pspF* mutants (Figure 3.3.5B). This increase could also be seen when cells were grown in the presence of ethanol stress, which is known to induce the Psp response (Figure 3.3.5C). While these are preliminary results, the influence on *yebE-lux* expression by the absence of either *pspA* or *pspF* when cells experience

stress exemplifies an unknown interaction between YebE and the Psp response which warrants further investigation.

3.4 Tables and Figures

Table 3.1.1. Mined RNA-Seq and SILAC data from Vogt *et al.* (210) and microarray data collected in Giannakopoulou *et al.* (232) for potential CpxRA upregulated genes.

Data Source	Dataset S3- Vogt <i>et al.</i> (2019)		Giannakopoulou <i>et al.</i> (2018)	Protein Function ³
Gene Name	Fold change RNA-Seq ¹	Fold change SILAC ¹	log2 fold change Δ cpxRA-WT microarray ²	
<i>htpX</i>	12.10	10.77	-0.93	Membrane-localized protease
<i>yebE</i>	24.52	5.36	-1.92	Inner membrane protein with transmembrane domain
<i>ygiB</i>	3.54	2.24	-0.99	Outer membrane protein
<i>tolC</i> ⁴	N/A	N/A	N/A	Outer membrane channel required for several efflux systems
<i>dps</i>	2.12	1.43	-2.49	DNA protection during starvation
<i>malE</i>	2.55	1.26	-5.88	Maltose/maltodextrin-binding periplasmic protein
<i>malG</i>	2.12	n.d.	-5.48	Maltose/maltodextrin transport system permease
<i>malK</i> ⁴	N/A	N/A	-4.27	Maltose/maltodextrin import ATP-binding protein
<i>lamB</i>	N/A	N/A	-5.91	Maltoporin in the outer membrane
<i>bssR</i>	3.72	n.d.	-3.36	Biofilm regulator involved in catabolite repression and stress response
<i>bdm</i>	2.81	n.d.	-2.54	Biofilm-dependent modulation protein

Bolded values indicate $P_{adj} < 0.05$ (RNA-Seq), $FDR < 0.05$ (SILAC), $t\text{-test} < 0.05$ (microarray).

¹Calculated wild-type/ Δ cpxRA

²Negative value indicates higher expression in wild-type (WT) DBS100

³Protein function as described by UniProtKB for *E. coli* K12

⁴Included due to potential operon leader of gene of interest

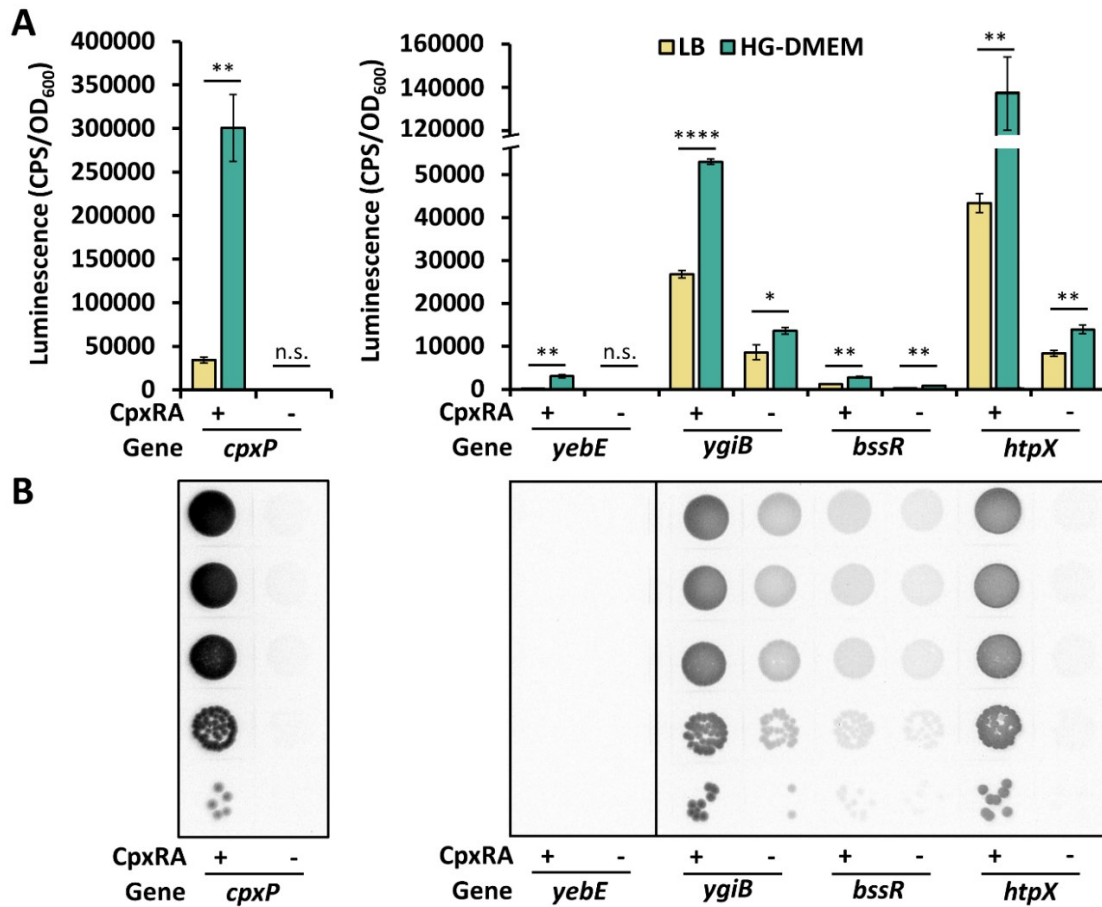


Figure 3.1.1. Confirmation of upregulated genes in the presence of CpxRA using *lux*-reporter assays in both LB and HG-DMEM. (A) Wild-type and $\Delta cpxRA$ strains harboring a *lux*-reporter plasmid for either the positive control, *cpxP*, or genes of interest *yebE*, *ygiB*, *bssR*, and *htpX* were grown in LB (yellow) and HG-DMEM buffered with 0.1M MOPS (teal) or (B) on LB agar plates. Data represents the mean and standard deviation of three biological replicate cultures. The asterisks indicate a statistically significant difference between the mean luminescence produced in LB compared to HG-DMEM for each strain and reporter tested (* $P < 0.05$, ** $P < 0.01$, **** $P < 0.0001$, n.s. not significant, Student's *t*-test). See Table S1 for significance values comparing wild-type and $\Delta cpxRA$ strains in each condition. All assays were completed at least twice, with one representative experiment shown.

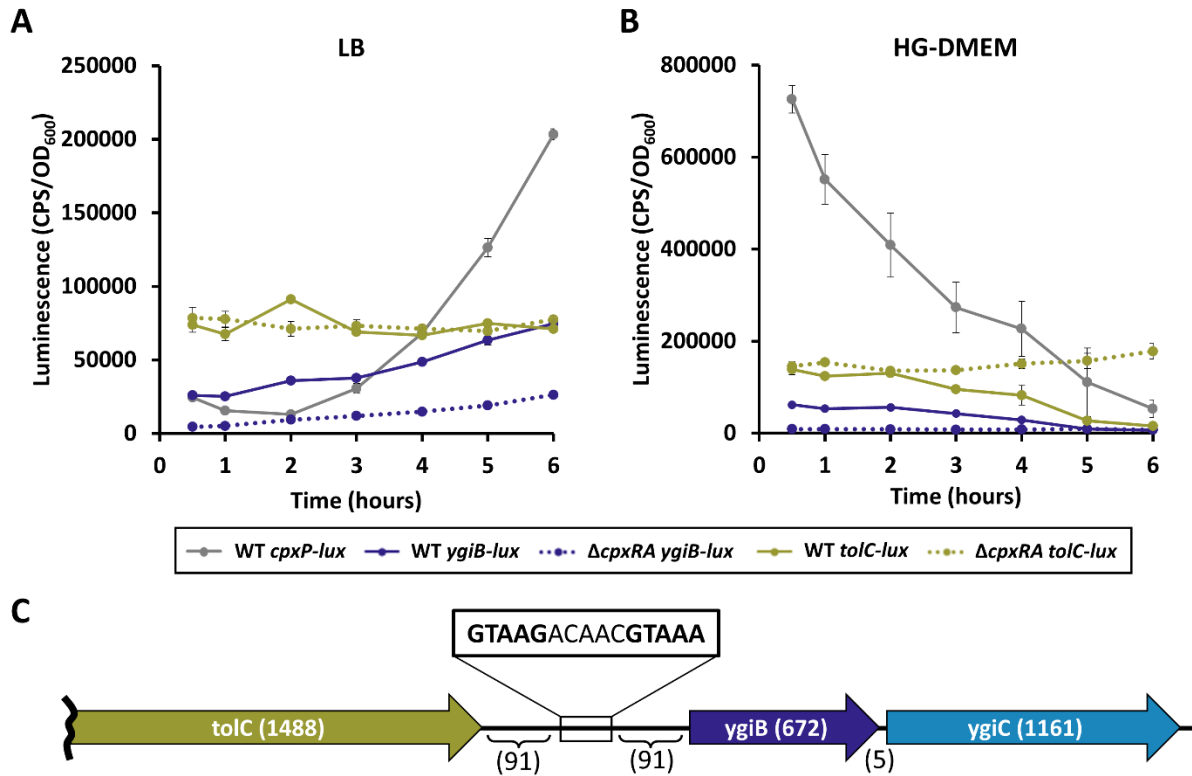


Figure 3.1.2. Expression of *ygiB*- and *tolC-lux* over time indicates CpxRA-dependent regulation. (A-B) Wild-type (solid line) and Δ *cpxRA* (dotted line) cells harboring either *ygiB-lux* (blue) or *tolC-lux* (green) reporter plasmids and wild-type cells containing *cpxP-lux* (gray) were grown in either (A) LB or (B) HG-DMEM without MOPS. Data represents the mean and standard deviation of three biological replicate cultures. (C) Diagram of *tolC* and *ygiBC* in *C. rodentium* DBS100. The CpxR putative binding site is indicated with the black outlined box. Numbers in brackets indicate the number of nucleotides.

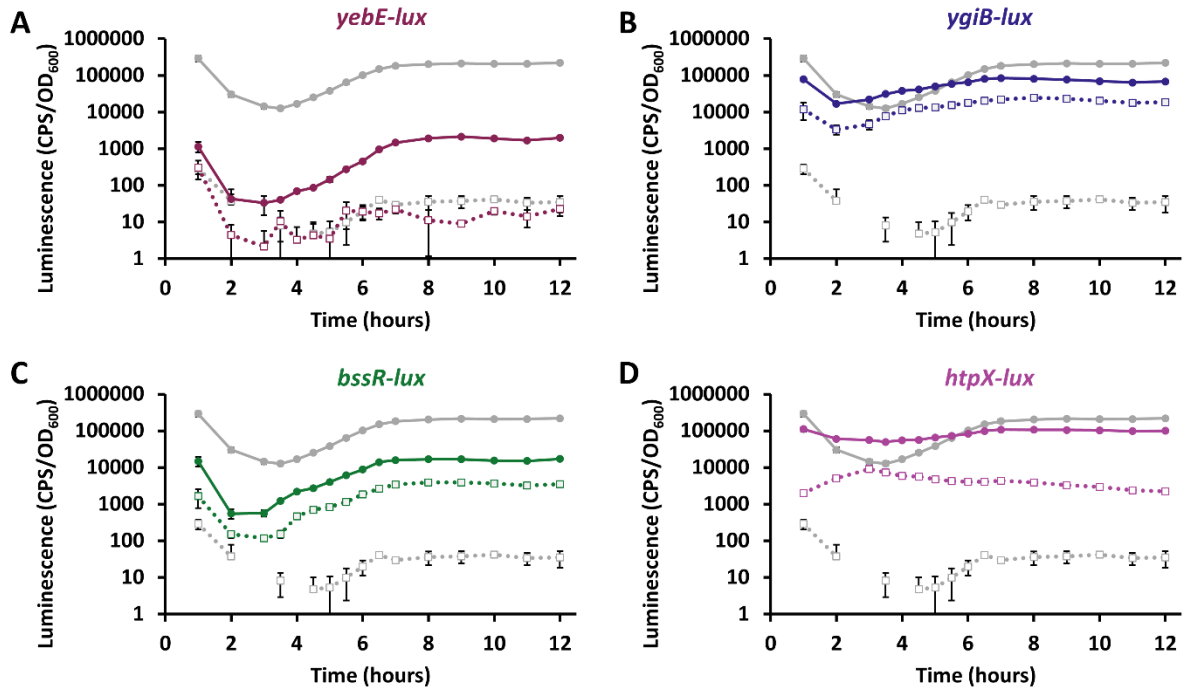


Figure 3.1.3. *yebE*, *ygiB*, and *bssR* exhibit expression profiles like that of *cpxP* over time in wild-type cells. Luminescence from wild-type (line with filled circle) and $\Delta cpxRA$ (dashed line with empty square) cells harboring *lux*-reporter plasmids grown in LB broth for 12 hours. The positive control *cpxP-lux* (gray), indicating Cpx activity, is plotted alongside the genes of interest: (A) *yebE* (dark purple), (B) *ygiB* (blue), (C) *bssR* (green), and (D) *htpX* (light purple). Data represents the mean and standard deviation of three biological replicate cultures. Gaps in data represent time points where no luminescence was detected thus could not be plotted on the log scale. The experiment was done twice with the results from one representative experiment shown.

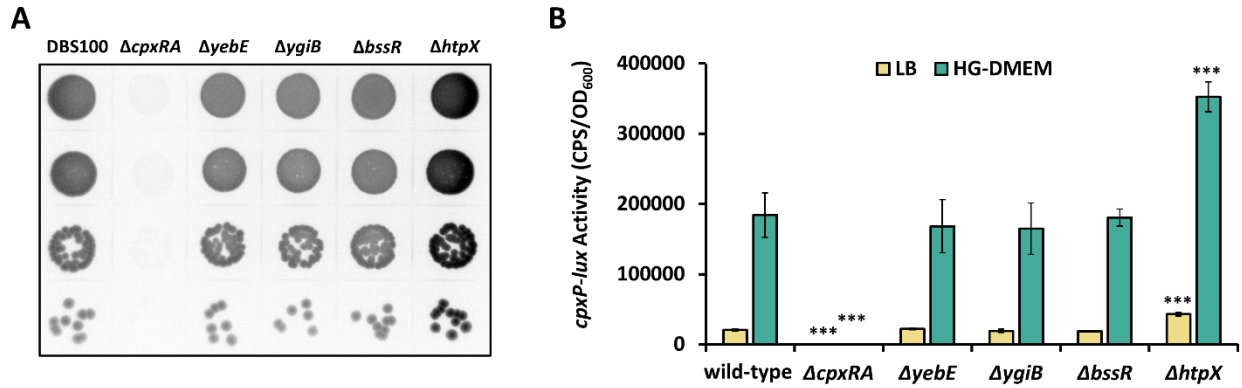


Figure 3.1.4. CpxRA is induced in the absence of *htpX*. (A) Wild-type and mutant strains harboring *cpxP-lux* reporters spotted on LB agar supplemented with kanamycin. (B) Strains harboring *cpxP-lux* reporter plasmids were grown in either LB (yellow) or HG-DMEM buffered with 0.1M MOPS (teal). The asterisks (***) indicate a statistically significant difference from the wild-type DBS100 strain in the same media type ($P < 0.001$, one-way ANOVA with Dunnett's multiple comparison test). Experiments were repeated twice with one set of representative data shown.

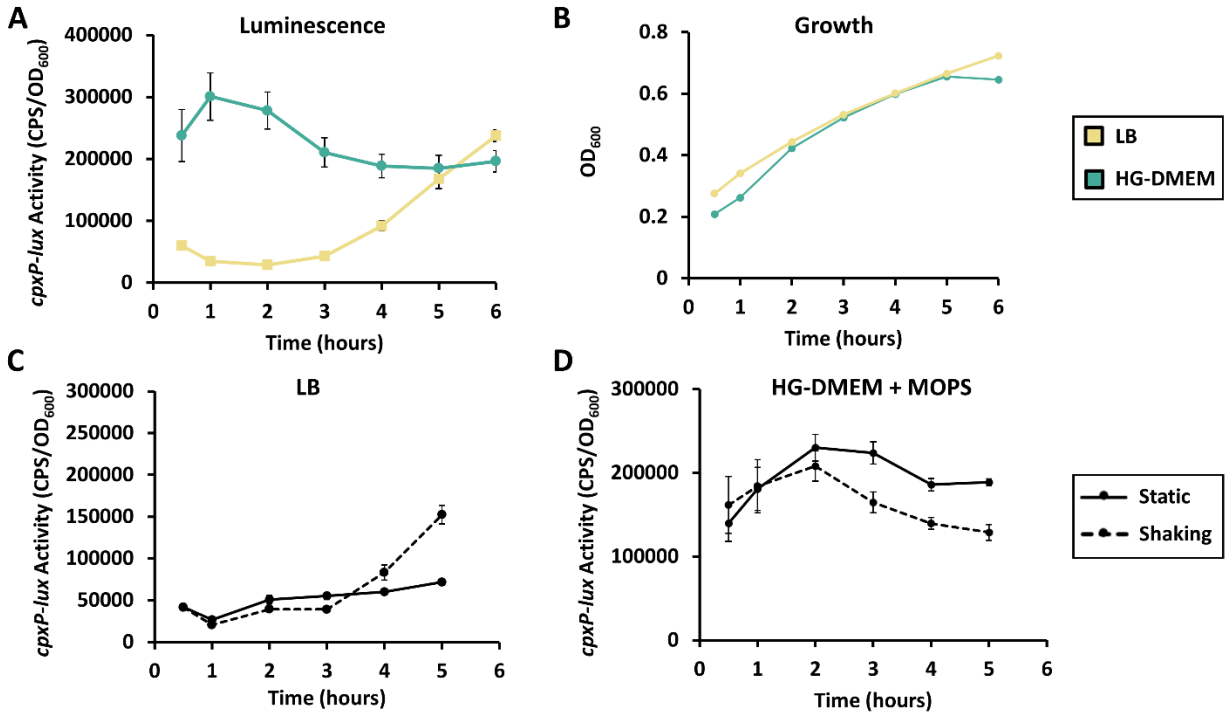


Figure 3.1.5. CpxRA activity is dependent on culturing conditions. (A) *cpxP-lux* activity and (B) growth measured in wild-type cells over time in either LB (yellow) or HG-DMEM buffered with 0.1M MOPS (teal). Cells were also grown in either (A) LB or (B) HG-DMEM buffered with 0.1M MOPS under static (solid line) or shaking (dashed line) conditions. Data represents the mean and standard deviation of three biological replicate cultures.

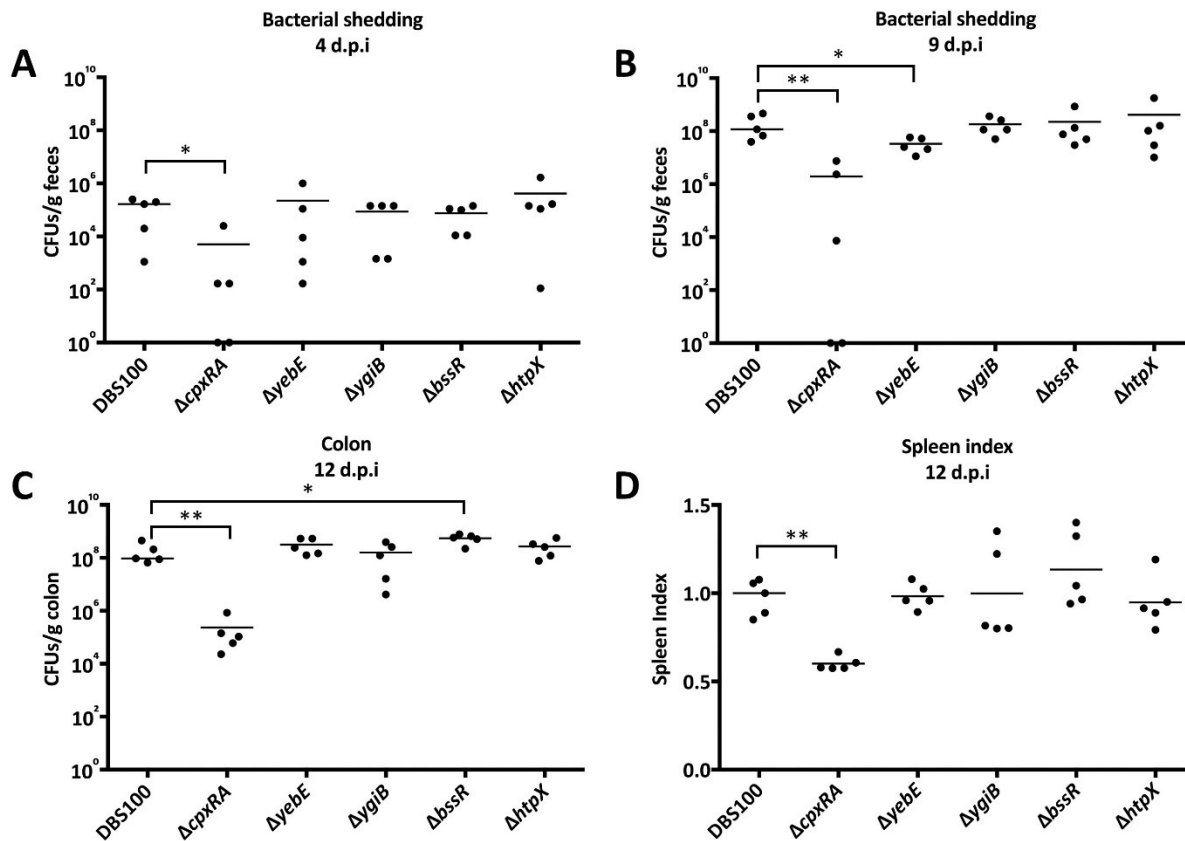


Figure 3.1.6. Genes of interest do not significantly contribute to *C. rodentium* colonization or virulence in C57Bl/6J mice. (A-C) Bacterial burden, per gram of feces at days 4 and 9 post-infection or the terminal centimeter of the colon on day 12, was measured in colony forming units (CFUs) by selective plating on MacConkey agar. (D) Spleens were harvested from euthanized mice and the spleen index was determined relative to mice infected with wild-type *C. rodentium*. (A-D) Horizontal lines indicate the median of n=5 mice and asterisks show significant differences between mice infected with wild-type versus those infected with a mutant strain (* $P < 0.05$, ** $P < 0.01$, Mann-Whitney U Test).

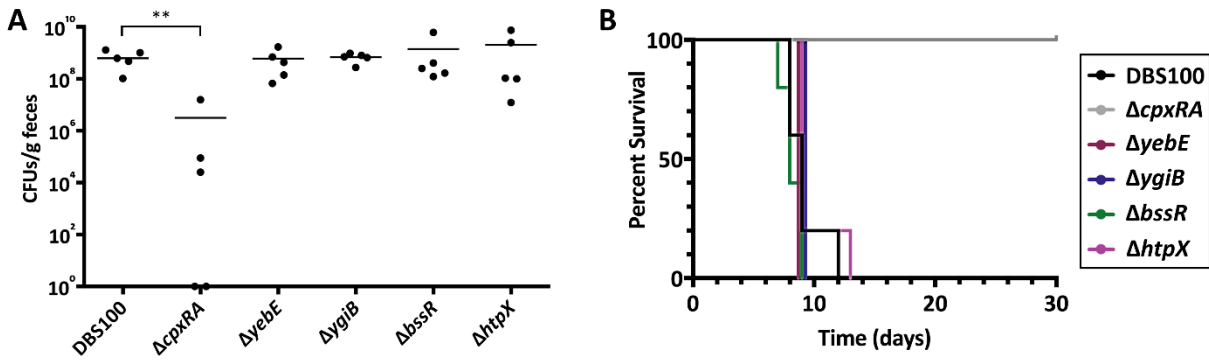


Figure 3.1.7. Genes upregulated by the Cpx ESR do not impact *C. rodentium* colonization or virulence in C3H/HeJ mice. (A) Colonization level was determined 4 days post-infection and measured in colony forming units (CFUs) per gram of feces. Horizontal lines indicate the median of n=5 mice and asterisks show significant differences between mice infected with wild-type versus those infected with a mutant strain (** $P < 0.01$, Mann-Whitney U Test). (B) Data depicts percent survival of mice infected with *C. rodentium* DBS100 strains over 30 days. Mice were euthanized if they reached any one of the following critical endpoints: 20% body weight loss, hunching and shaking, inactivity, or body condition score of < 2 .

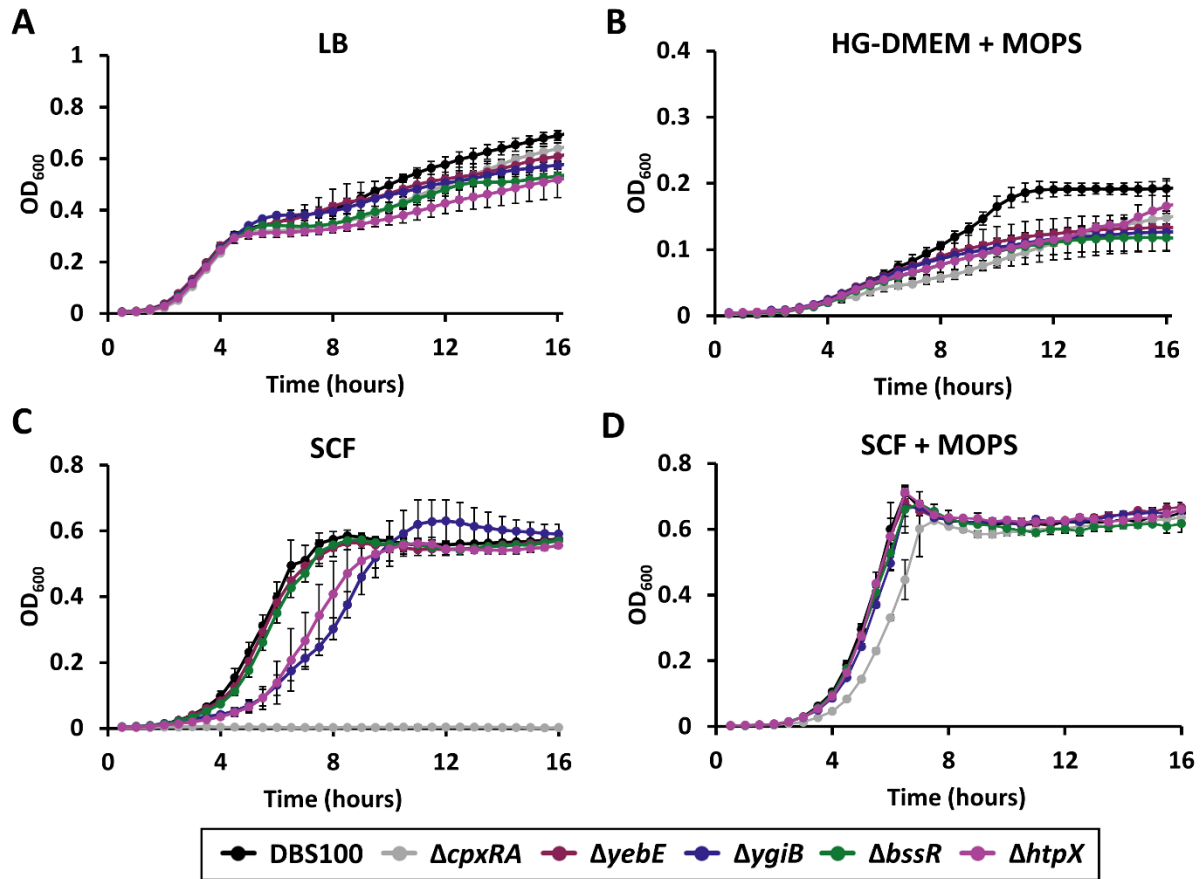


Figure 3.1.8. Simulated colonic fluid (SCF) promotes *C. rodentium* growth whilst indicating fitness defects in $\Delta cpxRA$, $\Delta ygiB$, and $\Delta htpX$. Strains were grown in (A) LB, (B) HG-DMEM with 0.1M MOPS, (C) SCF, and (D) SCF with 0.1M MOPS. Data represents the mean of three biological replicates and the error bars indicate the standard deviation. The experiment was completed twice with the data from one experiment shown.

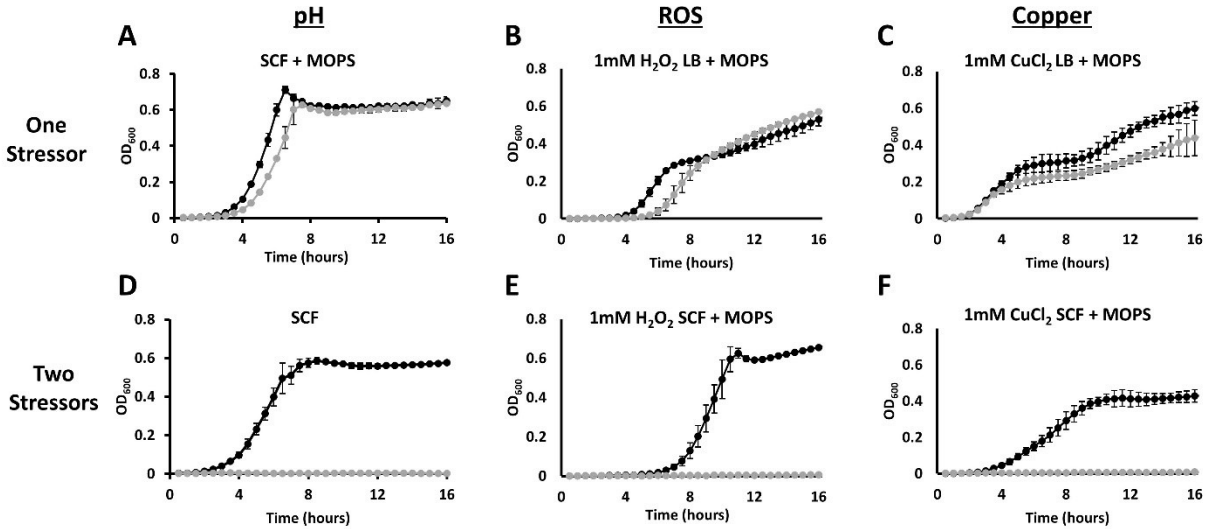


Figure 3.1.9. Simulated colonic fluid (SCF) highlights severe fitness defects in $\Delta cpxRA$ cells in response to sub-inhibitory levels of pH, oxidative, and copper stress. Strains were grown in (A, E, F) SCF with 0.1M MOPS, (B, C) LB with 0.1M MOPS or (D) SCF. Sub-inhibitory levels of the stressors (B, E) H₂O₂ to stimulate oxidative stress and (C, F) CuCl₂ for copper stress were added to cultures containing wild-type (black) or $\Delta cpxRA$ (grey) cells. Data represents the mean of three biological replicates and the error bars indicate the standard deviation. The experiments were completed three times with one representative experiment of each stressor shown.

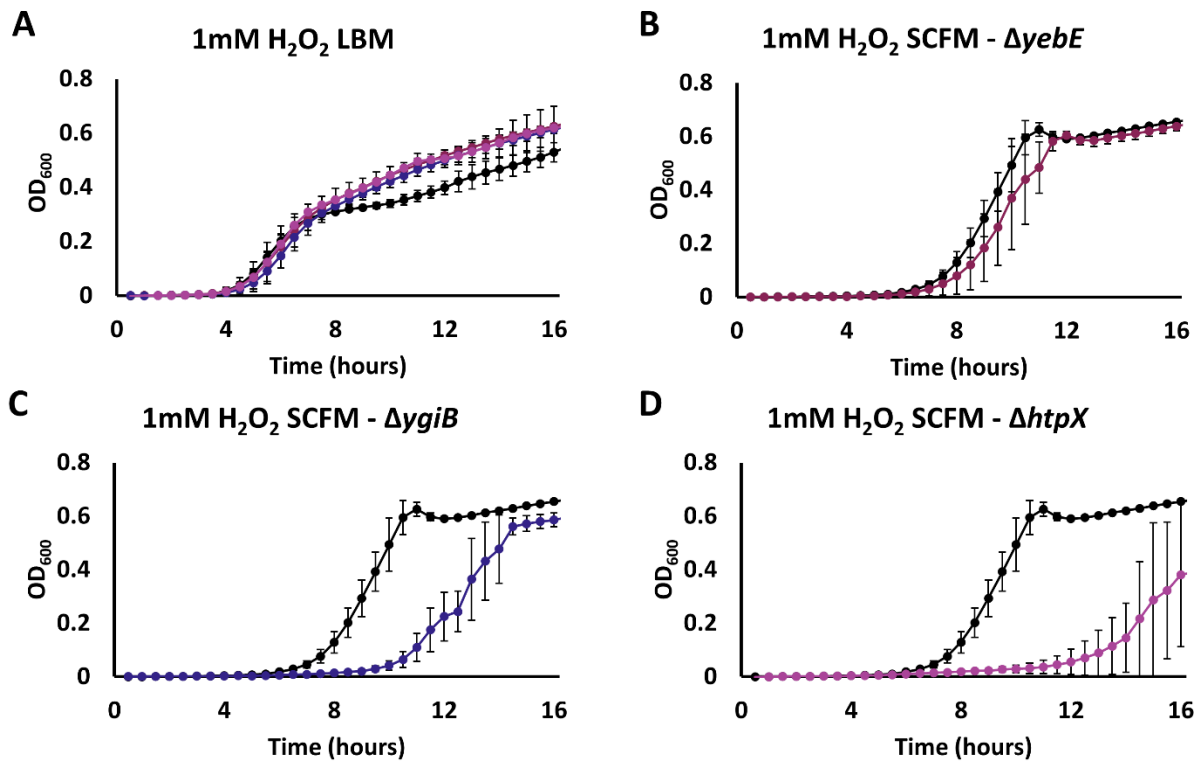


Figure 3.1.10. $\Delta yebE$, $\Delta ygiB$ and $\Delta htpX$ cells experience fitness defects in simulated colonic fluid (SCF) with oxidative stress. Strains were grown in (A) LB with 0.1M MOPS or (B-D) SCF with 0.1M MOPS. Sub-inhibitory levels of 1mM H₂O₂ was added to all wells containing either wild-type (black), $\Delta yebE$ (dark purple), $\Delta ygiB$ (blue), or $\Delta htpX$ (light purple) cells. Data represents the mean of three biological replicates and the error bars indicate the standard deviation. The experiments were completed three times with one representative experiment of each stressor shown.

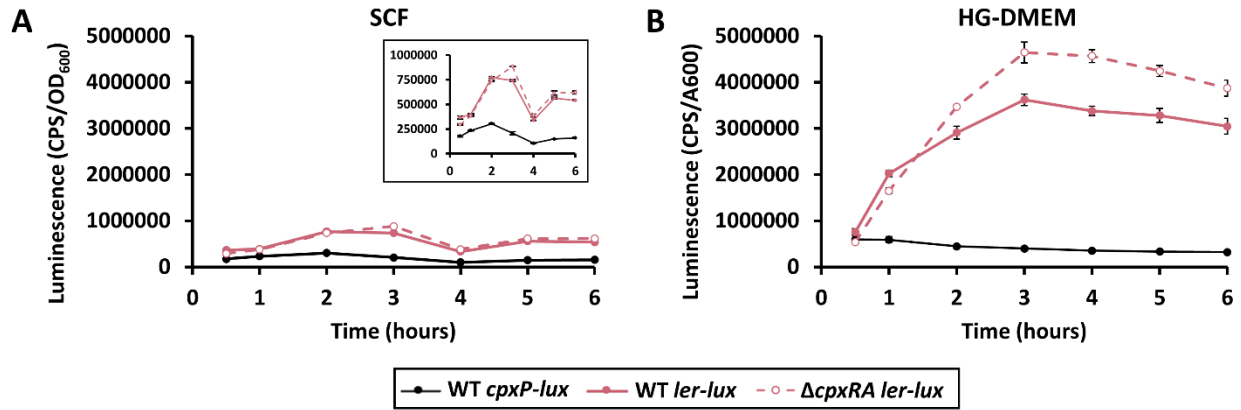


Figure 3.2.1. *C. rodentium* Δ *cpxRA* mutants show altered expression of LEE regulator, *ler*, in virulence-inducing conditions. Wild-type (solid line) and Δ *cpxRA* (dotted line) cells harboring *ler-lux* (pink) reporter plasmids and wild-type cells containing *cpxP-lux* (black) were grown in either (A) SCF buffered with 0.1M MOPS or (B) HG-DMEM buffered with 0.1M MOPS. Data represents the mean and standard deviation of three biological replicate cultures.

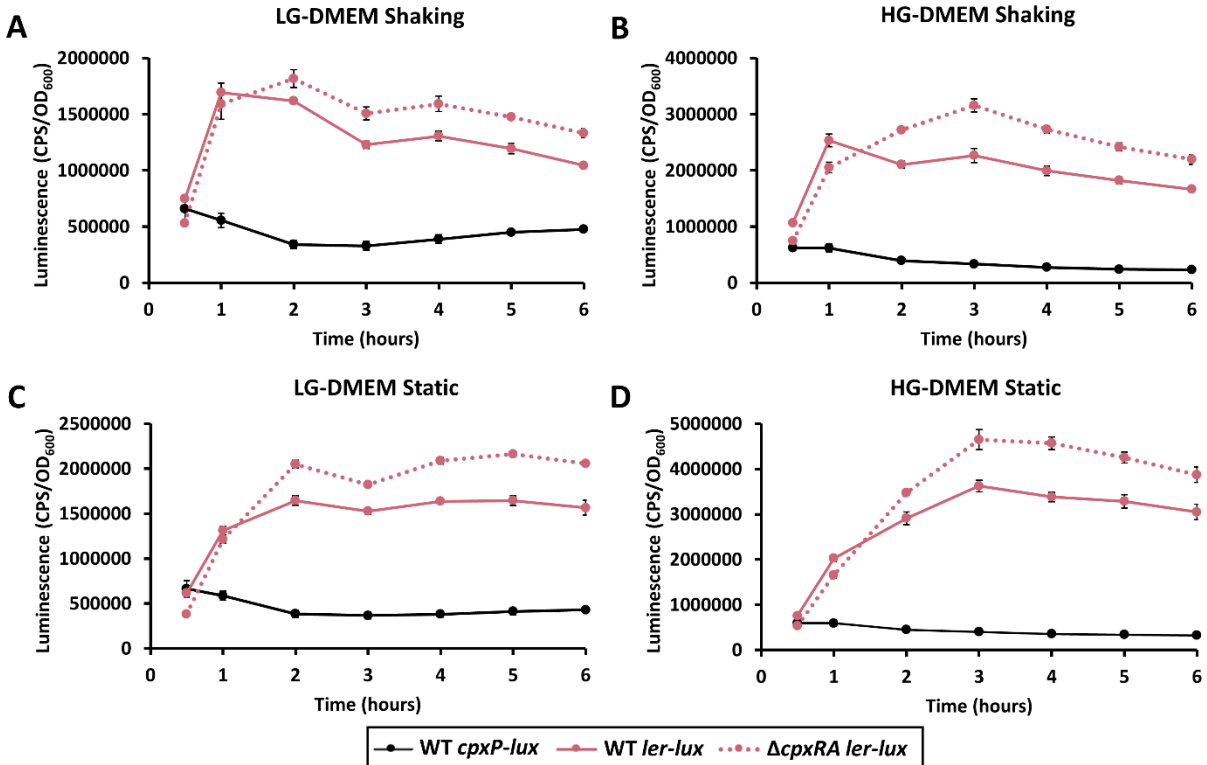


Figure 3.2.2. Expression of the LEE master regulator, *ler*, over time indicates reduced expression in the presence of CpxRA. Wild-type (solid line) and Δ *cpxRA* (dotted line) cells harboring *ler-lux* (pink) reporter plasmids and wild-type cells containing *cpxP-lux* (black) were grown under static and shaking conditions in either (A and C) low-glucose DMEM buffered with 0.1M MOPS or (B and D) HG-DMEM buffered with 0.1M MOPS. Data represents the mean and standard deviation of three biological replicate cultures. (D) Same data as presented in Figure 3.2.1B.

Table 3.2.1. Mined RNA-Seq and SILAC data from Vogt *et al.* (210) and microarray data collected in Giannakopoulou *et al.* (232) for potential CpxRA downregulated genes.

Data Source	Dataset S3- Vogt <i>et al.</i> (2019)		Giannakopoulou <i>et al.</i> (2018)	Protein Function ⁴
Gene Name ¹	Fold change RNA-Seq ²	Fold change SILAC ²	log2 fold change Δ cpxRA-WT microarray ³	
<i>pspA</i>	0.31	0.46	4.49	Phage shock protein A
<i>pspF</i>	2.03	1.04	1.10	Psp operon transcriptional activator
<i>cfcA</i> (ROD_RS22960)	N/A	N/A	-0.86	Putative type IV pilin
<i>cfcC</i> (ROD_RS22970)	N/A	N/A	1.99	Putative type IV pilus biogenesis protein
<i>kfcC</i> (ROD_RS20355)	0.39	0.46	0.22	Putative fimbrial subunit
<i>kfcF</i> (ROD_RS26805)	0.46	n.d.	1.65	Putative fimbrial subunit
<i>cts1G</i> (ROD_RS13655)	N/A	N/A	2.83	VgrG family T6SS protein
<i>espV</i> (ROD_RS09465)	N/A	N/A	2.43	Putative T3SS effector protein
<i>mpc</i> (ROD_RS14755)	N/A	N/A	1.74	T3SS regulator (LEE-encoded)
<i>yehD</i> (ROD_RS11070)	0.35	n.d.	-0.61	Fimbrial protein

Bolded values indicate $P_{adj} < 0.05$ (RNA-Seq), $FDR < 0.05$ (SILAC), $t\text{-test} < 0.05$ (microarray).

¹Locus tag for *C. rodentium* ICC168

²Calculated wild-type/ Δ cpxRA

³Positive value indicates lower expression in wild-type (WT) DBS100

⁴Protein function as described by UniProtKB for *C. rodentium* ICC168

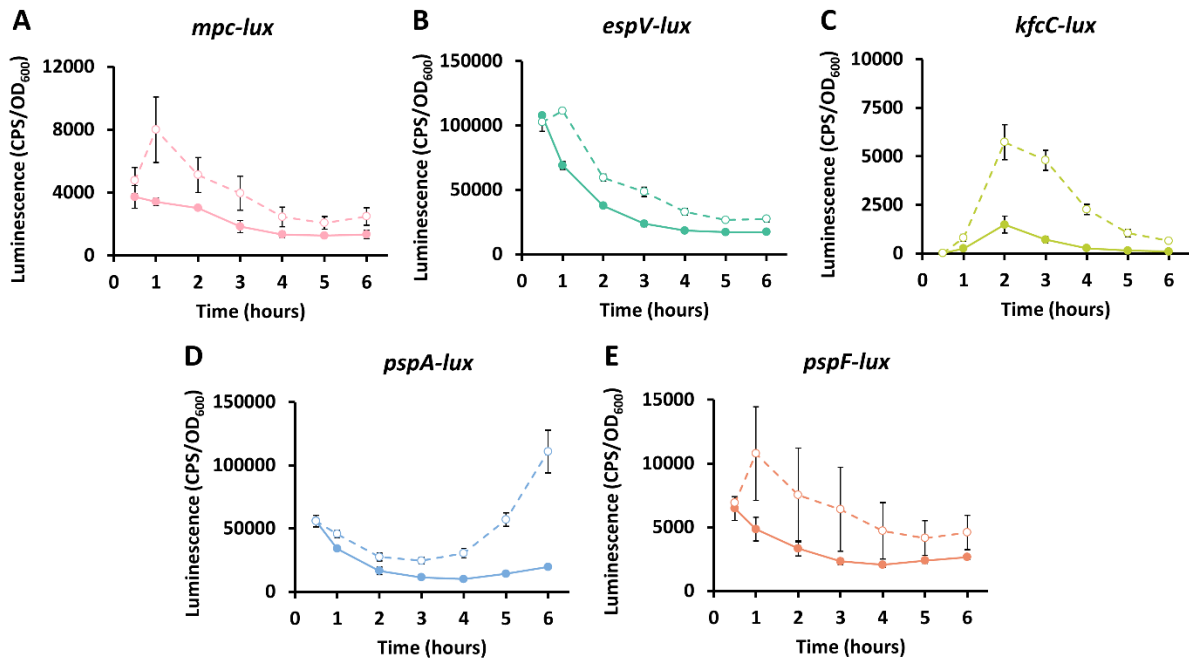


Figure 3.2.3. Virulence genes and the Psp response components, *pspA* and *pspF*, have reduced expression in the presence of CpxRA. Wild-type (solid line) and $\Delta cpxRA$ (dotted line) cells harboring reporter plasmids for the genes of interest *mpc* (A, pink), *espV* (B, green/blue), operon leader *kfcC* (C, yellow/green), *pspA* (D, blue), and *pspF* (E, orange) were grown in HG-DMEM buffered with 0.1M MOPS. Data represents the mean and standard deviation of three biological replicate cultures. The experiment was done twice with the results from one representative experiment shown.

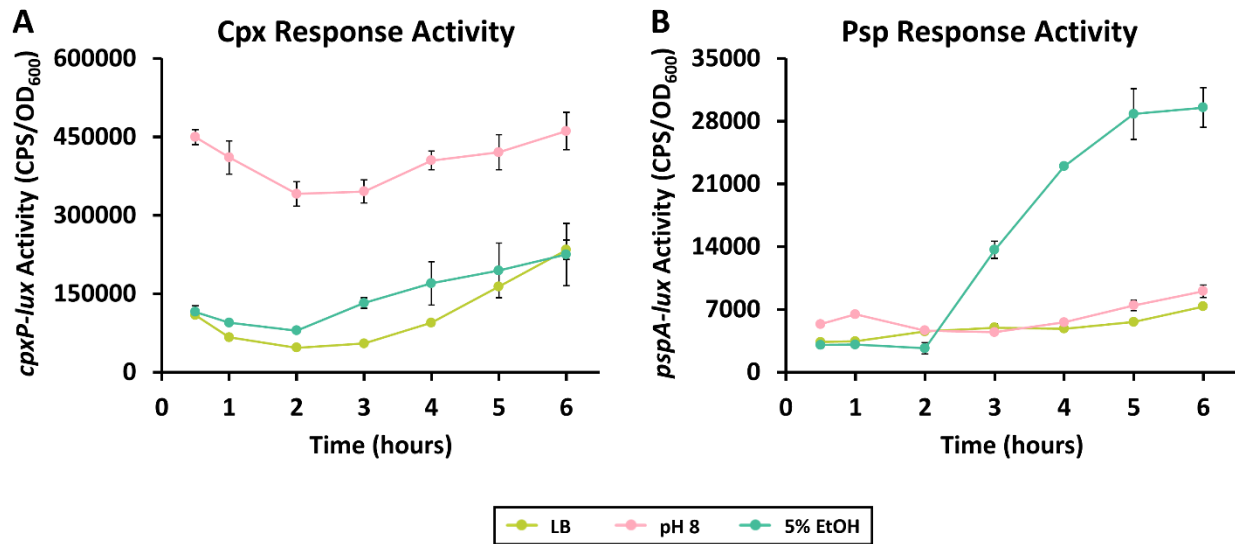


Figure 3.3.1. The activity of the Cpx response is strongly induced by alkaline pH while the Psp response is strongly induced by ethanol stress over time. Wild-type cells harboring either the reporter plasmid (A) *cpxP-lux* or (B) *pspA-lux* were grown in either LB (green), LB pH 8 buffered with 0.1M MOPS (pink), or LB with 5% ethanol (blue). Data represents the mean and standard deviation of three biological replicate cultures.

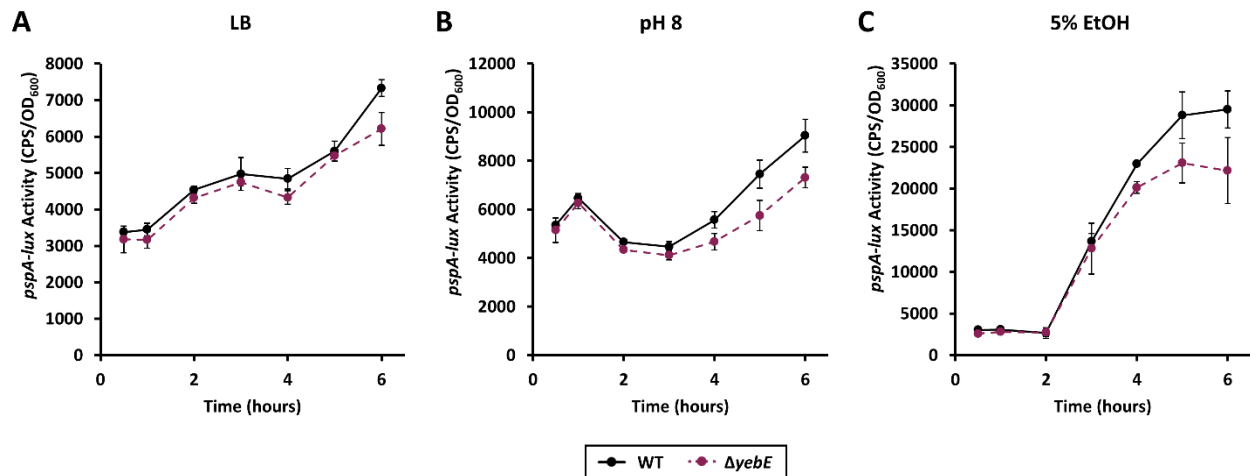


Figure 3.3.2. $\Delta yebE$ mutants exhibit lower levels of Psp activity relative to wild-type cells. Wild-type (solid line) and $\Delta yebE$ (dashed line and dark purple) cells harboring the reporter plasmid *pspA-lux*, indicative of the activity of the Psp response, were grown in either (A) LB, (B) LB pH 8 buffered with 0.1M MOPS, or (C) LB with 5% ethanol. Data represents the mean and standard deviation of three biological replicate cultures. The experiment was done twice with the results from one representative experiment shown.

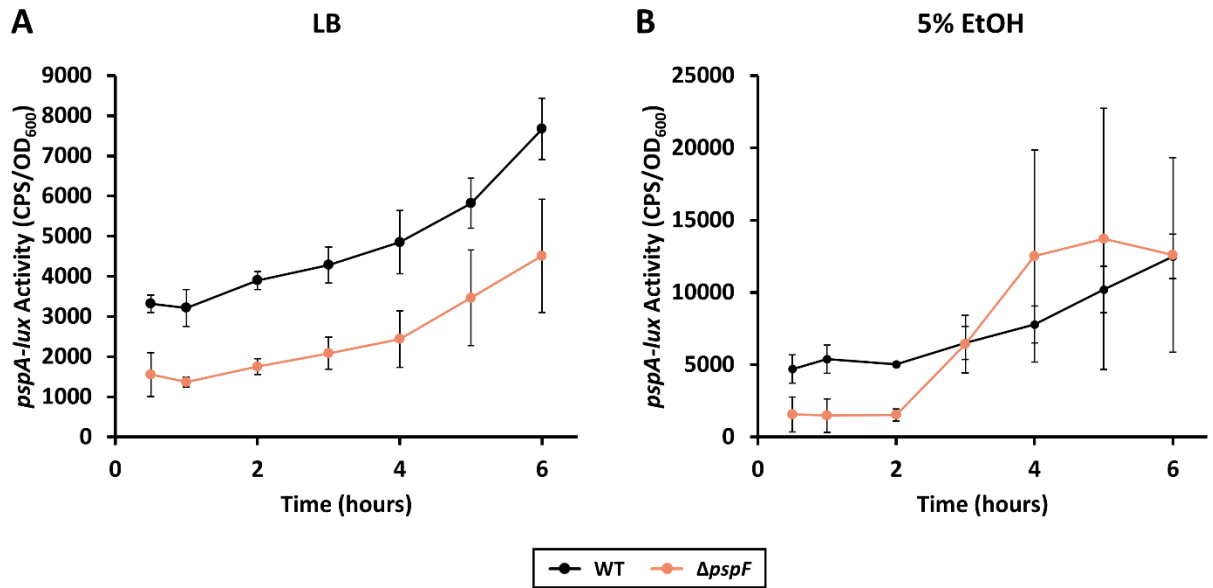


Figure 3.3.3. The Psp response regulator PspF is required for full and proper expression of *pspA* over time. Wild-type (black) and Δ *pspF* (orange) cells harboring the reporter plasmid *pspA-lux*, indicative of the activity of the Psp response, were grown in either (A) LB or (B) LB with 5% ethanol. Data represents the mean and standard deviation of three biological replicate cultures.

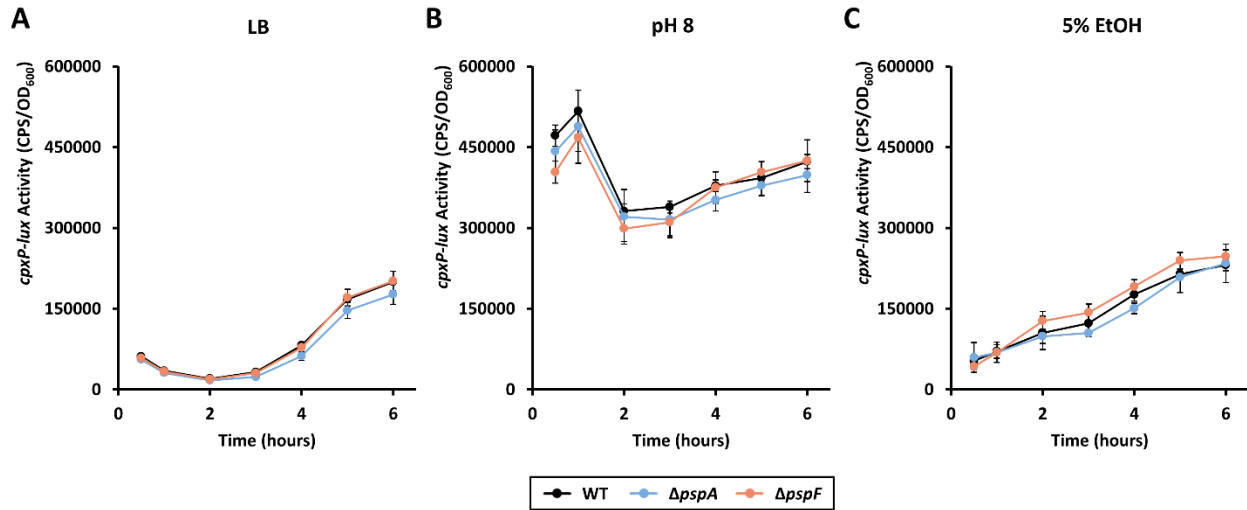


Figure 3.3.4. The activity of the Cpx response does not depend on the presence of an intact Psp response. Wild-type (black), $\Delta pspA$ (blue), and $\Delta pspF$ (orange) cells harboring the reporter plasmid *cpxP-lux*, indicative of the activity of the Cpx response, were grown in either (A) LB, (B) LB pH 8 buffered with 0.1M MOPS, or (C) LB with 5% ethanol. Data represents the mean and standard deviation of three biological replicate cultures.

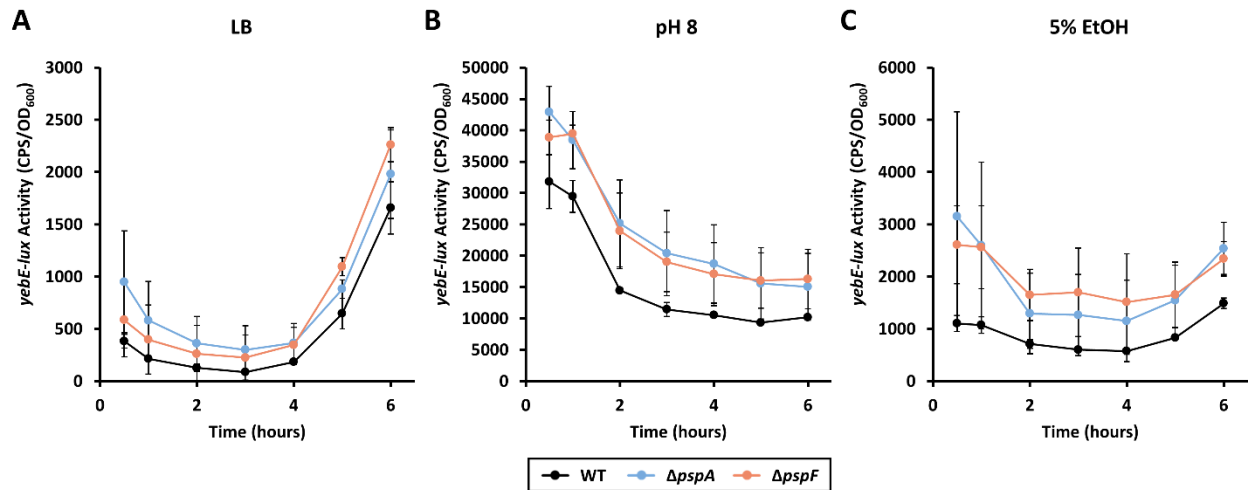


Figure 3.3.5. The absence of the Psp response members, *pspA* and *pspF*, moderately increases the expression of *yebE*. Wild-type (black), $\Delta pspA$ (blue), and $\Delta pspF$ (orange) cells harboring the reporter plasmid *yebE-lux* were grown in either (A) LB, (B) LB pH 8 buffered with 0.1M MOPS, or (C) LB with 5% ethanol. Data represents the mean and standard deviation of three biological replicate cultures.

Chapter 4. Discussion

4.1 Induction of the Cpx ESR over time is condition-specific

Throughout this study, we identified numerous growth conditions which influenced the activity of the Cpx ESR. HG-DMEM is commonly used for inducing the expression of virulence factors *in vitro* (70, 242). A previous study published microarray data indicating that HG-DMEM also moderately induced *cpxP* gene expression in EPEC cells overexpressing NlpE, relative to cells grown in LB, though they did not comment on this result being DMEM-dependent (241). Whilst DMEM has been used in previous Cpx-related studies to induce virulence gene expression, to our knowledge this is the first study to distinctly demonstrate a strong induction of the Cpx ESR in HG-DMEM relative to LB (Figure 3.1.1A) (210, 212, 230, 241, 243, 244). The Cpx ESR is associated with monitoring proper membrane protein biogenesis, the repression of virulence factors, and maintaining cell wall integrity (145). Therefore, its increased level of activity in HG-DMEM highlights the importance of stringent regulation of envelope functions under conditions where virulence factor expression is upregulated and suggests that the proper coordination of virulence factor production with envelope homeostasis may be just as important as their presence for pathogenesis *in vivo*.

Interestingly, while previous studies have shown that Cpx ESR activity is highest in late exponential or early stationary phase in LB, we found the activity of the Cpx ESR in HG-DMEM, indicated by the expression of the *cpxP-lux* reporter, was highest during log phase growth and reduced over time (Figure 3.1.5A-B) (204, 205). If HG-DMEM was a simple activator of the Cpx ESR, one would expect the pattern of expression for the positive control, *cpxP*, to remain the same albeit with the luminescence levels increased, however this was not observed (Figure 3.1.5A). These observations over time indicate the dynamic nature of the Cpx ESR and how the integration of numerous, likely intrinsic and extrinsic, signals can alter its

activity. While single time points can indicate activation or repression by the Cpx ESR, collecting data over time allows for a further understanding of the reliance a gene's expression has on the Cpx ESR throughout growth as evidenced by Figure 3.1.3.

In addition, not only did the media affect the activity levels of the Cpx ESR over time but also cultures grown in shaking versus static conditions impacted the level of Cpx activity in a media-dependent manner (Figure 3.1.5C-D). Expression of the *cpxP-lux* reporter was influenced differently by a shaking versus static culture depending on the medium used as opposed to the speed of growth, as both cultures grew faster in shaking conditions (data not shown). Previous studies have shown that static and shaking cultures can impact gene regulation and resulting phenotypes. In *Salmonella enterica*, it has been shown that the expression of *hilA* is CpxA-dependent in low pH and its expression is increased when cultures are grown statically (252). In uropathogenic *E. coli*, the agglutination titer was opposite for wild-type and strains lacking the small RNA, RyfA, when either grown shaking or statically in both LB and human urine (253). Therefore, our study highlights the importance of culture conditions on the activity of the Cpx ESR and prompts questions as to the nature of the envelope stressors in the media tested and by extension how those conditions could impact the physiology of growing cells.

4.2 Elucidating the regulation of uncharacterized genes by the Cpx ESR

One of the objectives of this study was to develop an understanding of the Cpx-dependent regulation for the relatively uncharacterized genes *yebE* and *ygiB*. In *E. coli*, YebE is an uncharacterized predicted inner membrane protein that shares homology with TerB-like proteins and contains putative metal binding sites (UniProtKB Accession no. P33218, GenBank

CAD6012101.1). According to the protein prediction software InterProScan and TMHMM Server v. 2.0, YebE has two transmembrane domains, a linker in the cytoplasm, and a large globular protein structure in the periplasm (254–257). YebE is a widely conserved protein largely in the classes alpha-, delta- and gammaproteobacteria with homologs identified in Pseudomonales, Enterobacterales, Rhizobiales, and Burkholderiales among others, as identified by the database eggNOG 5.0 (258). Previous genome screens and microarrays have correlated the induction of *yebE* expression in *E. coli* with fluoroquinolone resistance, and in response to alkaline pH, copper stress, and UV irradiation though minimal work has been done to characterize the function of the encoded protein (189, 259, 260). *yebE* is unique in this study as its expression appears to rely largely on the presence of the Cpx ESR in the conditions tested (Figure 3.1.1A, Figure 3.1.3A). While other genes, like *ygiB*, *bssR*, and *htpX*, maintained expression in the Δ *cpxRA* mutant, the expression of *yebE* was mostly abolished in LB, and in wild-type *C. rodentium* closely resembled the expression pattern of *cpxP* over time (Figure 3.1.1A, Figure 3.1.3A). While we have found that YebE is not required for colonization nor virulence *in vivo*, our results indicate the encoded protein could perhaps aid in maintaining cell membrane integrity and/or mediating oxidative stress during growth in simulated colonic fluid providing direction for future study of this gene (Figure 3.1.10B).

YgiB is a predicted outer membrane lipoprotein which was originally suggested to be encoded in an operon with *tolC* (239). According to the bioinformatic database EcoCyc's transcription unit predictor, *ygiB* in *E. coli* MG1655 is transcribed along with *tolC* from promoters upstream of *tolC* (BioCyc ID: TU0-14701) (239, 261, 262). However, the *ygiB-lux* reporter constructed for this thesis contained only the base pairs in between the predicted end of *tolC* and approximately 50 base pairs downstream from the predicted translation start site of *ygiB*

and did not contain any previously known or predicted promoters (239, 261, 262). Therefore, our results indicate that *ygiB* is under the control of its own promoter and can be differentially expressed from *tolC* by the Cpx ESR in that *ygiB* expression is induced upon stress while *tolC* is reduced (Figure 3.1.2A-B).

Currently the only major phenotypes associated with *ygiB* include an exacerbation of $\Delta tolC$ growth defects in minimal media with glucose when cells are lacking the YgiBC and YjfMC proteins as well as an induction of expression during mature biofilm formation (239, 263). YjfMC are homologous to YgiBC but are encoded in a different section of the *E. coli* chromosome (239). When grown in simulated colonic fluid in the presence of hydrogen peroxide to induce oxidative stress, $\Delta ygiB$ cells were unable to grow until approximately 10 hours post-inoculation where apparent suppressor mutations developed as indicated by the large deviations in growth between biological replicates (Figure 3.1.10C). In addition, albeit slight, we found that $\Delta ygiB$ cells have a reduced growth rate relative to wild-type cells in the presence of copper stress when grown in SCF (data not shown). Numerous studies have shown that *tolC* is required for resistance to bile as a part of the AcrAB-TolC efflux pump in *E. coli* as well as colonization *in vivo* for various pathogenic bacteria (92, 264–267). Given the exacerbation of the $\Delta tolC$ mutant growth defect with the absence of *ygiBC* demonstrated by Dhamdhare *et al.* (2010), the differential regulation of *tolC* and *ygiB* by the Cpx ESR seen in this study, and the susceptibility of $\Delta ygiB$ cells to additional stressors when grown in SCF containing bile, it is intriguing to suggest that perhaps YgiB complements the function of TolC in stressful conditions under the control of the Cpx ESR. In other words, the Cpx ESR may act to minimize large membrane proteins like TolC from integrating into a stressed membrane and instead upregulate YgiB to

carry out similar functions in the meantime. Since evidence for the function of *ygiB* is largely lacking in current literature, these results could provide an interesting avenue for future work.

4.3 SCF is beneficial for determining colonization efficacy and susceptibilities of mutants to stressors

While HG-DMEM has been a frequent media used to induce virulence gene expression and mimic an *in vivo* environment prior to conducting animal model experiments, we chose to investigate the fitness of our mutants in a medium relevant to the conditions present in the colon by using SCF (70, 242). SCF is a relatively uncommon media in individual pathogen fitness studies as in the past it has primarily been used for determining drug solubility and delivery systems which involve looking at the microbiota's effect on drug release (268, 269). A more frequently used gastrointestinal fluid is simulated gastric fluid (SGF) which has been used to demonstrate acid-tolerance of pathogens like EPEC, EHEC, *Vibrio cholerae*, *Listeria monocytogenes*, and *Salmonella* (81, 270–272). One study in *Salmonella* demonstrated differences in cell viability upon exposure to gastrointestinal fluids where they found gastric juice with a pH of 4 or 5 in conjunction with bile salts from simulated intestinal juice reduced cell viability greater than acidic pH alone (272). In this study we show that simulating the conditions *C. rodentium* cells face during colonization of the colon using SCF was able to uncover growth defects and susceptibilities in $\Delta cpxRA$ cells and the mutants of our genes of interest that would have been unidentified in LB or HG-DMEM (Figure 3.1.8, Figure 3.1.9, Figure 3.1.10). Of note, wild-type *C. rodentium* grew to a significantly higher OD in SCF relative to LB and HG-DMEM and had an increased growth rate relative to that in HG-DMEM

suggesting that this media simulates an environment this gastrointestinal pathogen has adapted to (Figure 3.1.8). In addition, the growth phenotypes in buffered SCF paralleled the *in vivo* colon colonization of each mutant thus highlighting the versatility and replicability of using simulated physiological conditions (Figure 3.1.7A, Figure 3.1.8D). Furthermore, mutant cells grown in SCF were more susceptible to extraneous stressors than wild-type *C. rodentium* which could allow for greater insight into the function of genes, like *yebE* and *ygiB*, which previously had no known associated growth phenotypes (Figure 3.1.10B-D).

Interestingly, the $\Delta cpxRA$ mutant had an increased lag phase when grown in the presence of oxidative stress in LB while growth was abolished in SCF with H₂O₂ (Figure 3.1.9B and E). As detailed thoroughly in recent reviews, it is understood that *C. rodentium* utilizes aerobic respiration to outcompete host microbiota during colonization (6, 103, 119). A previous study found that deletion of the *cydAB* genes in *C. rodentium*, which contribute to aerobic respiration in low-oxygen environments, resulted in a severe reduction of growth *in vivo* (101, 273). Following this, it was determined that disruption to the mitochondrial respiration of intestinal epithelial cells is largely responsible for *C. rodentium* infection causing oxygenation of the mucosal surface (102). The Cpx ESR has been implicated in the regulation of aerobic respiration in EPEC where it has been shown that removal of *cpxRA* reduced the oxygen consumption capabilities of cells which was attributed to problems with cytochrome *bo₃* oxidase biogenesis or function (274). Similar conclusions have been made in *Salmonella typhimurium* which also utilizes aerobic respiration to expand in the gastrointestinal tract and experiences colonization defects in the absence of CpxRA (275, 276).

A follow up study to Lopez *et al.* (101) found that prior to expansion by aerobic respiration, *C. rodentium* utilizes host derived H₂O₂ as an electron acceptor during anaerobic

respiration via cytochrome *c* peroxidase (*ccp*) (116). Both wild-type and Δ *ccp* mutant cells could survive in LB in the presence of mM concentrations of H₂O₂, though in the absence of *ccp* there was increased expression of the catalase-peroxidase, *katG*, suggesting that cells were experiencing higher levels of oxidative stress. In the RNA-seq data from Vogt *et al.* (210), *katG* expression was also significantly induced in the *cpxRA* mutant grown in HG-DMEM which suggests the cells were experiencing elevated levels of oxidative stress (data not shown). Given that rapid expansion by aerobic respiration is a proposed mechanism of *C. rodentium* pathogenesis in overcoming colonization resistance and the production of reactive oxygen species by intestinal epithelial cells is an important defense mechanism, our results utilizing SCF support the implication that the Cpx ESR is required to successfully adapt to encountered oxidative stressors during colonization in the gastrointestinal tract (101, 124, 277, 278).

The formulation of SCF used in this study, with the substitution of ox bile for porcine bile, was developed by Beumer *et al.* (235) with the intention of isolating non-culturable but viable *Campylobacter jejuni* coccoid cells. The recipe for this media proved unique from other versions of colonic fluid that have been used to study EHEC as it contained proteose-peptone, used porcine bile as opposed to bile salts, as well as lacked Bacto tryptone (279, 280). Utilizing formulations different from those in this study, Musken *et al.* (279) used simulated intestinal fluids mimicking the ileum and colon to demonstrate differential expression of a major fimbrial subunit in sorbitol-fermenting EHEC while Polzin *et al.* (280) found that EHEC proteins involved in nucleotide biosynthesis and the expression of Shiga toxins were increased in simulated ileal and colonic environments. In addition, it was found that outer membrane vesicle (OMV) production and cytotoxicity, which is an important virulence factor, as well as OMV-associated Shiga toxin 2a in EHEC was increased in both simulated ileal and colonic

environments (281). On the other hand, OMV cytotoxicity and OMV-associated Shiga toxin 2a were not increased in DMEM which was confirmed with RT-qPCR for *stx_{2a}* expression (281). These studies, in conjunction with the data presented here, highlight the importance of using a physiologically relevant environment when it comes to monitoring gene and protein expression in cells to predict gastrointestinal survival, colonization, and virulence. While we found that HG-DMEM is superior at inducing the expression of the virulence factor *ler*, we propose that SCF would be a useful medium to screen genes that have the potential to be involved in or required for colonization (Figure 3.2.1).

4.4 The presence of the Cpx ESR negatively impacts the expression of master LEE regulator, *ler*

Previous studies have shown that the Cpx ESR negatively impacts the expression of virulence factors. In EPEC, overexpression of the response regulator CpxR reduced the activation of LEE1, LEE4, and LEE5 while the removal of CpxR resulted in increased expression of all five LEE operons when in a non-pathogenic *E. coli* background that lacked *ler* indicating the regulation of the LEE by the Cpx ESR was likely *ler*-independent (244). In EHEC, it has also been shown that the Cpx ESR negatively regulates virulence factors, including those that are LEE-encoded through Sigma factor 32 and the Lon protease (243). On the other hand, a recent study by Kumar *et al.* (282) proposed a model for EHEC suggesting that CpxR upregulates the expression of *ler* directly and that serotonin is an inhibitor of the Cpx ESR which results in reduced transcription of the LEE. The authors used RT-qPCR and growth in low-glucose DMEM to show that *ler* was reduced in the absence of CpxR in EHEC and was reduced

in *C. rodentium* $\Delta cpxA$ (282). Due to these findings, we wished to verify the impact of the Cpx ESR on the expression of *ler* to determine whether the avirulence associated with the $\Delta cpxRA$ mutant could be due to reduced expression of the LEE in *C. rodentium*. Unlike Kumar *et al.* (282), our data indicates that in SCF, the impact of the Cpx ESR on *ler* expression is minimal with a slight increase in expression in the absence of the Cpx ESR (Figure 3.2.1A). We also found that in both high- or low-glucose DMEM, in static and shaking conditions, the expression of *ler* is consistently higher in the absence of the Cpx ESR (Figure 3.2.1B, Figure 3.2.2). Therefore, our data suggests the colonization and virulence phenotypes observed for the $\Delta cpxRA$ mutant is not due to reduced expression of *ler* but perhaps could be in part from the overexpression of *ler* which may contribute to reduced fitness and inappropriately timed virulence mechanisms *in vivo*.

4.5 Virulence factors are more stringently expressed in the presence of CpxRA

Originally known as 10036 in EHEC and *orf12* in EPEC, *mpc* (multiple point controller) was first characterized as a regulatory protein of the LEE in EHEC (41). *mpc* is the operon leader of polycistronic LEE3, which encodes numerous structural proteins of the T3SS apparatus like EscV, a translocase, and EscN, the ATPase (41–44). In EPEC, *orf12* is required for T3SS protein secretion, pedestal formation, and virulence *in vivo* (18). In terms of regulatory function, *mpc* translation is required for the expression of downstream genes while overexpression represses *ler* activity (41, 44). Using RT-qPCR, Sun *et al.* (2016), found that the expression of *mpc* was under tight control as transcripts levels remained low relative to the other LEE3 genes. Interestingly,

our results suggest that in the absence of CpxRA, the expression of *mpc* is significantly increased relative to wild-type cells in a virulence-inducing condition (Figure 3.2.3A). Given that the transcription of *mpc* has been suggested to be under stringent regulation for proper T3SS expression, it is intriguing that the presence of the Cpx ESR would influence its expression (41, 44). Due to the complex regulation of *mpc* including that exerted by Ler and histone-like nucleoid structuring protein (H-NS), which also regulate each other and are influenced by secondary regulators like SspA, the nature of the interaction between the Cpx ESR on *mpc* transcription has yet to be determined (46, 49, 62, 283). One hypothesis is that in the absence of CpxRA, *ler* expression is increased which subsequently increases the expression of the entire LEE, including *mpc* (Figure 3.2.1 and Figure 3.2.2) (50, 55). On the other hand, it is possible that the change in expression of *mpc* is an indirect result from having the removal of the Cpx ESR impact the functionality of the inner membrane which could subsequently impact sensors or regulators associated with the T3SS (145, 185, 187). To this end, Mpc, also known as Orf12 and CesL, is proposed to be a class I chaperone that interacts with SepL and SepD, which have been identified as gate keepers of initial T3SS translocator and effector secretion through interaction with basal apparatus components EscU and EscV (53, 284–287). Under host-adapted conditions, transcript levels of *mpc* isolated from *C. rodentium* were increased relative to bacteria grown anaerobically on fecal media suggesting that the expression of *mpc* is important *in vivo*, perhaps for the critical and *in vivo* induced timing of LEE gene expression (288). Although the T3SS secreted protein profile in *C. rodentium* has been shown to be unimpacted by the absence of *cpxRA in vitro*, suggesting the T3SS remains functional, it could be postulated that the timing of the secretion or order with which the proteins are secreted could be affected *in vivo* in a $\Delta cpxRA$ mutant with contribution from the dysregulation of *mpc* (210, 231).

EspV, an effector protein that is dependent on T3SS translocation in EPEC 2348/69 but not EHEC O157:H7, has been shown *in vitro* via ectopic expression and in cell culture to induce morphological changes like condensed nuclei, dendritic-like projections, and cell rounding in eukaryotic cells (247, 289). Despite this, it is not required for *C. rodentium* colonization or virulence as a $\Delta espV$ mutant infection was insignificantly different from that of wild-type cells in both C3H/He and C57Bl6 mice (247). While the function of EspV is relatively uncharacterized in *C. rodentium*, the reduced expression of *espV-lux* in the presence of CpxRA provides an avenue for future research (Figure 3.2.3B). Previous research has shown differential effects of the presence of the Cpx ESR on effector protein expression. In the microarray data generated by Giannakopoulou *et al.* (232), the absence of CpxRA downregulated the expression of T3SS effector protein *espO*, which has been implicated in stimulating the secretion of IL-22 and antimicrobial peptides with higher $\Delta espO$ bacterial burdens present in late infections due to reduced immune response (290, 291). IL-22 is important for controlling *C. rodentium* early infection and clearance of pathogens (292, 293). On the other hand, the RNA-seq data from Vogt *et al.* (210) indicated significantly lower expression of numerous T3SS effector proteins in the presence of CpxRA and through verification by RT-qPCR, determined the Cpx ESR influenced the non-LEE encoded effector *nleB1* transcriptionally. This suggests that the presence of CpxRA can differentially impact the expression of numerous effector proteins in *C. rodentium* which may, individually or collectively, contribute negatively to the colonization and virulence defects associated with a $\Delta cpxRA$ mutant.

The *kfc* operon (C-H) has been implicated in a moderate disruption to *C. rodentium* colonization duration *in vivo* and is induced by bicarbonate-mediated induction of RegA through removal of H-NS repression (64, 65). Both *kfcC* and *kfcF* were chosen for luminescent reporter

construction however no luminescence was produced from the *kfcF-lux* plasmid in HG-DMEM (data not shown). On the other hand, *kfcC* was moderately expressed in HG-DMEM and experienced a significant increase in expression relative to WT in the absence of CpxRA (Figure 3.2.3C). Vogt *et al.* (210) previously hypothesized that the reduction in expression of *kfc* in the presence of CpxRA may constitute a mechanism for preventing high amounts of large protein complexes from being assembled in a stressed inner membrane. Previous RNA-seq data has indicated that *kfcC* expression is induced under host-adapted conditions relative to LB in *C. rodentium* (288). Therefore, regulation or control over this induction could be important for overall fitness *in vivo*. Our results support the conclusions by Vogt *et al.* (210) where the Δ *cpxRA* mutant had increased activation of the *kfcC* promoter which we determined is prolonged over time and may be detrimental *in vivo*.

4.6 The Cpx ESR influences the activity of the Psp response

The Psp response was originally characterized following *E. coli* infection by filamentous phage and was later found to be induced in response to heat, ethanol, and osmotic shock (Figure 1.2) (251, 294). *pspA* encodes Phage Shock Protein A (PspA) and functions as a negative regulator for the Psp response as well as an effector protein by forming a multimeric complex that associates with the inner membrane seemingly to dissipate disruptions to PMF (155, 245, 246). *pspF* is a regulatory enhancer protein transcribed in the opposite direction from *pspABCDE* and enhances the expression of the *psp* operon by binding upstream of *pspA* (163, 165). To our knowledge, there has been no work conducted to characterize the Psp response in *C. rodentium*. As evidenced by the luminescent reporters shown in Figure 3.2.3D-E and Figure 3.3.2, *C. rodentium* expresses both *pspA* and *pspF*. In *E. coli*, the Psp response is thought to maintain

proton motive force and induction has been associated with biofilm formation and disruptions to bacterial protein secretion/translocation (mislocalized secretins), indicating that it is likely under the control of multiple signals (155, 166, 246, 251, 263, 295–297). The results presented in Figure 3.2.3D-E indicate that the Psp response is more active in the absence of CpxRA. The Cpx ESR upregulates factors like DegP and DsbA, a periplasmic protease and chaperone, respectively, which are involved in the maintenance of envelope protein folding and degradation (188, 207, 211). In addition, sRNAs associated with the Cpx ESR, CpxQ and CyaR, have been implicated in the maintenance of PMF suggesting another source for Psp-induction in the absence of CpxRA (reviewed by (298)). The rapid increase of expression starting 3 hours post-resuspension of *pspA-lux* over time in the $\Delta cpxRA$ mutant corresponds with previous findings in *E. coli* where *pspA-lac* expression rapidly increased approximately 3 hours after exposure to antibiotics that affect lipid biosynthesis as well as protein translocation (Figure 3.2.3D) (299).

Another two-component system, ArcAB, has been associated with the activity of the Psp response under certain conditions. ArcAB is required for full induction of the Psp response by protein-IV secretin stress in a PspBC-dependent manner via the sensor kinase ArcB (166). In this study, Jovanovic *et al.* (166), also tested *pspA-lac* expression in a $\Delta cpxA$ mutant using β -galactosidase assays and exposed the cells to various stressors, including ethanol, where they determined that the induction of the Psp response was unaffected by the absence of *cpxA* in *E. coli* MG1655. The absence of an effect on the Psp response by a $\Delta cpxA$ mutant is intriguing in conjunction with our results, suggesting that expression of *pspA* by the Cpx ESR may be CpxR-dependent, though this requires further experimentation as the differences observed could also be organism- or condition-specific (Figure 3.2.3D-E) (166).

pspF encodes a σ^{54} transcriptional activator and is under the control of a σ^{70} promoter where its expression is maintained at a low level regardless of stressors encountered (163, 165). The transcription of *pspF* in *E. coli* is inhibited by 6S RNA at elevated pH as well as negatively self-regulated by PspF in wild-type cells *in vitro* (165, 300). Therefore, it was unexpected to identify a rapid increase in expression of *pspF-lux* between 0.5 and 1 hour in the $\Delta cpxRA$ mutant which remained increased relative to wild-type cells throughout the 6-hour assay (Figure 3.2.3E). In addition, the large error bars for *pspF-lux* expression in the $\Delta cpxRA$ mutant indicate possible dysregulation or uncontrolled expression of *pspF* in stressful conditions like HG-DMEM (Figure 3.2.3E). Given that the transcription of *pspF* is tightly controlled and the activity of the Psp response relies on the abundance of the transcriptional activator relative to PspA, the influence of the Cpx ESR on the transcription of *pspF* could suggest that CpxR acts as a negative regulator of *pspF*. On the other hand, the absence of CpxRA could indirectly activate the expression of *pspF* either from increased membrane stress experienced by the cell from removal of the Cpx ESR or via other transcriptional regulators like sRNAs.

The Psp response has been shown to be required for virulence in *Yersinia enterocolitica* and the intracellular pathogen *Salmonella* Typhimurium (168, 301, 302). In the case of *Y. enterocolitica*, the Psp response is required to mediate stress on the membrane caused by the production of a T3SS, and more specifically the secretin YscC (168, 169). Our data suggests that the LEE-encoded T3SS of *C. rodentium* could have altered expression in the $\Delta cpxRA$ mutant in HG-DMEM from the data collected for the *ler-lux* and *mpc-lux* constructs, which could result in T3SS-mediated stress on the inner membrane leading to the induction of the Psp response (Figure 3.2.2, Figure 3.2.3A, Figure 3.2.3D-E). Altogether, while it is unclear from the results presented here whether the impact of the Cpx ESR on the components of the Psp response, *pspA*

and *pspF*, is direct from aiding in the regulation of *pspF* transcription or is derived from other factors influenced by the presence of CpxRA, like membrane homeostasis or virulence mechanisms, it is evident that maintaining inner membrane integrity in HG-DMEM is important for *C. rodentium*.

Given that our results in Figure 3.2.3D-E indicate an interaction between the Cpx ESR and Psp response, it was important to identify conditions that could differentially regulate both envelope stress responses to further investigate this connection. To this end, we determined that alkaline pH did not induce the Psp response and ethanol stress only moderately induced the Cpx response (Figure 3.3.1). This lack of connection between the Cpx ESR and the Psp response induction is supported by results from *Y. enterocolitica* where overexpression of secretins only induced the Psp response and there was little overlap between the induction of the Psp, Cpx, and RpoE responses (303). In addition to differential-inducing conditions, the activity of *cpxP-lux* was measured in the absence of two Psp components, PspA and PspF. The Δ *pspA* mutant would be unable to elicit the effector functions like maintenance of PMF while the Δ *pspF* mutant has reduced Psp response activity in LB and extremely dysregulated activity in ethanol stress (Figure 3.3.3) (155). This was somewhat surprising in that previous studies have reported the absence of *pspF* abolishes the expression of the Psp operon though this difference could be explained by varying experimental conditions, reporters or bacterial species (164, 166, 218). Regardless, we found that the absence of either PspA or PspF does not impact the activity of the Cpx response as indicated by the expression of *cpxP-lux* in LB and in both Cpx- and Psp-inducing conditions (Figure 3.3.4). This supports the notion provided by Bury-Moné *et al.* (218), that the Cpx ESR may modulate envelope stress response in general while other stress responses, including the Psp response, have a more specialized function in maintaining envelope integrity. They also found

that the regulon of PspF overlaps with that of CpxR indicating potential for crosstalk (218). Overall, our results support the conclusion that the presence of the Cpx ESR impacts the expression of both *pspA* and *pspF* and by extension the activity of the Psp response, while the activity of the Cpx response is independent from a fully functional Psp response.

4.7 Interactions identified between Cpx-regulated YebE and the Psp response

Novel to the field of study involving the Psp response, we have identified an interaction between the presence of YebE on the activity of the Psp response as well as the presence of a complete Psp response on the expression of YebE. Based on a high-throughput genetic screen produced by Babu *et al.* (250), there was predicted interactions between *yebE* and *pspACE* (BioGRID alias: Y75_p1822) (248, 249). This is particularly significant in that PspACE constitute the components of the Psp response which occupy the cytoplasm (PspA), inner membrane (PspC), and periplasm (PspE), while YebE is an uncharacterized inner membrane protein predicted to have regions in the cytoplasm, inner membrane, and periplasm (UniProtKB Accession no. P33218, GenBank CAD6012101.1) (see Figure 1.2 for Psp response model) (155, 245, 254–257). Beyond localization predictions, a connection can be seen in microarray analysis of fluoroquinolone-resistant *E. coli* strains where *yebE*, *pspC*, *pspE*, and *pspD* were all upregulated relative to fluoroquinolone-sensitive *E. coli* (259). Similarly, in *E. coli* cells overexpressing an outer membrane esterase autotransporter, the expression of YebE, the Cpx ESR, and the Psp response was significantly increased suggesting induction by envelope stress (229). In support of a more direct connection between YebE and the Psp response, we have shown in the absence of YebE, the activity of the Psp response indicated by *pspA-lux* activity is reduced over time in both alkaline pH and in ethanol stress (Figure 3.3.2B-C). Therefore, it is

possible that through uncharacterized interactions, YebE could be important for the signaling or stabilization of the Psp response components at the inner membrane, which results in a moderately stronger induction of *pspA-lux* expression in stressful conditions (Figure 3.3.2B-C).

Furthering this connection, our results also indicate that in the absence of either *pspA* or *pspF*, the expression of *yebE* is induced (Figure 3.3.5). Our previous data indicates that YebE expression relies heavily on the presence of the Cpx ESR as in a $\Delta cpxRA$ mutant, *yebE-lux* activity is essentially abolished (Figure 3.1.1A and Figure 3.1.3A). In addition, the induction is strongest in alkaline pH relative to ethanol stress, which is a condition that strongly induces the Cpx ESR where one would expect subsequently higher levels of *yebE* expression (Figure 3.3.1A, Figure 3.3.5). On the other hand, it is interesting that while the presence of the Psp response components seemingly doesn't impact the expression of *cpxP-lux*, it does influence the expression of *yebE-lux* which suggests that perhaps other factors influence the expression of *yebE* beyond only the Cpx ESR (Figure 3.3.4, Figure 3.3.5). With these observations in combination, it could be hypothesized that *yebE* expression is induced in response to general membrane stress which is further exacerbated in the absence of the Psp stress response.

Future work should include elucidating whether the interaction between YebE and the Psp response is Cpx-dependent as well as identifying if these transcriptional effects are also evident at the protein-level. It would also be important to experimentally confirm the localization of YebE and to determine if protein-protein interactions exist between YebE and the inner membrane components of the Psp response, namely PspACE. In addition, it would be interesting to determine if more specific stressors, such as problems with protein secretion or direct disruptions to PMF with carbonyl cyanide-m-chlorophenylhydrazone (CCCP) known to induce *pspA* expression, would more clearly elucidate the influence of YebE on the Psp response and

vice versa (304). Utilizing overexpression vectors of YebE could further elucidate its role in cell physiology and the impact of YebE on the Psp response. To identify a connection between the Cpx ESR and the Psp response, determining if *pspF* is directly regulated by CpxR using either an electrophoretic mobility shift assay or identifying and deleting putative CpxR binding sites followed with a reporter assay would shed light on the proposed crosstalk between these two responses. It would also be important to determine if the effects of YebE on the Psp response and vice versa are CpxRA dependent utilizing double knockouts. While it is tempting to suggest that the Cpx response somehow regulates the Psp response through YebE, further research is required to identify if a direct mechanism exists.

4.8 Concluding remarks

This thesis resulted in three major sections of findings broadly categorized into Cpx upregulated genes and the role of the Cpx response in pathogenesis, genes downregulated by the Cpx ESR, and the interactions between the Cpx ESR, YebE, and the Psp response. In the first objective, uncharacterized members of the *C. rodentium* Cpx regulon were investigated to determine if they were responsible for the avirulent phenotype exhibited *in vivo*. Our results demonstrate that neither *yebE*, *ygiB*, *bssR*, nor *htpX* are required for virulence, although they each require the Cpx ESR for maximal expression in multiple conditions and over different growth phases. In addition, we provide evidence that fitness defects exacerbated in a simulated gut environment likely contribute to the colonization defect and attenuation of virulence exhibited by Δ *cpxRA* mutant cells. The second objective shifted the focus to genes downregulated by the CpxRA which were confirmed using luminescent reporters grown in HG-DMEM. A major theme highlighted in this objective was that the virulence factors, such as *ler*,

mpc, *espV*, and *kfcC*, were downregulated in the presence of CpxRA and highlighted a potential importance in the timing of the expression of virulence mechanisms in terms of physiologically relevant conditions like SCF and HG-DMEM. Lastly, we uncovered a novel interaction between the Cpx ESR, YebE, and the Psp response. While the nature of these interactions requires further study, it contributes interesting observations to the currently uncharacterized protein YebE and highlights a one-way crosstalk between the Cpx ESR and the Psp response. In general, this thesis contributes to the scientific community by providing novel growth phenotypes associated with the $\Delta cpxRA$ mutant, highlights the importance of using physiologically relevant conditions when studying mechanisms that could be translatable *in vivo*, and provides a foundation for future research to investigate the uncharacterized protein YebE and its connection to envelope stress.

References

1. Lenz A, Tomkins J, Fabich AJ. 2015. Draft genome sequence of *Citrobacter rodentium* DBS100 (ATCC 51459), a primary model of enterohemorrhagic *Escherichia coli* virulence. *Genome Announc* 3:e00415-15.
2. Schauer DB, Zabel BA, Pedraza IF, O'Hara CM, Steigerwalt AG, Brenner DJ. 1995. Genetic and biochemical characterization of *Citrobacter rodentium* sp. nov. *J Clin Microbiol* 33:2064–2068.
3. Schauer DB, Falkow S. 1993. Attaching and effacing locus of a *Citrobacter freundii* biotype that causes transmissible murine colonic hyperplasia. *Infect Immun* 61:2486–2492.
4. Schauer DB, Falkow S. 1993. The *eae* gene of *Citrobacter freundii* biotype 4280 is necessary for colonization in transmissible murine colonic hyperplasia. *Infect Immun* 61:4654–4661.
5. Baker DG. 1998. Natural pathogens of laboratory mice, rats, and rabbits and their effects on research. *Clin Microbiol Rev* 11:231–266.
6. Mullineaux-Sanders C, Sanchez-Garrido J, Hopkins EGD, Shenoy AR, Barry R, Frankel G. 2019. *Citrobacter rodentium*–host–microbiota interactions: immunity, bioenergetics and metabolism. *Nat Rev Microbiol* 17:701–715.
7. Khan MA, Bouzari S, Ma C, Rosenberger CM, Bergstrom KSB, Gibson DL, Steiner TS, Vallance BA. 2008. Flagellin-dependent and -independent inflammatory responses following infection by enteropathogenic *Escherichia coli* and *Citrobacter rodentium*. *Infect Immun* 76:1410–1422.
8. Barthold SW, Coleman GL, Bhatt PN, Osbaldiston GW, Jonas AM. 1976. The etiology of transmissible murine colonic hyperplasia. *Lab Anim Sci* 26:889–894.
9. Mundy R, MacDonald TT, Dougan G, Frankel G, Wiles S. 2005. *Citrobacter rodentium* of mice and man. *Cell Microbiol* 7:1697–1706.

10. Collins JW, Keeney KM, Crepin VF, Rathinam VAK, Fitzgerald KA, Finlay BB, Frankel G. 2014. *Citrobacter rodentium*: Infection, inflammation and the microbiota. *Nat Rev Microbiol* 12:612–623.
11. Luperchio SA, Schauer DB. 2001. Molecular pathogenesis of *Citrobacter rodentium* and transmissible murine colonic hyperplasia. *Microbes Infect* 3:333–340.
12. Simmons CP, Goncalves NS, Ghaem-Maghami M, Bajaj-Elliott M, Clare S, Neves B, Frankel G, Dougan G, MacDonald TT. 2002. Impaired resistance and enhanced pathology during infection with a noninvasive, attaching-effacing enteric bacterial pathogen, *Citrobacter rodentium*, in mice lacking IL-12 or IFN- γ . *J Immunol* 168:1804–1812.
13. Vallance BA, Deng W, Jacobson K, Finlay BB. 2003. Host susceptibility to the attaching and effacing bacterial pathogen *Citrobacter rodentium*. *Infect Immun* 71:3443–3453.
14. Diez E, Zhu L, Teatero SA, Paquet M, Roy MF, Loredó-Ostí JC, Malo D, Gruenheid S. 2011. Identification and characterization of *CriI*, a locus controlling mortality during *Citrobacter rodentium* infection in mice. *Genes Immun* 12:280–290.
15. Teatero SA, Thomassin JL, Zhu L, Diez E, Malo D, Gruenheid S. 2011. The *CriI* locus is the common genetic cause of susceptibility to *Citrobacter rodentium* infection in C3H and FVB mouse strains. *Gut Microbes* 2:173-177.
16. Papapietro O, Teatero S, Thanabalasuriar A, Yuki KE, Diez E, Zhu L, Kang E, Dhillon S, Muise AM, Durocher Y, Marcinkiewicz MM, Malo D, Gruenheid S. 2013. R-Spondin 2 signalling mediates susceptibility to fatal infectious diarrhoea. *Nat Commun* 4:1898.
17. Mundy R, Girard F, Fitzgerald AJ, Frankel G. 2006. Comparison of colonization dynamics and pathology of mice infected with enteropathogenic *Escherichia coli*, enterohaemorrhagic *E. coli* and *Citrobacter rodentium*. *FEMS Microbiol Lett* 265:126–132.
18. Deng W, Puente JL, Gruenheid S, Li Y, Vallance BA, Vázquez A, Barba J, Ibarra JA, O'Donnell P, Metalnikov P, Ashman K, Lee S, Goode D, Pawson T, Finlay BB. 2004. Dissecting virulence: Systematic and functional analyses of a pathogenicity island. *Proc*

- Natl Acad Sci U S A 101:3597–3602.
19. Petty NK, Bulgin R, Crepin VF, Cerdeño-Tárraga AM, Schroeder GN, Quail MA, Lennard N, Corton C, Barron A, Clark L, Toribio AL, Parkhill J, Dougan G, Frankel G, Thomson NR. 2010. The *Citrobacter rodentium* genome sequence reveals convergent evolution with human pathogenic *Escherichia coli*. *J Bacteriol* 192:525–538.
 20. Robinson CM, Sinclair JF, Smith MJ, O'Brien AD. 2006. Shiga toxin of enterohemorrhagic *Escherichia coli* type O157:H7 promotes intestinal colonization. *Proc Natl Acad Sci U S A* 103:9667–9672.
 21. Eppinger M, Cebula TA. 2015. Future perspectives, applications and challenges of genomic epidemiology studies for food-borne pathogens: A case study of enterohemorrhagic *Escherichia coli* (EHEC) of the O157:H7 serotype. *Gut Microbes* 6:194–201.
 22. Bugarel M, Martin A, Fach P, Beutin L. 2011. Virulence gene profiling of enterohemorrhagic (EHEC) and enteropathogenic (EPEC) *Escherichia coli* strains: A basis for molecular risk assessment of typical and atypical EPEC strains. *BMC Microbiol* 11:142.
 23. Vallance BA, Chan C, Robertson ML, Finlay BB. 2002. Enteropathogenic and enterohemorrhagic *Escherichia coli* infections: Emerging themes in pathogenesis and prevention. *Can J Gastroenterol* 16:771–778.
 24. Donnenberg MS, Finlay BB. 2013. Combating enteropathogenic *Escherichia coli* (EPEC) infections: the way forward. *Trends Microbiol* 21:317–319.
 25. Baldini MM, Kaper JB, Levine MM, Candy DCA, Moon HW. 1983. Plasmid-mediated adhesion in enteropathogenic *Escherichia coli*. *J Pediatr Gastroenterol Nutr* 2:534–538.
 26. Sohel I, Puente JL, Ramer SW, Bieber D, Wu CY, Schoolnik GK. 1996. Enteropathogenic *Escherichia coli*: Identification of a gene cluster coding for bundle-forming pilus morphogenesis. *J Bacteriol* 178:2613–2628.
 27. Stone KD, Zhang HZ, Carlson LK, Donnenberg MS. 1996. A cluster of fourteen genes

- from enteropathogenic *Escherichia coli* is sufficient for the biogenesis of a type IV pilus. *Mol Microbiol* 20:325–337.
28. Tobe T, Sasakawa C. 2001. Role of bundle-forming pilus of enteropathogenic *Escherichia coli* in host cell adherence and in microcolony development. *Cell Microbiol* 3:579–585.
 29. Girôn JA, Ho ASY, Schoolnik GK. 1991. An inducible bundle-forming pilus of enteropathogenic *Escherichia coli*. *Science* 254:710–713.
 30. Mundy R, Pickard D, Wilson RK, Simmons CP, Dougan G, Frankel G. 2003. Identification of a novel type IV pilus gene cluster required for gastrointestinal colonization of *Citrobacter rodentium*. *Mol Microbiol* 48:795–809.
 31. Caballero-Flores GG, Croxen MA, Martínez-Santos VI, Finlay BB, Puente JL. 2015. Identification and regulation of a novel *Citrobacter rodentium* gut colonization fimbria (Gcf). *J Bacteriol* 197:1478–1491.
 32. Gueguen E, Cascales E. 2013. Promoter swapping unveils the role of the *Citrobacter rodentium* CTS1 type VI secretion system in interbacterial competition. *Appl Environ Microbiol* 79:32–38.
 33. Mellies JL, Barron AMS, Carmona AM. 2007. Enteropathogenic and enterohemorrhagic *Escherichia coli* virulence gene regulation. *Infect Immun* 75:4199–4210.
 34. Phillips AD, Navabpour S, Hicks S, Dougan G, Wallis T, Frankel G. 2000. Enterohaemorrhagic *Escherichia coli* O157:H7 target Peyer's patches in humans and cause attaching/effacing lesions in both human and bovine intestine. *Gut* 47:377–381.
 35. Law RJ, Gur-Arie L, Rosenshine I, Finlay BB. 2013. *In vitro* and *in vivo* model systems for studying enteropathogenic *Escherichia coli* infections. *Cold Spring Harb Perspect Med* 3:a009977.
 36. Lewis SB, Cook V, Tighe R, Schüller S. 2015. Enterohemorrhagic *Escherichia coli* colonization of human colonic epithelium *in vitro* and *ex vivo*. *Infect Immun* 83:942–949.
 37. Wiles S, Clare S, Harker J, Huett A, Young D, Dougan G, Frankel G. 2004. Organ

- specificity, colonization and clearance dynamics *in vivo* following oral challenges with the murine pathogen *Citrobacter rodentium*. *Cell Microbiol* 6:963–972.
38. Wiles S, Pickard KM, Peng K, MacDonald TT, Frankel G. 2006. *In vivo* bioluminescence imaging of the murine pathogen *Citrobacter rodentium*. *Infect Immun* 74:5391–5396.
 39. Deng W, Li Y, Vallance BA, Finlay BB. 2001. Locus of enterocyte effacement from *Citrobacter rodentium*: Sequence analysis and evidence for horizontal transfer among attaching and effacing pathogens. *Infect Immun* 69:6323–6335.
 40. Woodward SE, Krekhno Z, Finlay BB. 2019. Here, there, and everywhere: How pathogenic *Escherichia coli* sense and respond to gastrointestinal biogeography. *Cell Microbiol* 21:e13107.
 41. Tsai NP, Wu YC, Chen JW, Wu CF, Tzeng CM, Syu W. 2006. Multiple functions of *l0036* in the regulation of the pathogenicity island of enterohaemorrhagic *Escherichia coli* O157:H7. *Biochem J* 393:591–599.
 42. Gauthier A, Puente JL, Finlay BB. 2003. Secretin of the enteropathogenic *Escherichia coli* type III secretion system requires components of the type III apparatus for assembly and localization. *Infect Immun* 71:3310–3319.
 43. Andrade A, Pardo JP, Espinosa N, Pérez-Hernández G, González-Pedrajo B. 2007. Enzymatic characterization of the enteropathogenic *Escherichia coli* type III secretion ATPase EscN. *Arch Biochem Biophys* 468:121–127.
 44. Sun WSW, Chen JW, Wu YC, Tsai HY, Kuo YL, Syu WJ. 2016. Expression regulation of polycistronic *lee3* genes of enterohaemorrhagic *Escherichia coli*. *PLoS One* 11:e0155578.
 45. Portaliou AG, Tsolis KC, Loos MS, Balabanidou V, Rayo J, Tsirigotaki A, Crepin VF, Frankel G, Kalodimos CG, Karamanou S, Economou A. 2017. Hierarchical protein targeting and secretion is controlled by an affinity switch in the type III secretion system of enteropathogenic *Escherichia coli*. *EMBO J* 36:3517–3531.
 46. Turner NCA, Connolly JPR, Roe AJ. 2018. Control freaks—signals and cues governing the regulation of virulence in attaching and effacing pathogens. *Biochem Soc Trans*

- 47:229–238.
47. Wan B, Zhang Q, Tao J, Zhou A, Yao YF, Ni J. 2016. Global transcriptional regulation by H-NS and its biological influence on the virulence of enterohemorrhagic *Escherichia coli*. *Gene* 588:115–123.
 48. Shin M. 2017. The mechanism underlying Ler-mediated alleviation of gene repression by H-NS. *Biochem Biophys Res Commun* 483:392–396.
 49. Bustamante VH, Santana FJ, Calva E, Puente JL. 2001. Transcriptional regulation of type III secretion genes in enteropathogenic *Escherichia coli*: Ler antagonizes H-NS-dependent repression. *Mol Microbiol* 39:664–678.
 50. Yang J, Tauschek M, Hart E, Hartland EL, Robins-Browne RM. 2010. Virulence regulation in *Citrobacter rodentium*: the art of timing. *Microb Biotechnol* 3:259–268.
 51. Barba J, Bustamante VH, Flores-Valdez MA, Deng W, Finlay BB, Puente JL. 2005. A positive regulatory loop controls expression of the locus of enterocyte effacement-encoded regulators Ler and GrlA. *J Bacteriol* 187:7918–7930.
 52. Jobichen C, Li M, Yerushalmi G, Yih WT, Mok YK, Rosenshine I, Ka YL, Sivaraman J. 2007. Structure of GrlR and the implication of its EDED motif in mediating the regulation of type III secretion system in EHEC. *PLoS Pathog* 3:e69.
 53. Díaz-Guerrero M, Gaytán MO, Soto E, Espinosa N, García-Gómez E, Marcos-Vilchis A, Andrade A, González-Pedrajo B. 2021. CesL regulates type III secretion substrate specificity of the enteropathogenic *E. coli* injectisome. *Microorganisms* 9:1047.
 54. Deng W, Yu HB, Li Y, Finlay BB. 2015. SepD/SepL-dependent secretion signals of the type III secretion system translocator proteins in enteropathogenic *Escherichia coli*. *J Bacteriol* 197:1263–1275.
 55. Platenkamp A, Mellies JL. 2018. Environment Controls LEE Regulation in Enteropathogenic *Escherichia coli*. *Front Microbiol* 9:1694.
 56. Connolly JPR, Finlay BB, Roe AJ. 2015. From ingestion to colonization: The influence of

- the host environment on regulation of the LEE encoded type III secretion system in enterohaemorrhagic *Escherichia coli*. *Front Microbiol* 6:658.
57. Friedberg D, Umanski T, Fang Y, Rosenshine M. 1999. Hierarchy in the expression of the locus of enterocyte effacement genes of enteropathogenic *Escherichia coli*. *Mol Microbiol* 34:941–952.
 58. Goldberg MD, Johnson M, Hinton JCD, Williams PH. 2001. Role of the nucleoid-associated protein Fis in the regulation of virulence properties of enteropathogenic *Escherichia coli*. *Mol Microbiol* 41:549–559.
 59. Madrid C, Balsalobre C, García J, Juárez A. 2007. The novel Hha/YmoA family of nucleoid-associated proteins: use of structural mimicry to modulate the activity of the H-NS family of proteins. *Mol Microbiol* 63:7–14.
 60. Sharma VK, Zuerner RL. 2004. Role of *hha* and *ler* in transcriptional regulation of the *esp* operon of enterohemorrhagic *Escherichia coli* O157:H7. *J Bacteriol* 186:7290–7301.
 61. Tauschek M, Yang J, Hocking D, Azzopardi K, Tan A, Hart E, Praszkiar J, Robins-Browne RM. 2010. Transcriptional analysis of the *grlRA* virulence operon from *Citrobacter rodentium*. *J Bacteriol* 192:3722–3734.
 62. Torres AG, López-Sánchez GN, Milflores-Flores L, Patel SD, Rojas-López M, Martínez De La Peña CF, Arenas-Hernández MMP, Martínez-Laguna Y. 2007. Ler and H-NS, regulators controlling expression of the long polar fimbriae of *Escherichia coli* O157:H7. *J Bacteriol* 189:5916–5928.
 63. Haack KR, Robinson CL, Miller KJ, Fowlkes JW, Mellies JL. 2003. Interaction of Ler at the LEE5 (*tir*) operon of enteropathogenic *Escherichia coli*. *Infect Immun* 71:384–392.
 64. Hart E, Yang J, Tauschek M, Kelly M, Wakefield MJ, Frankel G, Hartland EL, Robins-Browne RM. 2008. RegA, an AraC-like protein, is a global transcriptional regulator that controls virulence gene expression in *Citrobacter rodentium*. *Infect Immun* 76:5247–5256.
 65. Yang J, Hart E, Tauschek M, Price GD, Hartland EL, Strugnell RA, Robins-Browne RM.

2008. Bicarbonate-mediated transcriptional activation of divergent operons by the virulence regulatory protein, RegA, from *Citrobacter rodentium*. *Mol Microbiol* 68:314–327.
66. Dong T, Coombes BK, Schellhorn HE. 2009. Role of RpoS in the virulence of *Citrobacter rodentium*. *Infect Immun* 77:501–507.
67. Cordone A, Lucchini S, De Felice M, Ricca E. 2011. Direct and indirect control of Lrp on LEE pathogenicity genes of *Citrobacter rodentium*. *FEMS Microbiol Lett* 325:64–70.
68. Jimenez AG, Ellermann M, Abbott W, Sperandio V. 2020. Diet-derived galacturonic acid regulates virulence and intestinal colonization in enterohaemorrhagic *Escherichia coli* and *Citrobacter rodentium*. *Nat Microbiol* 5:368–378.
69. Gaytán MO, Martínez-Santos VI, Soto E, González-Pedrajo B. 2016. Type three secretion system in attaching and effacing pathogens. *Front Cell Infect Microbiol* 6:129.
70. Deng W, Vallance BA, Li Y, Puente JL, Finlay BB. 2003. *Citrobacter rodentium* translocated intimin receptor (Tir) is an essential virulence factor needed for actin condensation, intestinal colonization and colonic hyperplasia in mice. *Mol Microbiol* 48:95–115.
71. Buschor S, Cuenca M, Uster SS, Schären OP, Balmer ML, Terrazos MA, Schürch CM, Hapfelmeier S. 2017. Innate immunity restricts *Citrobacter rodentium* A/E pathogenesis initiation to an early window of opportunity. *PLoS Pathog* 13:e1006476.
72. Hu JL, Nie SP, Min FF, Xie MY. 2012. Polysaccharide from seeds of *Plantago asiatica* L. increases short-chain fatty acid production and fecal moisture along with lowering pH in mouse colon. *J Agric Food Chem* 60:11525–11532.
73. Jones RCW, Otsuka E, Wagstrom E, Jensen CS, Price MP, Gebhart GF. 2007. Short-term sensitization of colon mechanoreceptors is associated with long-term hypersensitivity to colon distention in the mouse. *Gastroenterology* 133:184–194.
74. McConnell EL, Basit AW, Murdan S. 2010. Measurements of rat and mouse gastrointestinal pH, fluid and lymphoid tissue, and implications for *in-vivo* experiments. *J*

Pharm Pharmacol 60:63–70.

75. De Biase D, Lund PA. 2015. The *Escherichia coli* acid stress response and its significance for pathogenesis, p 49-88. In Sariaslani S, Gadd GM (ed), Advances in applied microbiology, vol 92. Elsevier Academic Press Inc, San Diego, CA.
76. Tennant SM, Hartland EL, Phumoonna T, Lyras D, Rood JI, Robins-Browne RM, Van Driel IR. 2008. Influence of gastric acid on susceptibility to infection with ingested bacterial pathogens. Infect Immun 76:639–645.
77. Sun FJ, Kaur S, Ziemer D, Banerjee S, Samuelson LC, De Lisle RC. 2003. Decreased gastric bacterial killing and up-regulation of protective genes in small intestine in gastrin-deficient mouse. Dig Dis Sci 48:976–985.
78. Cheng C, Wakefield MJ, Yang J, Tauschek M, Robins-Browne RM. 2012. Genome-wide analysis of the Pho regulon in a *pstCA* Mutant of *Citrobacter rodentium*. PLoS One 7:e50682.
79. Price SB, Cheng CM, Kaspar CW, Wright JC, Degraives FJ, Penfound TA, Castanie-Cornet MP, Foster JW. 2000. Role of *rpoS* in acid resistance and fecal shedding of *Escherichia coli* O157:H7. Appl Environ Microbiol 66:632–637.
80. Aquino P, Honda B, Jaini S, Lyubetskaya A, Hosur K, Chiu JG, Ekladius I, Hu D, Jin L, Sayeg MK, Stettner AI, Wang J, Wong BG, Wong WS, Alexander SL, Ba C, Bensussen SI, Bernstein DB, Braff D, Cha S, Cheng DI, Cho JH, Chou K, Chuang J, Gastler DE, Grasso DJ, Greifenberger JS, Guo C, Hawes AK, Israni D V., Jain SR, Kim J, Lei J, Li H, Li D, Li Q, Mancuso CP, Mao N, Masud SF, Meisel CL, Mi J, Nykyforchyn CS, Park M, Peterson HM, Ramirez AK, Reynolds DS, Rim NG, Saffie JC, Su H, Su WR, Su Y, Sun M, Thommes MM, Tu T, Varongchayakul N, Wagner TE, Weinberg BH, Yang R, Yaroslavsky A, Yoon C, Zhao Y, Zollinger AJ, Stringer AM, Foster JW, Wade J, Raman S, Broude N, Wong WW, Galagan JE. 2017. Coordinated regulation of acid resistance in *Escherichia coli*. BMC Syst Biol 11:1.
81. Pienaar JA, Singh A, Barnard TG. 2019. Acid-happy: Survival and recovery of enteropathogenic *Escherichia coli* (EPEC) in simulated gastric fluid. Microb Pathog

- 128:396–404.
82. Bergholz TM, Whittam TS. 2006. Variation in acid resistance among enterohaemorrhagic *Escherichia coli* in a simulated gastric environment. *J Appl Microbiol* 102:352–362.
 83. Cheville AM, Arnold KW, Buchrieser C, Cheng CM, Kaspar CW. 1996. *rpoS* regulation of acid, heat, and salt tolerance in *Escherichia coli* O157:H7. *Appl Environ Microbiol* 62:1822–1824.
 84. Coldewey SM, Hartmann M, Schmidt DS, Engelking U, Ukena SN, Gunzer F. 2007. Impact of the *rpoS* genotype for acid resistance patterns of pathogenic and probiotic *Escherichia coli*. *BMC Microbiol* 7:21.
 85. Mata GMSC, Ferreira GM, Spira B. 2017. RpoS role in virulence and fitness in enteropathogenic *Escherichia coli*. *PLoS One* 12:e0180381.
 86. Battesti A, Majdalani N, Gottesman S. 2011. The RpoS-mediated general stress response in *Escherichia coli**. *Annu Rev Microbiol* 65:189–213.
 87. Xu Y, Zhao Z, Tong W, Ding Y, Liu B, Shi Y, Wang J, Sun S, Liu M, Wang Y, Qi Q, Xian M, Zhao G. 2020. An acid-tolerance response system protecting exponentially growing *Escherichia coli*. *Nat Commun* 11:1496.
 88. Smith A, Bhagwat AA. 2013. Hypervirulent-host-associated *Citrobacter rodentium* cells have poor acid tolerance. *Curr Microbiol* 66:522–526.
 89. Begley M, Gahan CGM, Hill C. 2005. The interaction between bacteria and bile. *FEMS Microbiol Rev* 29:625–651.
 90. Prouty AM, Brodsky IE, Falkow S, Gunn JS. 2004. Bile-salt-mediated induction of antimicrobial and bile resistance in *Salmonella typhimurium*. *Microbiology* 150:775–783.
 91. Lin C, Wang Y, Le M, Chen KF, Jia YG. 2021. Recent Progress in Bile Acid-Based Antimicrobials. *Bioconjug Chem* 32:395–410.
 92. Thanassi DG, Cheng LW, Nikaido H. 1997. Active efflux of bile salts by *Escherichia coli*. *J Bacteriol* 179:2512–2518.

93. Otake T, Fujimoto M, Hoshino Y, Ishihara T, Haneda T, Okada N, Miki T. 2020. Twin-arginine translocation system is involved in *Citrobacter rodentium* fitness in the intestinal tract. *Infect Immun* 88:e00892-19.
94. Tremblay S, Romain G, Roux M, Chen XL, Brown K, Gibson DL, Ramanathan S, Menendez A. 2017. Bile acid administration elicits an intestinal antimicrobial program and reduces the bacterial burden in two mouse models of enteric infection. *Infect Immun* 85:e00942-16.
95. Kitamoto S, Nagao-Kitamoto H, Kuffa P, Kamada N. 2016. Regulation of virulence: the rise and fall of gastrointestinal pathogens. *J Gastroenterol* 51:195–205.
96. Wallace N, Zani A, Abrams E, Sun Y. 2016. The impact of oxygen on bacterial enteric pathogens, p 179-204. *In* Sariaslani S, Gadd GM (ed), *Advances in applied microbiology*, vol 95. Elsevier Academic Press Inc, San Diego, CA.
97. Paiva CN, Bozza MT. 2014. Are reactive oxygen species always detrimental to pathogens? *Antioxid Redox Signal* 20:1000–1034.
98. Albenberg L, Esipova T V., Judge CP, Bittinger K, Chen J, Laughlin A, Grunberg S, Baldassano RN, Lewis JD, Li H, Thom SR, Bushman FD, Vinogradov SA, Wu GD. 2014. Correlation between intraluminal oxygen gradient and radial partitioning of intestinal microbiota. *Gastroenterology* 147:1055-1063.
99. Tropini C, Earle KA, Huang KC, Sonnenburg JL. 2017. The gut microbiome: connecting spatial organization to function. *Cell Host Microbe* 21:433–442.
100. Suzuki TA, Nachman MW. 2016. Spatial heterogeneity of gut microbial composition along the gastrointestinal tract in natural populations of house mice. *PLoS One* 11:e0163720.
101. Lopez CA, Miller BM, Rivera-chávez F, Velazquez EM, Byndloss MX, Chávez-arroyo A, Lokken KL, Tsolis RM, Winter SE, Bäumlér AJ. 2016. Virulence factors enhance *Citrobacter rodentium* expansion through aerobic respiration 353:1249–1254.
102. Berger CN, Crepin VF, Roumeliotis TI, Wright JC, Carson D, Pevsner-Fischer M, Furniss

- RCD, Dougan G, Dori-Bachash M, Yu L, Clements A, Collins JW, Elinav E, Larrouy-Maumus GJ, Choudhary JS, Frankel G. 2017. *Citrobacter rodentium* subverts ATP flux and cholesterol homeostasis in intestinal epithelial cells *in vivo*. *Cell Metab* 26:738-752.
103. Caballero-Flores G, Pickard JM, Núñez G. 2021. Regulation of *Citrobacter rodentium* colonization: virulence, immune response and microbiota interactions. *Curr Opin Microbiol* 63:142–149.
104. Schroeder BO. 2019. Fight them or feed them: how the intestinal mucus layer manages the gut microbiota. *Gastroenterol Rep* 7:3–12.
105. Bhullar K, Zarepour M, Yu H, Yang H, Croxen M, Stahl M, Finlay BB, Turvey SE, Vallance BA. 2015. The serine protease autotransporter Pic modulates *Citrobacter rodentium* pathogenesis and its innate recognition by the host. *Infect Immun* 83:2636–2650.
106. Wlodarska M, Willing B, Keeney KM, Menendez A, Bergstrom KS, Gill N, Russell SL, Vallance BA, Finlay BB. 2011. Antibiotic treatment alters the colonic mucus layer and predisposes the host to exacerbated *Citrobacter rodentium*-induced colitis. *Infect Immun* 79:1536–1545.
107. Gustafsson JK, Navabi N, Rodriguez-Piñeiro AM, Alomran AHA, Premaratne P, Fernandez HR, Banerjee D, Sjövall H, Hansson GC, Lindén SK. 2013. Dynamic changes in mucus thickness and ion secretion during *Citrobacter rodentium* infection and clearance. *PLoS One* 8:e84430.
108. Wlodarska M, Willing BP, Bravo DM, Finlay BB. 2015. Phytonutrient diet supplementation promotes beneficial Clostridia species and intestinal mucus secretion resulting in protection against enteric infection. *Sci Rep* 5:9253.
109. Sharba S, Venkatakrishnan V, Padra M, Winther M, Gabl M, Sundqvist M, Wang J, Forsman H, Linden SK. 2019. Formyl peptide receptor 2 orchestrates mucosal protection against *Citrobacter rodentium* infection. *Virulence* 10:610–624.
110. Desai MS, Seekatz AM, Koropatkin NM, Kamada N, Hickey CA, Wolter M, Pudlo NA,

- Kitamoto S, Terrapon N, Muller A, Young VB, Henrissat B, Wilmes P, Stappenbeck TS, Núñez G, Martens EC. 2016. A dietary fiber-deprived gut microbiota degrades the colonic mucus barrier and enhances pathogen susceptibility. *Cell* 167:1339-1353.
111. Montrose DC, Nishiguchi R, Basu S, Staab HA, Zhou XK, Wang H, Meng L, Johncilla M, Cubillos-Ruiz JR, Morales DK, Wells MT, Simpson KW, Zhang S, Dogan B, Jiao C, Fei Z, Oka A, Herzog JW, Sartor RB, Dannenberg AJ. 2021. Dietary fructose alters the composition, localization, and metabolism of gut microbiota in association with worsening colitis. *Cell Mol Gastroenterol Hepatol* 11:525–550.
112. Vollaard E, Clasener H. 1994. Colonization resistance. *Antimicrob Agents Chemother* 38:409–414.
113. Lawley TD, Walker AW. 2012. Intestinal colonization resistance. *Immunology* 138:1–11.
114. Shealy NG, Yoo W, Byndloss MX. 2021. Colonization resistance: metabolic warfare as a strategy against pathogenic Enterobacteriaceae. *Curr Opin Microbiol* 64:82–90.
115. Kim S, Covington A, Pamer EG. 2017. The intestinal microbiota: Antibiotics, colonization resistance, and enteric pathogens. *Immunol Rev* 279:90–105.
116. Miller BM, Liou MJ, Zhang LF, Nguyen H, Litvak Y, Schorr EM, Jang KK, Tiffany CR, Butler BP, Bäumlér AJ. 2020. Anaerobic respiration of NOX1-derived hydrogen peroxide licenses bacterial growth at the colonic surface. *Cell Host Microbe* 28:789-797.
117. Osbelt L, Thiemann S, Smit N, Lesker TR, Schröter M, Gálvez EJC, Schmidt-Hohagen K, Pils MC, Mühlen S, Dersch P, Hiller K, Schlüter D, Neumann-Schaal M, Strowig T. 2020. Variations in microbiota composition of laboratory mice influence *Citrobacter rodentium* infection via variable short-chain fatty acid production. *PLoS Pathog* 16:e1008448.
118. An J, Zhao X, Wang Y, Noriega J, Gewirtz AT, Zou J. 2021. Western-style diet impedes colonization and clearance of *Citrobacter rodentium*. *PLoS Pathog* 17:e1009497.
119. Liang Q, Vallance BA. 2021. What’s for dinner? How *Citrobacter rodentium*’s metabolism helps it thrive in the competitive gut. *Curr Opin Microbiol* 63:76–82.

120. Kamada N, Kim Y-G, Sham HP, Vallance BA, Puente JL, Martens EC, Núñez G. 2012. Regulated virulence controls the ability of a pathogen to compete with the gut microbiota. *Science* 336:1325–1329.
121. Caballero-Flores G, Pickard JM, Fukuda S, Inohara N, Núñez G. 2020. An enteric pathogen subverts colonization resistance by evading competition for amino acids in the gut. *Cell Host Microbe* 28:526–533.
122. Connolly JPR, Slater SL, O’Boyle N, Goldstone RJ, Crepin VF, Gallego DR, Herzyk P, Smith DGE, Douce GR, Frankel G, Roe AJ. 2018. Host-associated niche metabolism controls enteric infection through fine-tuning the regulation of type 3 secretion. *Nat Commun* 9:4187.
123. Bailey MT, Dowd SE, Parry NMA, Galley JD, Schauer DB, Lyte M. 2010. Stressor exposure disrupts commensal microbial populations in the intestines and leads to increased colonization by *Citrobacter rodentium*. *Infect Immun* 78:1509–1519.
124. Mullineaux-Sanders C, Collins JW, Ruano-Gallego D, Levy M, Pevsner-Fischer M, Glegola-Madejska IT, Sångfors AM, Wong JLC, Elinav E, Crepin VF, Frankel G. 2017. *Citrobacter rodentium* relies on commensals for colonization of the colonic mucosa. *Cell Rep* 21:3381–3389.
125. Curtis MM, Hu Z, Klimko C, Narayanan S, Deberardinis R, Sperandio V. 2014. The gut commensal *Bacteroides thetaiotaomicron* exacerbates enteric infection through modification of the metabolic landscape. *Cell Host Microbe* 16:759–769.
126. Rodrigues DM, Sousa AJ, Johnson-Henry KC, Sherman PM, Gareau MG. 2012. Probiotics are effective for the prevention and treatment of *Citrobacter rodentium*-induced colitis in mice. *J Infect Dis* 206:99–109.
127. Mao T, Su CW, Ji Q, Chen CY, Wang R, Vijaya Kumar D, Lan J, Jiao L, Shi HN. 2021. Hyaluronan-induced alterations of the gut microbiome protects mice against *Citrobacter rodentium* infection and intestinal inflammation. *Gut Microbes* 13:e1972757.
128. Fanning S, Hall LJ, Cronin M, Zomer A, MacSharry J, Goulding D, Motherway MOC,

- Shanahan F, Nally K, Dougan G, Van Sinderen D. 2012. Bifidobacterial surface-exopolysaccharide facilitates commensal-host interaction through immune modulation and pathogen protection. *Proc Natl Acad Sci U S A* 109:2108–2113.
129. Vong L, Pinnell LJ, Määttänen P, Yeung CW, Lurz E, Sherman PM. 2015. Selective enrichment of commensal gut bacteria protects against *Citrobacter rodentium*-induced colitis. *Am J Physiol - Gastrointest Liver Physiol* 309:G181–G192.
130. Lin R, Piao M, Song Y. 2019. Dietary quercetin increases colonic microbial diversity and attenuates colitis severity in *Citrobacter rodentium*-infected mice. *Front Microbiol* 10:1092.
131. Johnson-Henry KC, Nadjafi M, Avitzur Y, Mitchell DJ, Ngan BY, Galindo-Mata E, Jones NL, Sherman PM. 2005. Amelioration of the effects of *Citrobacter rodentium* infection in mice by pretreatment with probiotics. *J Infect Dis* 191:2106–2117.
132. Silhavy TJ, Kahne D, Walker S. 2010. The bacterial cell envelope. *Cold Spring Harb Perspect Biol* 2:a000414.
133. Gronow S, Brade H. 2001. Lipopolysaccharide biosynthesis: which steps do bacteria need to survive? *J Endotoxin Res* 7:3–23.
134. Needham BD, Trent MS. 2013. Fortifying the barrier: the impact of lipid A remodelling on bacterial pathogenesis. *Nat Rev Microbiol* 11:467–481.
135. Hagan CL, Silhavy TJ, Kahne D. 2011. β -barrel membrane protein assembly by the Bam complex. *Annu Rev Biochem* 80:189–210.
136. Tikhonova EB, Zgurskaya HI. 2004. AcrA, AcrB, and TolC of *Escherichia coli* form a stable intermembrane multidrug efflux complex. *J Biol Chem* 279:32116–32124.
137. Du D, Wang Z, James NR, Voss JE, Klimont E, Ohene-Agyei T, Venter H, Chiu W, Luisi BF. 2014. Structure of the AcrAB-TolC multidrug efflux pump. *Nature* 509:512–515.
138. Konovalova A, Silhavy TJ. 2015. Outer membrane lipoprotein biogenesis: Lol is not the end. *Philos Trans R Soc Lond B Biol Sci* 370:20150030.

139. Braun V. 1975. Covalent lipoprotein from the outer membrane of *Escherichia coli*. *Biochim Biophys Acta* 415:335–377.
140. Tsirigotaki A, De Geyter J, Šoštarić N, Economou A, Karamanou S. 2017. Protein export through the bacterial Sec pathway. *Nat Rev Microbiol* 15:21–36.
141. Dalbey RE, Kuhn A, Zhu L, Kiefer D. 2014. The membrane insertase YidC. *Biochim Biophys Acta* 1843:1489–1496.
142. Cymer F, Von Heijne G, White SH. 2015. Mechanisms of integral membrane protein insertion and folding. *J Mol Biol* 427:999–1022.
143. Patel R, Smith SM, Robinson C. 2014. Protein transport by the bacterial Tat pathway. *Biochim Biophys Acta* 1843:1620–1628.
144. Hengge-Aronis R. 1999. Interplay of global regulators and cell physiology in the general stress response of *Escherichia coli*. *Curr Opin Microbiol* 2:148–152.
145. Hews CL, Cho T, Rowley G, Raivio TL. 2019. Maintaining integrity under stress: envelope stress response regulation of pathogenesis in gram-negative bacteria. *Front Cell Infect Microbiol* 9:313.
146. Dartigalongue C, Missiakas D, Raina S. 2001. Characterization of the *Escherichia coli* σ^E regulon. *J Biol Chem* 276:20866–20875.
147. De Las Peñas A, Connolly L, Gross CA. 1997. The σ^E -mediated response to extracytoplasmic stress in *Escherichia coli* is transduced by RseA and RseB, two negative regulators of σ^E . *Mol Microbiol* 24:373–385.
148. Alba BM, Leeds JA, Onufryk C, Lu CZ, Gross CA. 2002. DegS and YaeL participate sequentially in the cleavage of RseA to activate the σ^E -dependent extracytoplasmic stress response. *Genes Dev* 16:2156–2168.
149. Kanehara K, Ito K, Akiyama Y. 2002. YaeL (EcfE) activates the σ^E pathway of stress response through a site-2 cleavage of anti- σ^E , RseA. *Genes Dev* 16:2147–2155.
150. Flynn JM, Levchenko I, Sauer RT, Baker TA. 2004. Modulating substrate choice: the

- SspB adaptor delivers a regulator of the extracytoplasmic-stress response to the AAA+ protease ClpXP for degradation. *Genes Dev* 18:2292–2301.
151. Baker TA, Sauer RT. 2012. ClpXP, an ATP-powered unfolding and protein-degradation machine. *Biochim Biophys Acta* 1823:15–28.
 152. Rowley G, Spector M, Kormanec J, Roberts M. 2006. Pushing the envelope: extracytoplasmic stress responses in bacterial pathogens. *Nat Rev Microbiol* 4:383–394.
 153. Flores-Kim J, Darwin AJ. 2016. The phage shock protein response. *Annu Rev Microbiol* 70:83–101.
 154. Recacha E, Fox V, Díaz-Díaz S, García-Duque A, Docobo-Pérez F, Pascual Á, Rodríguez-Martínez JM. 2021. Disbalancing envelope stress responses as a strategy for sensitization of *Escherichia coli* to antimicrobial agents. *Front Microbiol* 12:653479.
 155. Joly N, Engl C, Jovanovic G, Huvet M, Toni T, Sheng X, Stumpf MPH, Buck M. 2010. Managing membrane stress: the phage shock protein (Psp) response, from molecular mechanisms to physiology. *FEMS Microbiol Rev* 34:797–827.
 156. Srivastava D, Moumene A, Flores-Kim J, Darwin AJ. 2017. Psp stress response proteins form a complex with mislocalized secretins in the *Yersinia enterocolitica* cytoplasmic membrane. *MBio* 8:e01088-17.
 157. Yamaguchi S, Gueguen E, Horstman NK, Darwin AJ. 2010. Membrane association of PspA depends on activation of the phage-shock-protein response in *Yersinia enterocolitica*. *Mol Microbiol* 78:429–443.
 158. Flores-Kim J, Darwin AJ. 2015. Activity of a bacterial cell envelope stress response is controlled by the interaction of a protein binding domain with different partners. *J Biol Chem* 290:11417–11430.
 159. Horstman NK, Darwin AJ. 2012. Phage shock proteins B and C prevent lethal cytoplasmic membrane permeability in *Yersinia enterocolitica*. *Mol Microbiol* 85:445–460.
 160. Maxson ME, Darwin AJ. 2006. PspB and PspC of *Yersinia enterocolitica* are dual

- function proteins: regulators and effectors of the phage-shock-protein response. *Mol Microbiol* 59:1610–1623.
161. Dworkin J, Jovanovic G, Model P. 2000. The PspA protein of *Escherichia coli* is a negative regulator of σ^{54} - dependent transcription. *J Bacteriol* 182:311–319.
 162. Yamaguchi S, Reid DA, Rothenberg E, Darwin AJ. 2013. Changes in Psp protein binding partners, localization and behaviour upon activation of the *Yersinia enterocolitica* phage shock protein response. *Mol Microbiol* 87:656–671.
 163. Jovanovic G, Weiner L, Model P. 1996. Identification, nucleotide sequence, and characterization of PspF, the transcriptional activator of the *Escherichia coli* stress-induced *psp* operon. *J Bacteriol* 178:1936–1945.
 164. Lloyd LJ, Jones SE, Jovanovic G, Gyaneshwar P, Rolfe MD, Thompson A, Hinton JC, Buck M. 2004. Identification of a new member of the phage shock protein response in *Escherichia coli*, the Phage Shock Protein G (PspG). *J Biol Chem* 279:55707–55714.
 165. Jovanovic G, Dworkin J, Model P. 1997. Autogenous control of PspF, a constitutively active enhancer-binding protein of *Escherichia coli*. *J Bacteriol* 179:5232–5237.
 166. Jovanovic G, Lloyd LJ, Stumpf MPH, Mayhew AJ, Buck M. 2006. Induction and function of the phage shock protein extracytoplasmic stress response in *Escherichia coli*. *J Biol Chem* 281:21147–21161.
 167. Standar K, Mehner D, Osadnik H, Berthelmann F, Hause G, Lünsdorf H, Brüser T. 2008. PspA can form large scaffolds in *Escherichia coli*. *FEBS Lett* 582:3585–3589.
 168. Darwin AJ, Miller VL. 2001. The *psp* locus of *Yersinia enterocolitica* is required for virulence and for growth *in vitro* when the Ysc type III secretion system is produced. *Mol Microbiol* 39:429–445.
 169. Darwin AJ. 2013. Stress relief during host infection: the phage shock protein response supports bacterial virulence in various ways. *PLoS Pathog* 9:e1003388.
 170. Flores-Kim J, Darwin AJ. 2012. Links between type III secretion and extracytoplasmic

- stress responses in *Yersinia*. *Front Cell Infect Microbiol* 2:125.
171. Casino P, Rubio V, Marina A. 2010. The mechanism of signal transduction by two-component systems. *Curr Opin Struct Biol* 20:763–771.
 172. Zschiedrich CP, Keidel V, Szurmant H. 2016. Molecular mechanisms of two-component signal transduction. *J Mol Biol* 428:3752–3775.
 173. Thomassin JL, Leclerc JM, Giannakopoulou N, Zhu L, Salmon K, Portt A, Daigle F, Le Moual H, Gruenheid S. 2017. Systematic analysis of two-component systems in *Citrobacter rodentium* reveals positive and negative roles in virulence. *Infect Immun* 85:e00654-16.
 174. Wall E, Majdalani N, Gottesman S. 2018. The complex Rcs regulatory cascade. *Annu Rev Microbiol* 72:111–139.
 175. Majdalani N, Heck M, Stout V, Gottesman S. 2005. Role of RcsF in signaling to the Rcs phosphorelay pathway in *Escherichia coli*. *J Bacteriol* 187:6770–6778.
 176. Castanié-Cornet MP, Cam K, Jacq A. 2006. RcsF is an outer membrane lipoprotein involved in the RcsCDB phosphorelay signaling pathway in *Escherichia coli*. *J Bacteriol* 188:4264–4270.
 177. Wall EA, Majdalani N, Gottesman S. 2020. IgaA negatively regulates the Rcs phosphorelay via contact with the RcsD phosphotransfer protein. *PLoS Genet* 16:e1008610.
 178. Schmöe K, Rogov V V., Rogova NY, Löhr F, Güntert P, Bernhard F, Dötsch V. 2011. Structural insights into Rcs phosphotransfer: the newly identified RcsD-ABL domain enhances interaction with the response regulator RcsB. *Structure* 19:577–587.
 179. Wehland M, Kiecker C, Coplin DL, Kelm O, Saenger W, Bernhard F. 1999. Identification of an RcsA/RcsB recognition motif in the promoters of exopolysaccharide biosynthetic operons from *Erwinia amylovora* and *Pantoea stewartii* subspecies *stewartii*. *J Biol Chem* 274:3300–3307.

180. Wehland M, Bernhard F. 2000. The RcsAB box. Characterization of a new operator essential for the regulation of exopolysaccharide biosynthesis in enteric bacteria. *J Biol Chem* 275:7013–7020.
181. Matsuoka Y, Shimizu K. 2011. Metabolic regulation in *Escherichia coli* in response to culture environments via global regulators. *Biotechnol J* 6:1330–1341.
182. Perraud AL, Weiss V, Gross R. 1999. Signalling pathways in two-component phosphorelay systems. *Trends Microbiol* 7:115–120.
183. Jianming D, Shiro luchi, Hoi-Shan K, Zhe L, Lin ECC. 1993. The deduced amino-acid sequence of the cloned *cpxR* gene suggests the protein is the cognate regulator for the membrane sensor, CpxA, in a two-component signal transduction system of *Escherichia coli*. *Gene* 136:227–230.
184. Raivio TL, Silhavy TJ. 1997. Transduction of envelope stress in *Escherichia coli* by the Cpx two- component system. *J Bacteriol* 179:7724–7733.
185. Vogt SL, Raivio TL. 2012. Just scratching the surface: an expanding view of the Cpx envelope stress response. *FEMS Microbiol Lett* 326:2–11.
186. Weber RF, Silverman PM. 1988. The Cpx proteins of *Escherichia coli* K12. Structure of the CpxA polypeptide as an inner membrane component. *J Mol Biol* 203:467–478.
187. Raivio TL. 2014. Everything old is new again: an update on current research on the Cpx envelope stress response. *Biochim Biophys Acta* 1843:1529–1541.
188. Pogliano J, Lynch AS, Belin D, Lin ECC, Beckwith J. 1997. Regulation of *Escherichia coli* cell envelope proteins involved in protein folding and degradation by the Cpx two-component system. *Genes Dev* 11:1169–1182.
189. Yamamoto K, Ishihama A. 2006. Characterization of copper-inducible promoters regulated by CpxA/CpxR in *Escherichia coli*. *Biosci Biotechnol Biochem* 70:1688–1695.
190. Price NL, Raivio TL. 2009. Characterization of the Cpx regulon in *Escherichia coli* strain MC4100. *J Bacteriol* 191:1798–1815.

191. Danese PN, Silhavy TJ. 1998. CpxP, a stress-combative member of the Cpx regulon. *J Bacteriol* 180:831–839.
192. Thede GL, Arthur DC, Edwards RA, Buelow DR, Wong JL, Raivio TL, Glover JNM. 2011. Structure of the periplasmic stress response protein CpxP. *J Bacteriol* 193:2149–2157.
193. Kwon E, Kim DY, Gross CA, Gross JD, Kim KK. 2010. The crystal structure *Escherichia coli* Spy. *Protein Sci* 19:2252–2259.
194. Raivio TL, Popkin DL, Silhavy TJ. 1999. The Cpx envelope stress response is controlled by amplification and feedback inhibition. *J Bacteriol* 181:5263–5272.
195. Raivio TL, Laird MW, Joly JC, Silhavy TJ. 2000. Tethering of CpxP to the inner membrane prevents spheroplast induction of the Cpx envelope stress response. *Mol Microbiol* 37:1186–1197.
196. Zhou X, Keller R, Volkmer R, Krauss N, Scheerer P, Hunke S. 2011. Structural basis for two-component system inhibition and pilus sensing by the auxiliary CpxP protein. *J Biol Chem* 286:9805–9814.
197. Tschauner K, Hörnschemeyer P, Müller VS, Hunke S. 2014. Dynamic Interaction between the CpxA sensor kinase and the periplasmic accessory protein CpxP mediates signal recognition in *E. coli*. *PLoS One* 9:e107383.
198. Isaac DD, Pinkner JS, Hultgren SJ, Silhavy TJ. 2005. The extracytoplasmic adaptor protein CpxP is degraded with substrate by DegP. *Proc Natl Acad Sci U S A* 102:17775–17779.
199. Snyder WB, Davis LJB, Danese PN, Cosma CL, Silhavy TJ. 1995. Overproduction of nlpE, a new outer membrane lipoprotein, suppresses the toxicity of periplasmic lacZ by activation of the Cpx signal transduction pathway. *J Bacteriol* 177:4216–4223.
200. Delhaye A, Laloux G, Collet JF. 2019. The lipoprotein NlpE is a cpx sensor that serves as a sentinel for protein sorting and folding defects in the *Escherichia coli* envelope. *J Bacteriol* 201:e00611-18.

201. Audrain B, Ferrières L, Zairi A, Soubigou G, Dobson C, Coppée JY, Beloin C, Ghigo JM. 2013. Induction of the Cpx envelope stress pathway contributes to *Escherichia coli* tolerance to antimicrobial peptides. *Appl Environ Microbiol* 79:7770–7779.
202. Hunke S, Keller R, Müller VS. 2012. Signal integration by the Cpx-envelope stress system. *FEMS Microbiol Lett* 326:12–22.
203. Mitchell AM, Silhavy TJ. 2019. Envelope stress responses: balancing damage repair and toxicity. *Nat Rev Microbiol* 17:417–428.
204. De Wulf P, Kwon O, Lin ECC. 1999. The CpxRA signal transduction system of *Escherichia coli*: growth-related autoactivation and control of unanticipated target operons. *J Bacteriol* 181:6772–6778.
205. Wolfe AJ, Parikh N, Lima BP, Zemaitaitis B. 2008. Signal integration by the two-component signal transduction response regulator CpxR. *J Bacteriol* 190:2314–2322.
206. DiGiuseppe PA, Silhavy TJ. 2003. Signal detection and target gene induction by the CpxRA two-component system. *J Bacteriol* 185:2432–2440.
207. Danese PN, Snyder WB, Cosma CL, Davis LJB, Silhavy TJ. 1995. The Cpx two-component signal transduction pathway of *Escherichia coli* regulates transcription of the gene specifying the stress-inducible periplasmic protease, DegP. *Genes Dev* 9:387–398.
208. Buelow DR, Raivio TL. 2005. Cpx signal transduction is influenced by a conserved N-terminal domain in the novel inhibitor CpxP and the periplasmic protease DegP. *J Bacteriol* 187:6622–6630.
209. MacRitchie DM, Acosta N, Raivio TL. 2012. DegP is involved in Cpx-mediated posttranscriptional regulation of the type III secretion apparatus in enteropathogenic *Escherichia coli*. *Infect Immun* 80:1766–1772.
210. Vogt SL, Scholz R, Peng Y, Guest RL, Scott NE, Woodward SE, Foster LJ, Raivio TL, Finlay BB. 2019. Characterization of the *Citrobacter rodentium* Cpx regulon and its role in host infection. *Mol Microbiol* 111:700–716.

211. Bardwell JCA, McGovern K, Beckwith J. 1991. Identification of a protein required for disulfide bond formation *in vivo*. *Cell* 67:581–589.
212. Vogt SL, Nevesinjac AZ, Humphries RM, Donnenberg MS, Armstrong GD, Raivio TL. 2010. The Cpx envelope stress response both facilitates and inhibits elaboration of the enteropathogenic *Escherichia coli* bundle-forming pilus. *Mol Microbiol* 76:1095–1110.
213. Miki T, Okada N, Kim Y, Abe A, Danbara H. 2008. DsbA directs efficient expression of outer membrane secretin EscC of the enteropathogenic *Escherichia coli* type III secretion apparatus. *Microb Pathog* 44:151–158.
214. Yamamoto K, Ishihama A. 2005. Transcriptional response of *Escherichia coli* to external copper. *Mol Microbiol* 56:215–227.
215. Kihara A, Akiyama Y, Ito K. 1998. Different pathways for protein degradation by the FtsH/HflKC membrane-embedded protease complex: an implication from the interference by a mutant form of a new substrate protein, YccA. *J Mol Biol* 279:175–188.
216. Daley DO, Rapp M, Granseth E, Melén K, Drew D, Von Heijne G. 2005. Global topology analysis of the *Escherichia coli* inner membrane proteome. *Science* 308:1321–1323.
217. Van Stelten J, Silva F, Belin D, Silhavy TJ. 2009. Effects of antibiotics and a proto-oncogene homolog on destruction of protein translocator SecY. *Science* 325:753–756.
218. Bury-Moné S, Nomane Y, Reymond N, Barbet R, Jacquet E, Imbeaud S, Jacq A, Bouloc P. 2009. Global analysis of extracytoplasmic stress signaling in *Escherichia coli*. *PLoS Genet* 5:e1000651.
219. Gerken H, Charlson ES, Cicirelli EM, Kenney LJ, Misra R. 2009. MzrA: a novel modulator of the EnvZ/OmpR two-component regulon. *Mol Microbiol* 72:1408–1422.
220. Gerken H, Misra R. 2010. MzrA-EnvZ interactions in the periplasm influence the EnvZ/OmpR two-component regulon. *J Bacteriol* 192:6271–6278.
221. Cai SJ, Inouye M. 2002. EnvZ-OmpR interaction and osmoregulation in *Escherichia coli*. *J Biol Chem* 277:24155–24161.

222. Batchelor E, Walther D, Kenney LJ, Goulian M. 2005. The *Escherichia coli* CpxA-CpxR envelope stress response system regulates expression of the porins OmpF and OmpC. *J Bacteriol* 187:5723–5731.
223. Nishino K, Honda T, Yamaguchi A. 2005. Genome-wide analyses of *Escherichia coli* gene expression responsive to the BaeSR two-component regulatory system. *J Bacteriol* 187:1763–1772.
224. Raffa RG, Raivio TL. 2002. A third envelope stress signal transduction pathway in *Escherichia coli*. *Mol Microbiol* 45:1599–1611.
225. Saha S, Lach SR, Konovalova A. 2021. Homeostasis of the Gram-negative cell envelope. *Curr Opin Microbiol* 61:99–106.
226. Majdalani N, Gottesman S. 2005. The Rcs phosphorelay: A complex signal transduction system. *Annu Rev Microbiol* 59:379–405.
227. Evans KL, Kannan S, Li G, de Pedro MA, Young KD. 2013. Eliminating a set of four penicillin binding proteins triggers the Rcs phosphorelay and Cpx stress responses in *Escherichia coli*. *J Bacteriol* 195:4415–4424.
228. Fei K, Chao HJ, Hu Y, Francis MS, Chen S. 2021. CpxR regulates the Rcs phosphorelay system in controlling the Ysc-Iop type III secretion system in *Yersinia pseudotuberculosis*. *Microbiol* 167:000998.
229. Petrovskaya LE, Ziganshin RH, Kryukova EA, Zlobinov A V., Gapizov SS, Shingarova LN, Mironov VA, Lomakina GY, Dolgikh DA, Kirpichnikov MP. 2021. Increased Synthesis of a Magnesium Transporter MgtA During Recombinant Autotransporter Expression in *Escherichia coli*. *Appl Bioch Biotechnol* 193:3672-3703.
230. Nevesinjac AZ, Raivio TL. 2005. The Cpx envelope stress response affects expression of the type IV bundle-forming pili of enteropathogenic *Escherichia coli*. *J Bacteriol* 187:672–686.
231. Thomassin JL, Giannakopoulou N, Zhu L, Gross J, Salmon K, Leclerc JM, Daigle F, Le Moual H, Gruenheid S. 2015. The CpxRA two-component system is essential for

- Citrobacter rodentium* virulence. Infect Immun 83:1919–1928.
232. Giannakopoulou N, Mendis N, Zhu L, Gruenheid S, Faucher SP, Le Moual H. 2018. The virulence effect of CpxRA in *Citrobacter rodentium* is independent of the auxiliary proteins NlpE and CpxP. Front Cell Infect Microbiol 8:320.
 233. Buffie CG, Pamer EG. 2013. Microbiota-mediated colonization resistance against intestinal pathogens. Nat Rev Immunol 13:790–801.
 234. McDonald C, Jovanovic G, Ces O, Buck M. 2015. Membrane stored curvature elastic stress modulates recruitment of maintenance proteins Pspa and Vipp1. mBio 6:e01188-15.
 235. Beumer RR, De Vries J, Rombouts FM. 1992. *Campylobacter jejuni* non-culturable coccoid cells. Int J Food Microbiol 15:153–163.
 236. Edwards RA, Keller LH, Schifferli DM. 1998. Improved allelic exchange vectors and their use to analyze 987P fimbria gene expression. Gene 207:149–157.
 237. Ferrières L, Hémerly G, Nham T, Guérout AM, Mazel D, Beloin C, Ghigo JM. 2010. Silent mischief: bacteriophage Mu insertions contaminate products of *Escherichia coli* random mutagenesis performed using suicidal transposon delivery plasmids mobilized by broad-host-range RP4 conjugative machinery. J Bacteriol 192:6418–6427.
 238. Ullman-Culleré MH, Foltz CJ. 1999. Body condition scoring: a rapid and accurate method for assessing health status in mice. Lab Anim Sci 49:319–323.
 239. Dhamdhare G, Zgurskaya HI. 2010. Metabolic shutdown in *Escherichia coli* cells lacking the outer membrane channel TolC. Mol Microbiol 77:743–754.
 240. Shimohata N, Chiba S, Saikawa N, Ito K, Akiyama Y. 2002. The Cpx stress response system of *Escherichia coli* senses plasma membrane proteins and controls HtpX, a membrane protease with a cytosolic active site. Genes Cells 7:653–662.
 241. Raivio TL, Leblanc SKD, Price NL. 2013. The *Escherichia coli* Cpx envelope stress response regulates genes of diverse function that impact antibiotic resistance and membrane integrity. J Bacteriol 195:2755–2767.

242. Kenny B, Abe A, Stein M, Finlay BB. 1997. Enteropathogenic *Escherichia coli* protein secretion is induced in response to conditions similar to those in the gastrointestinal tract. *Infect Immun* 65:2606–2612.
243. De la Cruz MA, Morgan JK, Ares MA, Yáñez-Santos JA, Riordan JT, Girón JA. 2016. The two-component system CpxRA negatively regulates the locus of enterocyte effacement of enterohemorrhagic *Escherichia coli* involving σ_{32} and Lon protease. *Front Cell Infect Microbiol* 6:11.
244. MacRitchie DM, Ward JD, Nevesinjac AZ, Raivio TL. 2008. Activation of the Cpx envelope stress response down-regulates expression of several locus of enterocyte effacement-encoded genes in enteropathogenic *Escherichia coli*. *Infect Immun* 76:1465–1475.
245. Darwin AJ. 2005. The phage-shock-protein response. *Mol Microbiol* 57:621–628.
246. Kobayashi R, Suzuki T, Yoshida M. 2007. *Escherichia coli* phage-shock protein A (PspA) binds to membrane phospholipids and repairs proton leakage of the damaged membranes. *Mol Microbiol* 66:100–109.
247. Arbeloa A, Oates C V., Marchès O, Hartland EL, Frankel G. 2011. Enteropathogenic and enterohemorrhagic *Escherichia coli* type III secretion effector EspV induces radical morphological changes in eukaryotic cells. *Infect Immun* 79:1067–1076.
248. Oughtred R, Stark C, Breitkreutz BJ, Rust J, Boucher L, Chang C, Kolas N, O'Donnell L, Leung G, McAdam R, Zhang F, Dolma S, Willems A, Coulombe-Huntington J, Chatr-Aryamontri A, Dolinski K, Tyers M. 2019. The BioGRID interaction database: 2019 update. *Nucleic Acids Res* 47:D529–D541.
249. Stark C, Breitkreutz BJ, Reguly T, Boucher L, Breitkreutz A, Tyers M. 2006. BioGRID: a general repository for interaction datasets. *Nucleic Acids Res* 34:D535–D539.
250. Babu M, Arnold R, Bundalovic-Torma C, Gagarinova A, Wong KS, Kumar A, Stewart G, Samanfar B, Aoki H, Wagih O, Vlasblom J, Phanse S, Lad K, Yeou Hsiung Yu A, Graham C, Jin K, Brown E, Golshani A, Kim P, Moreno-Hagelsieb G, Greenblatt J,

- Houry WA, Parkinson J, Emili A. 2014. Quantitative genome-wide genetic interaction screens reveal global epistatic relationships of protein complexes in *Escherichia coli*. *PLoS Genet* 10:e1004120.
251. Brissette JL, Russel M, Weiner L, Model P. 1990. Phage shock protein, a stress protein of *Escherichia coli*. *Proc Natl Acad Sci U S A* 87:862–866.
252. Nakayama SI, Kushiro A, Asahara T, Tanaka RI, Hu L, Kopecko DJ, Watanabe H. 2003. Activation of *hila* expression at low pH requires the signal sensor CpxA, but not the cognate response regulator CpxR, in *Salmonella enterica* serovar Typhimurium. *Microbiology* 149:2809–2817.
253. Bessaiah H, Pokharel P, Loucif H, Kulbay M, Sasseville C, Habouria H, Sébastien Houle, Bernier J, Massé É, Van Grevenynghe J, Dozois CM. 2021. The RyfA small RNA regulates oxidative and osmotic stress responses and virulence in uropathogenic *Escherichia coli*. *PLoS Pathog* 17:e1009617.
254. Jones P, Binns D, Chang HY, Fraser M, Li W, McAnulla C, McWilliam H, Maslen J, Mitchell A, Nuka G, Pesseat S, Quinn AF, Sangrador-Vegas A, Scheremetjew M, Yong SY, Lopez R, Hunter S. 2014. InterProScan 5: Genome-scale protein function classification. *Bioinformatics* 30:1236–1240.
255. Blum M, Chang HY, Chuguransky S, Grego T, Kandasamy S, Mitchell A, Nuka G, Paysan-Lafosse T, Qureshi M, Raj S, Richardson L, Salazar GA, Williams L, Bork P, Bridge A, Gough J, Haft DH, Letunic I, Marchler-Bauer A, Mi H, Natale DA, Necci M, Orengo CA, Pandurangan AP, Rivoire C, Sigrist CJA, Sillitoe I, Thanki N, Thomas PD, Tosatto SCE, Wu CH, Bateman A, Finn RD. 2021. The InterPro protein families and domains database: 20 years on. *Nucleic Acids Res* 49:D344–D354.
256. Sonnhammer EL, von Heijne G, Krogh A. 1998. A hidden Markov model for predicting transmembrane helices in protein sequences. *Proc Int Conf Intell Syst Mol Biol* 6:175–182.
257. Krogh A, Larsson B, Von Heijne G, Sonnhammer ELL. 2001. Predicting transmembrane protein topology with a hidden Markov model: Application to complete genomes. *J Mol*

- Biol 305:567–580.
258. Huerta-Cepas J, Szklarczyk D, Heller D, Hernández-Plaza A, Forslund SK, Cook H, Mende DR, Letunic I, Rattei T, Jensen LJ, Von Mering C, Bork P. 2019. EggNOG 5.0: A hierarchical, functionally and phylogenetically annotated orthology resource based on 5090 organisms and 2502 viruses. *Nucleic Acids Res* 47:D309–D314.
 259. Yamane T, Enokida H, Hayami H, Kawahara M, Nakagawa M. 2012. Genome-wide transcriptome analysis of fluoroquinolone resistance in clinical isolates of *Escherichia coli*. *Int J Urol* 19:360–368.
 260. Maurer LM, Yohannes E, Bondurant SS, Radmacher M, Slonczewski JL. 2005. pH regulates genes for flagellar motility, catabolism, and oxidative stress in *Escherichia coli* K-12. *J Bacteriol* 187:304–319.
 261. Romero PR, Karp PD. 2004. Using functional and organizational information to improve genome-wide computational prediction of transcription units on pathway-genome databases. *Bioinformatics* 20:709–717.
 262. Keseler IM, Gama-Castro S, Mackie A, Billington R, Bonavides-Martínez C, Caspi R, Kothari A, Krummenacker M, Midford PE, Muñiz-Rascado L, Ong WK, Paley S, Santos-Zavaleta A, Subhraveti P, Tierrafria VH, Wolfe AJ, Collado-Vides J, Paulsen IT, Karp PD. 2021. The EcoCyc Database in 2021. *Front Microbiol* 12:711077.
 263. Beloin C, Valle J, Latour-Lambert P, Faure P, Kzreminski M, Balestrino D, Haagensen JAJ, Molin S, Prensier G, Arbeille B, Ghigo JM. 2004. Global impact of mature biofilm lifestyle on *Escherichia coli* K-12 gene expression. *Mol Microbiol* 51:659–674.
 264. Fralick JA. 1996. Evidence that TolC is required for functioning of the Mar/AcrAB efflux pump of *Escherichia coli*. *J Bacteriol* 178:5803–5805.
 265. Paul S, Alegre KO, Holdsworth SR, Rice M, Brown JA, Mcveigh P, Kelly SM, Law CJ. 2014. A single-component multidrug transporter of the major facilitator superfamily is part of a network that protects *Escherichia coli* from bile salt stress. *Mol Microbiol* 92:872–884.

266. Imuta N, Nishi J, Tokuda K, Fujiyama R, Manago K, Iwashita M, Sarantuya J, Kawano Y. 2008. The *Escherichia coli* efflux pump TolC promotes aggregation of enteroaggregative *E. coli* 042. *Infect Immun* 76:1247–1256.
267. Piddock LJV. 2006. Clinically relevant chromosomally encoded multidrug resistance efflux pumps in bacteria. *Clin Microbiol Rev* 19:382–402.
268. Coombes Z, Yadav V, McCoubrey LE, Freire C, Basit AW, Conlan RS, Gonzalez D. 2020. Progestogens are metabolized by the gut microbiota: implications for colonic drug delivery. *Pharmaceutics* 12:760.
269. Yadav V, Gaisford S, Merchant HA, Basit AW. 2013. Colonic bacterial metabolism of corticosteroids. *Int J Pharm* 457:268–274.
270. Singh A, Barnard TG. 2016. Surviving the acid barrier: responses of pathogenic *Vibrio cholerae* to simulated gastric fluid. *Appl Microbiol Biotechnol* 100:815–824.
271. Koseki S, Mizuno Y, Sotome I. 2011. Modeling of pathogen survival during simulated gastric digestion. *Appl Environ Microbiol* 77:1021–1032.
272. Kim S, Ryu K, Biswas D, Ahn J. 2014. Survival, prophage induction, and invasive properties of lysogenic *Salmonella* Typhimurium exposed to simulated gastrointestinal conditions. *Arch Microbiol* 196:655–659.
273. Leclerc J, Rosenfeld E, Trainini M, Martin B, Meuric V, Bonnaure-Mallet M, Baysse C. 2015. The cytochrome *bd* oxidase of *Porphyromonas gingivalis* contributes to oxidative stress resistance and dioxygen tolerance. *PLoS One* 10:e0143808.
274. Guest RL, Wang J, Wong JL, Raivio TL. 2017. A bacterial stress response regulates respiratory protein complexes to control envelope stress adaptation. *J Bacteriol* 199:e00153-17.
275. Fujimoto M, Goto R, Haneda T, Okada N. 2018. *Salmonella enterica* serovar Typhimurium cpxra two-component system contributes to gut colonization in *Salmonella*-induced colitis. *Infect Immun* 86:e00280-18.

276. Rivera-Chávez F, Zhang LF, Faber F, Lopez CA, Byndloss MX, Olsan EE, Xu G, Velazquez EM, Lebrilla CB, Winter SE, Bäumlér AJ. 2016. Depletion of butyrate-producing *Clostridia* from the gut microbiota drives an aerobic luminal expansion of *Salmonella*. *Cell Host Microbe* 19:443–454.
277. Lupp C, Robertson ML, Wickham ME, Sekirov I, Champion OL, Gaynor EC, Finlay BB. 2007. Host-mediated inflammation disrupts the intestinal microbiota and promotes the overgrowth of Enterobacteriaceae. *Cell Host Microbe* 2:119–129.
278. Lambeth JD, Neish AS. 2014. Nox enzymes and new thinking on reactive oxygen: a double-edged sword revisited. *Annu Rev Pathol Mech Dis* 9:119–145.
279. Müsken A, Bielaszewska M, Greune L, Schweppe CH, Müthing J, Schmidt H, Schmidt MA, Karch H, Zhang W. 2008. Anaerobic conditions promote expression of Sfp fimbriae and adherence of sorbitol-fermenting enterohemorrhagic *Escherichia coli* O157:NM to human intestinal epithelial cells. *Appl Environ Microbiol* 74:1087–1093.
280. Polzin S, Huber C, Eylert E, Elsenhans I, Eisenreich W, Schmidt H. 2013. Growth media simulating ileal and colonic environments affect the intracellular proteome and carbon fluxes of enterohemorrhagic *Escherichia coli* O157: H7 strain EDL933. *Appl Environ Microbiol* 79:3703–3715.
281. Bauwens A, Kunsmann L, Marejková M, Zhang W, Karch H, Bielaszewska M, Mellmann A. 2017. Intrahost milieu modulates production of outer membrane vesicles, vesicle-associated Shiga toxin 2a and cytotoxicity in *Escherichia coli* O157:H7 and O104:H4. *Environ Microbiol Rep* 9:626–634.
282. Kumar A, Russell RM, Pifer R, Menezes-Garcia Z, Cuesta S, Narayanan S, MacMillan JB, Sperandio V. 2020. The serotonin neurotransmitter modulates virulence of enteric pathogens. *Cell Host Microbe* 28:41-53.
283. Hansen AM, Jin DJ. 2012. SspA up-regulates gene expression of the LEE pathogenicity island by decreasing H-NS levels in enterohemorrhagic *Escherichia coli*. *BMC Microbiol* 12:231.

284. Younis R, Bingle LEH, Rollauer S, Munera D, Busby SJ, Johnson S, Deane JE, Lea SM, Frankel G, Pallen MJ. 2010. SepL resembles an aberrant effector in binding to a class 1 type III secretion chaperone and carrying an N-terminal secretion signal. *J Bacteriol* 192:6093–6098.
285. Deng W, Li Y, Hardwidge PR, Frey EA, Pfuetzner RA, Lee S, Gruenheid S, Strynacka NCJ, Puente JL, Finlay BB. 2005. Regulation of type III secretion hierarchy of translocators and effectors in attaching and effacing bacterial pathogens. *Infect Immun* 73:2135–2146.
286. Serapio-Palacios A, Finlay BB. 2020. Dynamics of expression, secretion and translocation of type III effectors during enteropathogenic *Escherichia coli* infection. *Curr Opin Microbiol* 54:67–76.
287. O’Connell CB, Creasey EA, Knutton S, Elliott S, Crowther LJ, Luo W, John Albert M, Kaper JB, Frankel G, Donnenberg MS. 2004. SepL, a protein required for enteropathogenic *Escherichia coli* type III translocation, interacts with secretion component SepD. *Mol Microbiol* 52:1613–1625.
288. Smith AD, Yan X, Chen C, Dawson HD, Bhagwat AA. 2016. Understanding the host-adapted state of *Citrobacter rodentium* by transcriptomic analysis. *Arch Microbiol* 198:353–362.
289. Tobe T, Beatson SA, Taniguchi H, Abe H, Bailey CM, Fivian A, Younis R, Matthews S, Marches O, Frankel G, Hayashi T, Pallen MJ. 2006. An extensive repertoire of type III secretion effectors in *Escherichia coli* O157 and the role of lambdoid phages in their dissemination. *Proc Natl Acad Sci U S A* 103:14941–14946.
290. Berger CN, Crepin VF, Roumeliotis TI, Wright JC, Serafini N, Pevsner-Fischer M, Yu L, Elinav E, Di Santo JP, Choudhary JS, Frankel G. 2018. The *Citrobacter rodentium* type III secretion system effector EspO affects mucosal damage repair and antimicrobial responses. *PLoS Pathog* 14:e1007406.
291. Ale A, Crepin VF, Collins JW, Constantinou N, Habibzay M, Babbie AC, Frankel G, Stumpf PH. 2017. Model of host-pathogen interaction dynamics links *in vivo* optical

- imaging and immune responses. *Infect Immun* 85:e00606-16.
292. Zheng Y, Valdez PA, Danilenko DM, Hu Y, Sa SM, Gong Q, Abbas AR, Modrusan Z, Ghilardi N, De Sauvage FJ, Ouyang W. 2008. Interleukin-22 mediates early host defense against attaching and effacing bacterial pathogens. *Nat Med* 14:282–289.
 293. Tsai PY, Zhang B, He WQ, Zha JM, Odenwald MA, Singh G, Tamura A, Shen L, Sailer A, Yeruva S, Kuo WT, Fu YX, Tsukita S, Turner JR. 2017. IL-22 upregulates epithelial claudin-2 to drive diarrhea and enteric pathogen clearance. *Cell Host Microbe* 21:671-681.
 294. Brissette JL, Weiner L, Ripmaster TL, Model P. 1991. Characterization and sequence of the *Escherichia coli* stress-induced *psp* operon. *J Mol Biol* 220:35–48.
 295. Kleerebezem M, Crielaard W, Tommassen J. 1996. Involvement of stress protein PspA (phage shock protein A) of *Escherichia coli* in maintenance of the protonmotive force under stress conditions. *EMBO J* 15:162–171.
 296. Engl C, Beek A Ter, Bekker M, De Mattos JT, Jovanovic G, Buck M. 2011. Dissipation of proton motive force is not sufficient to induce the phage shock protein response in *Escherichia coli*. *Curr Microbiol* 62:1374–1385.
 297. Jones SE, Lloyd LJ, Tan KK, Buck M. 2003. Secretion defects that activate the phage shock response of *Escherichia coli*. *J Bacteriol* 185:6707–6711.
 298. Grabowicz M, Silhavy TJ. 2017. Envelope stress responses: an interconnected safety net. *Trends Biochem Sci* 42:232–242.
 299. Bergler H, Abraham D, Aschauer H, Turnowsky F. 1994. Inhibition of lipid biosynthesis induces the expression of the *pspA* gene. *Microbiology* 140:1937–1944.
 300. Trotochaud AE, Wassarman KM. 2006. 6S RNA regulation of *pspF* transcription leads to altered cell survival at high pH. *J Bacteriol* 188:3936–3943.
 301. Karlinsey JE, Maguire ME, Becker LA, Crouch ML V., Fang FC. 2010. The phage shock protein PspA facilitates divalent metal transport and is required for virulence of *Salmonella enterica* sv. Typhimurium. *Mol Microbiol* 78:669–685.

302. Darwin AJ, Miller VL. 1999. Identification of *Yersinia enterocolitica* genes affecting survival in an animal host using signature-tagged transposon mutagenesis. *Mol Microbiol* 32:51–62.
303. Maxson ME, Darwin AJ. 2004. Identification of inducers of the *Yersinia enterocolitica* phage shock protein system and comparison to the regulation of the RpoE and Cpx extracytoplasmic stress responses. *J Bacteriol* 186:4199–4208.
304. Weiner L, Model P. 1994. Role of an *Escherichia coli* stress-response operon in stationary-phase survival. *Proc Natl Acad Sci U S A* 91:2191–2195.

Appendices

Appendix Table and Figures

Table S1. Average CPS/OD₆₀₀ of three biological replicates 1-hour post-resuspension in LB and high-glucose DMEM with MOPS for *cpxP*-, *yebE*-, *ygiB*-, *bssR*-, and *htpX-lux* reporter plasmids.

Gene	CpxRA?	LB ¹	<i>P</i> -value ²	HG-DMEM ¹	<i>P</i> -value ²
<i>cpxP</i>	+	34643	0.0032	300779	0.00539
	-	0		42	
<i>yebE</i>	+	144	0.00772	3071	0.00442
	-	1		24	
<i>ygiB</i>	+	26800	0.00053	53025	0.0000005
	-	8567		13605	
<i>bssR</i>	+	1198	0.00035	2823	0.00135
	-	212		841	
<i>htpX</i>	+	43422	0.00056	137294	0.00621
	-	8366		13962	

¹Values (CPS/OD₆₀₀) are the same as those represented in Figure 1A

²*P*-value indicates significant difference between wild-type and Δ *cpxRA* mutant cells grown in the same condition (LB or HG-DMEM), Student's *t*-test

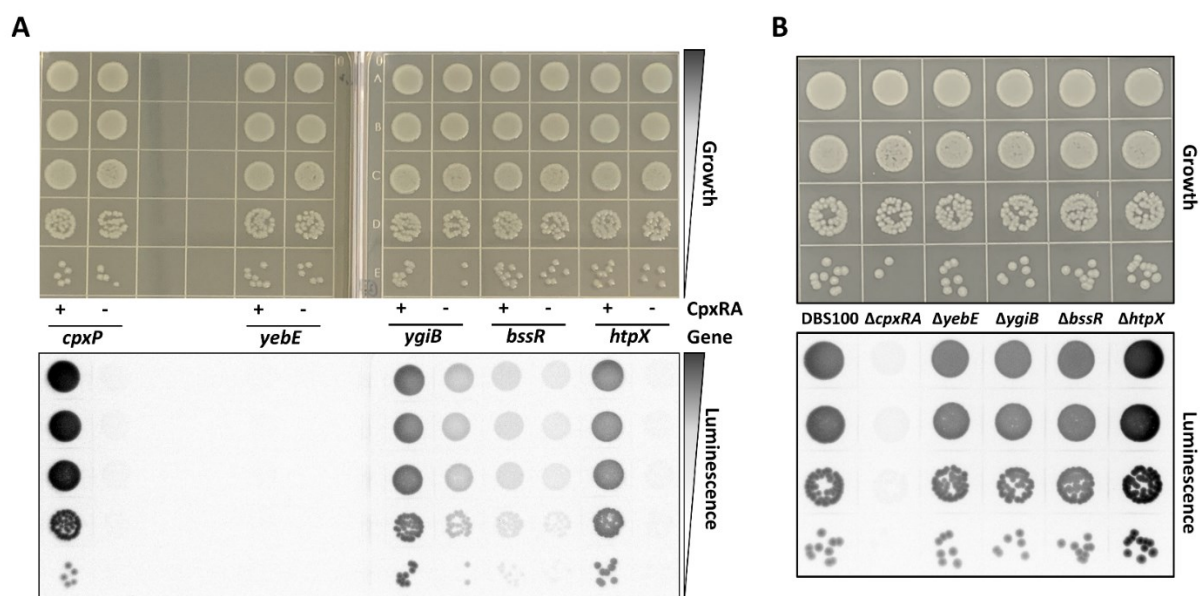


Figure S1. Luminescence on solid LB agar for reporters of confirmed Cpx regulon members and *cpxP-lux* in Cpx-regulated gene mutants. (A) Wild-type and $\Delta cpxRA$ strains harboring *lux*-reporter plasmids for each gene of interest and (B) wild-type and mutant strains harboring *cpxP-lux* reporter plasmids were grown overnight, standardized to OD₆₀₀ 1, serially diluted to 10⁻⁶, spotted on LB supplemented with kanamycin. Plates were pictured (top) after 18 hours of growth at 37°C and luminescence (bottom) was imaged using a ChemiDoc MP imaging system (Bio-Rad). All assays (A and B) were completed at least twice, with one representative experiment shown.

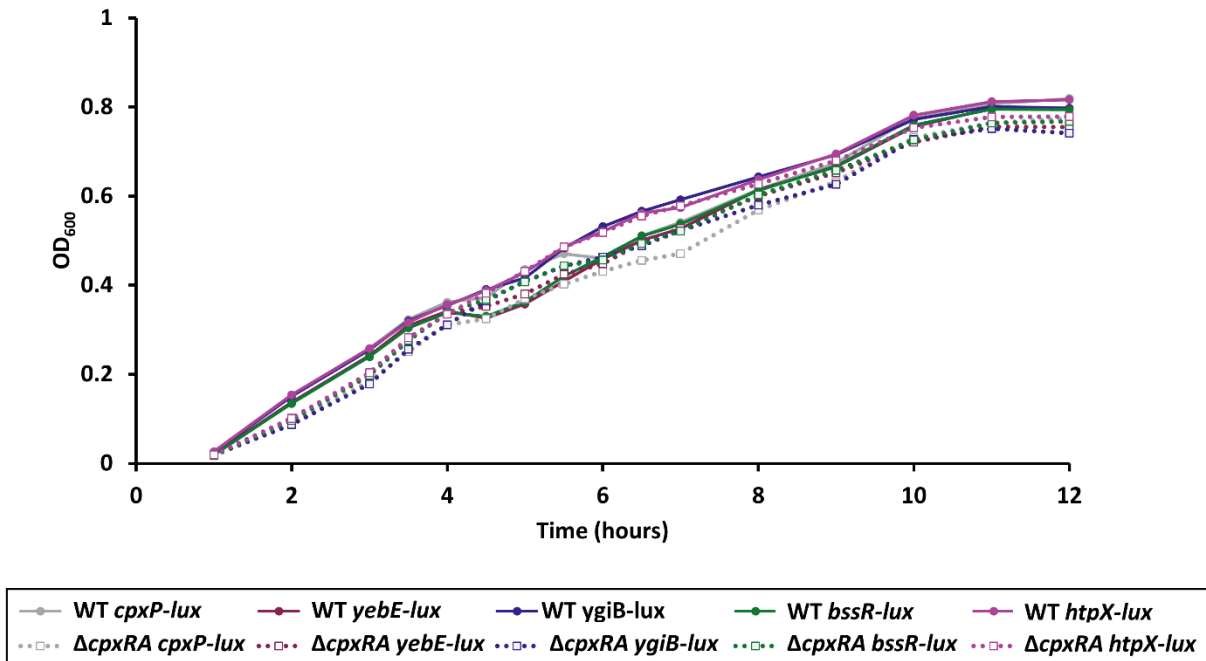


Figure S2. Growth curve of luminescent reporter strains grown and measured over 12 hours. Strains harboring *lux*-reporter plasmids were grown overnight and inoculated 1:100 in LB broth supplemented with kanamycin in a black walled 96-well plate and incubated at 37°C shaking. OD measurements were taken alongside luminescence measurements to ensure even growth between strains.